Transcriptomic and secretomic profiling of isolated leukocytes exposed to alpha-particle and photon radiation

Applications in biodosimetry

Matthew Howland
Hon. B. Sc. Biochemistry
University of Ottawa (2011)

A thesis submitted to the Faculty of Graduate and Postdoctoral Studies in partial fulfillment of the requirements for:

Master of Science in Biochemistry

Department of Biochemistry, Microbiology and Immunology
Faculty of Medicine
University of Ottawa

1 Abstract

The general public is at risk of ionising-radiation exposure. The development of high-throughput methods to triage exposures is warranted. Current biodosimetry techniques are low-throughput and encumbered by time and technical expertise. Although there has been an emergence of gene-profiling tools for the purpose of photon biodosimetry, similar capacities do not exist for alpha-particle radiation. Herein is the first genomic study useful for alpha-particle radiation biodosimetric triage. This work has identified robust alpha-particle induced gene-based biomarkers in isolated, ex-vivo irradiated leukocytes from multiple donors. It was found that alpha-particle and photon radiation elicited similar transcriptional responses, which could potentially be distinguished by aggregate-signature analysis. Although no distinct genes were sole indicators of exposure type, clustering algorithms and principal component analysis were able to demarcate radiation type with some success. By comparing the biological effects elicited by photon and alpha-particle radiation, significant contributions have been made to the field of radiation biodosimetry.

2 Acknowledgements

My success has been only partially my own – I am indebted to many, and without them, this thesis would not be. I would like to thank:

My parents first and foremost, for instilling in me a sense of curiosity and encouraging me with near infinite patience.

Dr. Vinita Chauhan, my direct supervisor and mentor, who has played a pivotal role in my development as a scientist. I am deeply grateful for her support and providing me with a myriad of opportunities.

Dr. Ross Milne, for being a supportive supervisor

Drs. Renaud Vincent and Jack Cornett, for guidance and scientific input

Dr. Lindsay Beaton, for her role as a sympathiser in the grad-student life style

Dr. Ruth Wilkins, for letting me work with a great degree of latitude

Sylvie Lachapelle for exceptional technical support

My friends, for having sat many hours listening to my scientific musings and tangents

Liz, for being so good, good to me

Canadian Safety and Security Program, for both project funding and exceptional opportunities

3 Table of Contents

4 List of Abbreviations

A Thrombospondin Type 1 Motif, Member 13 (ADAMTS13),

Acute Radiation Syndrome (ARS)

Analysis of Variance (ANOVA)

Ataxia–Telangiectasia Mutated (ATM)

B-Cell Lymphoma 2 (Bcl-2)

Background Corrected Fluorescence intensity (BFI)

Bcl-2-Associated Death Promoter (BAD)

Benjamini-Hochberg (BH)

c-Jun N-Terminal Kinases (JNK)

Comparative Threshold (Ct)

Complete Blood Count (CBC)

Dicentric Assay (DCA)

DNA Double Strand Breaks (DNA DSBs)

Enzyme-Linked Immuno-Sorbent Assay (ELISA)

False Discovery Rate (FDR)

Fetal Bovine Serum (FBS)

Fluorescein Isothiocyanate (FITC)

Forward Scatter (FSC)

Growth Arrest and DNA Damage 45A (GADD45A)

Granulocyte-Colony Stimulating Factor (G-CSF)

Granulocyte Macrophage-Colony Stimulating Factor (GM-CSF)

Gray (Gy)

Growth and Differentiation Factor 15 (GDF-15)

Interleukin (IL)

International Atomic Energy Association (IAEA)

International Commission on Radiation Protection (ICRP)

International Nuclear and Radiological Events Scale (INES)

Linear models for microarray data (LIMMA)

Linear Energy Transfer (LET)

Lipocalin-2/Neutrophil Gelatinase-Associated Lipocalin (LCN2/NGAL)

Microarray Technology (MA)

MicroRNA (miRNA)

Mylar Based Plastic Dishes (MD)

Myeloperoxidase (MPO)

National Council on Radiation Protection and Measurements (NCRP)

Ingenuity Pathway Analysis (IPA)

Peripheral Blood Mononuclear Cells (PBMCs)

Peroxiredoxin-2 (PRDX2)

Phosphate Buffered Saline (PBS)

Phosphorylated H2AX (Gamma-H2AX)

Principal Component Analysis (PCA)

Propidium Iodide (PI)

Protein Kinase B (Akt)

Quantitative Real Time Polymerase Chain Reaction (qPCR)

Relative Biological Effectiveness (RBE)

Radiological Dispersal Device (RDD)

Reactive Oxygen Species (ROS)

Side Scatter (SSC)

Serum Amyloid A (SAA)

Soluble Intercellular Adhesion Molecule 1 (sICAM-1),

Soluble Vascular Cell Adhesion Protein 1 (sVCAM-1)

Standard Deviation (SD)

Superoxide Dismutase [Cu-Zn] (SOD1)

Superoxide Dismutase 2 (SOD2)

TBS Serum Triton (TST)

Thioredoxin (TXN1)

Transforming Growth Factor Beta (TGF-β)

Tris-Phosphate Buffered Saline (TBS)

Tumor Protein 53 (p53)

White Blood Cells (WBCs)

5 List of Figures

6 List of Tables

7 Introduction

7.1 Threats of Public Radiation Exposure

There has been a growing consensus in the international community that nuclear terrorism is an escalating global concern. This is evidenced by the first ever Nuclear Security Summit (2010) held in Washington and the follow-up Seoul Korea Nuclear Security Summit (2012) (Nayan 2012). Furthermore, there is emerging agreement that it is not a matter of if, but of when, a nuclear accident or deliberately precipitated event will occur (Conklin and Liotta 2005). The threat of such an incident and subsequent public radiation exposure can arise from a variety of sources, including inter-state conflicts, malicious organizations/individuals and accidents (Bhattacharjee 2010).

7.1.1 Emerging Concerns

Nuclear trafficking is a global concern with well-documented incidents world-wide. There have been assaults on nuclear facilities in Pakistan (2007, 2008) (Gregory 2011) and South Africa (2007) (Bhattacharjee 2010). During the period of 1993 to 2011, the International Atomic Energy Association (IAEA) has documented 2164 nuclear material incidents or malicious acts. Of these, 588 involved the theft or loss of nuclear or radioactive materials. A further 18 of these incidents involved the alpha-particle emitting isotopes plutonium or highly enriched uranium. A bomb equivalent to that dropped on Nagasaki can be assembled with 6kg of plutonium (Kazi 2009), or crudely constructed with 50kg of highly enriched uranium. Radiological dispersal devices (RDD) can be fabricated with even less and more varied materials, are more likely to be employed than conventional nuclear weapons (Bechtel 2007), and could be readily constructed (Sutton and Bromley 2005). The Los Alamos and

Argonne National Laboratories have conducted a thorough review of RDD source material and have postulated that four of the nine isotopes most likely to be employed in a RDD are alpha-particle emitters. Furthermore, Los Alamos has rated these alpha-particle emitting isotopes as more likely candidates for use, due to their minimal shielding requirements and ease of concealment (Van Tuyle, Strub et al. 2003). These isotopes include Plutonium, Americium, Polonium and Radium (Peterson, MacDonell et al. 2007). There has been considerable effort put forward to simulate RDD blasts in controlled environments, using realistic source sizes of these isotopes with varying sophistication in RDD engineering (Harper, Musolino et al. 2007).

7.1.2 Documented Incidents

The IAEA also introduced an International Nuclear and Radiological Events Scale (INES) in 1990 to facilitate communication with the public about radio-nuclear events (IAEA 2008). Under the 1986 agreement, nuclear incidents of a certain magnitude are required to be reported by member states (Brumfiel 2011), and this tool is used by the national regulators during an emergency. A thorough review of reported nuclear incidents has been compiled since 2009 (Nenot 2009), including both accidental releases and malicious acts. High profile incidents affecting hundreds of thousands of individuals include nuclear reactor concerns and radioactive material releases in Chernobyl (1986) (Saenko, Ivanov et al. 2011) and Fukushima (2011) (Thielen 2012). Serious accidents have also happened in the medical field, such as mis-calibrations of medical sources, resulting in both overexposures and underexposures (Cohen, Schultheiss et al. 1995) (Ash and Bates 1994). These errors resulted in severe complications in over 1000 patients. There have also been serious accidents with orphaned radioactive sources being inadvertently handled by scrap-metal collectors; the most severe incident to date having occurred in Goiania, Brazil (Rosenthal,

de Almeida et al. 1991). In this particular case, scrap merchants disassembled a source which was then both sold and played with, resulting in the need to triage approximately 100,000 people. Almost 30 people required extreme medical intervention, including skin grafts and amputations. There have also been incidents of radioactive scrap metal being smelted and contaminating metal products. Other unintended exposures have resulted from equipment malfunctions as well as industrial overexposures (Nenot 1998). Malevolent uses of radioactive materials against specific people have also been documented. One case in the United States involved a father intentionally irradiating his son. A second documented case in France, wherein an individual seeking to injure a colleague, placed a radioactive source underneath their colleague's car seat. Assassinations for apparent political reasons have been conducted using alpha-particle emitting radioactive isotopes, such as the case of former KGB dissident Alexander Litvenenko (McFee and Leikin 2009). The use of alpha-particle emitting Polonium-210 was a confounding factor in his diagnosis; despite displaying symptoms consistent with radiation sickness, original hospital assessment was focussed on possible gamma-ray emitter contamination. Even though this was a relatively targeted assassination, with the poison being administered in the victim's tea, over 100 people from the surrounding area showed signs of internal contamination (Maguire, Fraser et al. 2010).

As discussed, there are numerous documented incidents in which civilians, sometimes numbering in the thousands, are exposed to radiation. The capability to rapidly identify these victims would be beneficial for providing timely medical intervention. The work presented in this thesis contributes to the field of radiation triage with specific focus on alpha-particle radiation.

7.2 Physics of Radiation

Radiation can be divided into two main branches, non-ionising and ionising radiation. In the context of nuclear incidents, the focus is primarily on ionising radiation, specifically, radiation with energy sufficient to induce bond breakages and induce ionising events in matter. Within an atom, nuclear particles are in continuous motion, resulting in continual collisions and energy transfer. In a stable nucleus there is insufficient energy for any nuclear particle to escape. In a radioactive atom there is a probability that, by pure chance, a nuclear particle acquires enough energy to escape. This results in the emission of energy from the atomic nucleus via a variety of possible mechanisms (Figure 1) (Johns and Cunningham 1983). There are numerous sub-types of ionising radiation, classified via the mechanism of energy release. Some of the major class distinctions include alpha-particle emission (charged helium ion), beta-particle emission (charged electron) or gamma/X-ray emission (neutral photon) (Andreo, Evans et al. 2005).

7.2.1 Alpha-Particle Decay

Alpha-particle decay occurs primarily in heavy nuclei and involves the emission of a charged two-proton two-neutron ion. This type of radiation is highly energetic, often on the order of MeV, but has limited penetrating power. As it moves through a given medium, an alpha-particle will cause intense ionization as it pulls electrons from surrounding atoms, on the order of 3000-7000 ion-pairs/mm through air. The pathway may extend several centimeters through air or micrometers through tissue.

7.2.2 Beta-Particle Decay

In the case of beta-particle decay, a neutron will change into a proton or vice versa and simultaneously emit a negatron or positron respectively. In either case the beta-particle will have the mass of an electron but the charge may be positive or negative, conserving the net charge of the atom. Beta particles generally have energy on the order of 0.1-2 MeV but with greater energy dispersion due to the formation of a small, neutral neutrino in the neutron/proton conversion. Beta-particles deposit their energy in a more turbulent way than alpha-particles, as the small mass of the electron can be easily deflected. This results in about 6-20 ion pairs/mm path through air. Due to their variable energy, beta-particles may travel from 10-2000 cm through air and up to 0.5 cm through tissue.

7.2.3 Photon Radiation

Ionising photon radiation nomenclature is based on their origin, with photons emitted from the nucleus called gamma-rays and those from electrons called X-rays. It is possible that after emission of an alpha- or beta-particle a nucleus will remain unstable, and as it drops to a stable potential, this excess energy is emitted in the form of a photon. As a photon has neither charge nor mass, it does not directly ionize matter in the same manner as a charged particle, but instead interacts via photoelectric effects or Compton scattering. In both mechanisms the photon energy is absorbed by a valence electron which then can be emitted from the atom. In the photoelectric effect, the energy of the electron will be equivalent to the incident energy of the gamma-ray photon minus the binding energy of the electron to the nucleus. In Compton scattering, a valence electron is emitted and another, lower energy X-ray photon is produced and emitted in a different direction. The energy spectrum of ionising photons can be quite variable but may range from anywhere up to 1 MeV. Due to their lack of charge and mass, photons may propagate almost 500 meters through air and 5 meters through tissue.

In summary, alpha-particles are the most densely ionising radiation but the least penetrating due to their relative size and charge. Gamma-rays possess no charge and no mass and are the least densely ionising but most penetrating form of radiation. Beta-particles exist between these two extremes.

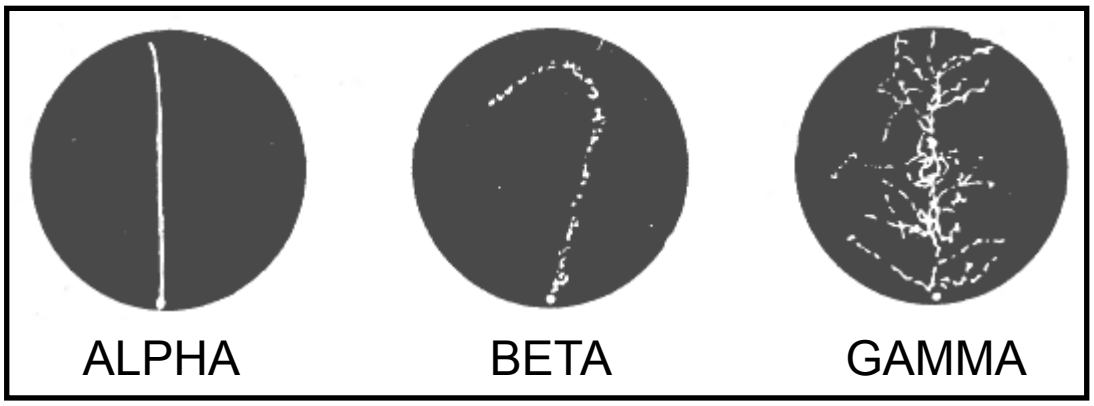

Figure 1: Cloud chamber photograph of alpha-particle, beta-particle and gamma-ray ionisation tracks. Alpha-particles display linear, dense ionising tracks with little deflection. Beta-particles are more sparsely ionising and turbulent. Gamma-rays show branched tracks with a forward disposition resultant from scattering. Reproduced from Johns and Cunningham (1983).

7.3 Radiobiology

7.3.1 Important Radiological Units

It is important to define several key radiological units and their relevance in a biological context. The International Commission on Radiation Units and Measurements has released a thorough report (ICRU 2011) on many radiological concepts and units but those which are important in the context of this thesis are:

Linear Energy Transfer (LET)

Defined as:

$$L_{\Delta} = \frac{dE_{\Delta}}{dl}$$

Units J / m

Linear energy transfer of a material for a given type of charged particle is a quotient of mean energy lost by the charged particle due to electronic interactions in traversing a distance, minus the mean sum of the kinetic energies in excess of delta of all the electrons realised by the charged particles.

Absorbed Dose

Defined as:

$$D = \frac{d\bar{\varepsilon}}{dm}$$

Units J / Kg

Absorbed dose is given by the quotient of mean energy imparted by ionizing radiation to a matter of mass. The special name for a unit of absorbed dose is a Gray (Gy).

Absorbed Dose Rate

Defined as:

$$\dot{D} = \frac{dD}{dt}$$

Units J/ Kg·s

Absorbed dose rate is defined by the change of absorbed dose with respect to time.

7.3.2 Time Scale and Modes of Radiation Damage within the Cell

The above noted equations are parameters with physical definitions, but it is important to place these definitions in the context of radiobiology. The mode of action of ionising radiation can be thought of in three distinct phases, centered around physical, chemical and biological interactions with radically different time scales (Boag 1975). The time scale and nature of these interactions is summarized in Figure 2

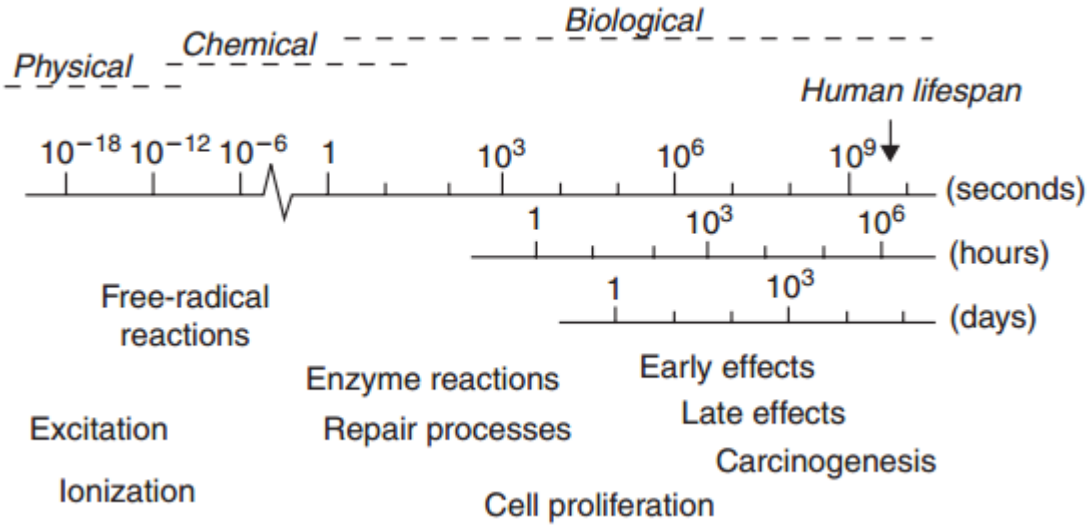

Figure 2: Logarithmic timeline demonstrating the time-scale and nature of interactions after exposure of humans to ionising radiation. Reproduced from Joiner and Van Der Kogel (2009).

Physical interactions are comprised of the interaction of the ionising particle and the atoms forming the cellular component in question. High-speed electrons will transverse a DNA molecule and a mammalian cell within the order of 10^{-18} s and 10^{-14} s respectively, resulting in 100,000 ionising events per 1 Gy dose to a 10 μm cell (Joiner and Van Der Kogel 2009). Within 10^{-12}s after exposure to ionising radiation, the ionising energy will have been distributed to various atomic species. This is followed by the chemical interaction of ionised atoms and free radicals, formed primarily by the radiolysis of water in the cytosol. These high-energy species are initially distributed in a non-homogenous manner, localized around ionising tracks. As they distribute through the cell, these chemical species will reach homogeneity within 10^{-7} s (Nagaishi and Kumagai 2011). The chemical species will have reacted and are generally resolved within 10^{-4} s after irradiation (Houee-Levin and Bobrowski 2013). The next phase consists of cellular effects and response, and encompasses a vast-time scale. It includes many facets of systems biology such as enzymatic reactions of immediate cellular perturbances and quenching of free-radicals to delayed effects such as the development of cancers in later life (Feinendegen, Hahnfeldt et al. 2008).

7.3.3 Relative Biological Effectiveness

In such a biological context, different radiation types can elicit different effects at the same physical radiation dose and the International Commission on Radiation Protection (ICRP) advocates the use of Relative Biological Effectiveness (RBE) and a radiation weighting factor to roughly quantify these differences (Valentin 2003). For the purposes of radiobiology, the ICRP defines RBE as being the ratio of the absorbed doses of two types of radiation that produce the same specified effect; low LET gamma and X-ray photon radiation is assigned a reference value of 1 and high LET radiation, such as alpha-particle

radiation, usually receives a weighting of 20. There are complications in the notion of RBE as it is end-point, dose, dose-rate, fraction and tissue specific (Valentin 2003). This has important ramifications in estimating absorbed doses in cases where physical dosimetry is absent.

One of the main differences between these radiation types is the physical track structure of dose deposition (Tabocchini, Campa et al. 2012) (Dingfelder 2012), and studies have shown that computationally, high LET DNA damage results in more complex lesions (Nikjoo, O'Neill et al. 1999) (Nikjoo, O'Neill et al. 2001). Many studies have shown varying biological effects elicited by changing radiation type or parameters (Asaithamby and Chen 2011) (Friedrich, Scholz et al. 2012) (Goodhead 1994), confirming computational modeling efforts. Track structure plays a vital role in eliciting biological effects, as one of the primary sites of damage to the cell via radiation damage is the DNA (Franken, ten Cate et al. 2011). High LET radiation such as alpha-particles deposit a large dose (~0.5Gy) per track through a cell (Lorimore, Goodhead et al. 1993) and does so on a picoseconds time scale (Kadhim, Hill et al. 2006). Low LET photon radiation such as X-rays and gamma-rays tend to produce a homogenous dose pattern across the cellular population with a dose of 1 Gy corresponding to ~1,000 tracks over a second time scale (Kadhim, Hill et al. 2006). High LET damage has a greater propensity of causing DNA double strand breaks (DSBs) (Figure 3) and this is the basis of many biological effects, as DNA DSBs are more deleterious to the cell (Jostes 1996) (Hall and Hei 2003).

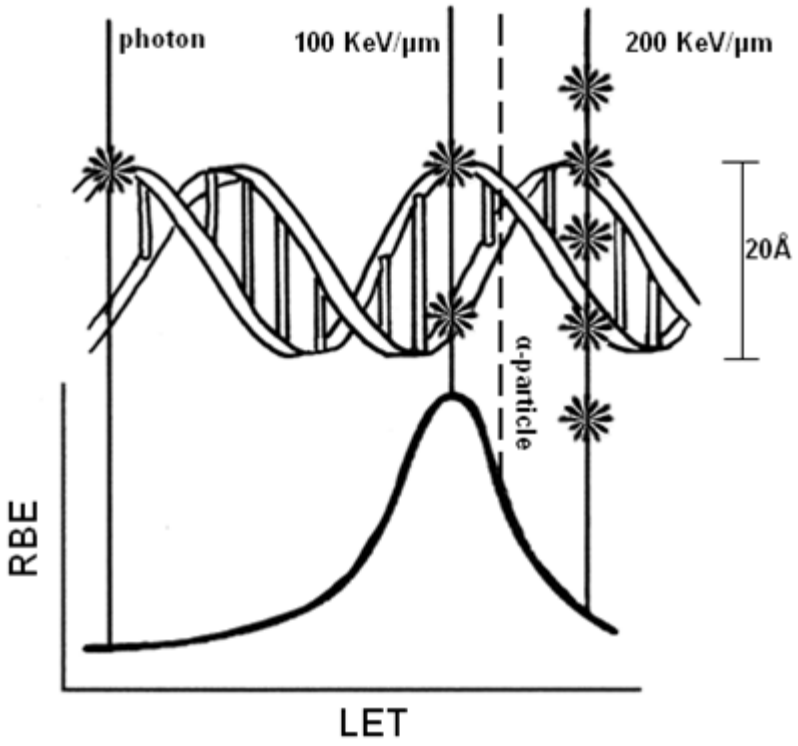

Figure 3: Schematic showing the relationship between increasing linear energy transfer and relative biological effect in the context of inducing DNA double strand breaks. Alpha-particle radiation is efficient at inducing such strand breakages relative to photon radiation, partially explaining the more pronounced and deleterious effects of high-LET radiation exposure. Adapted from Hall and Hei (2003).

7.4 Medical Symptoms of Radiation Exposure

7.4.1 Acute Radiation Syndrome

Exposure to acute doses of radiation can lead to acute radiation syndrome (ARS) or "radiation sickness", which effects most of the body's major systems, and is characterized by varied prodromal, latent and manifest periods (Waselenko, MacVittie et al. 2004). The prodromal phase usually occurs within the first 48 hours, but may become apparent up to 6 days post-irradiation. The latent phase is marked by improved symptoms and a short-term transient recovery. The manifest illness period may last for weeks after the initial on-set and transient recovery phases. As radiation is a genotoxic agent, systems with high rates of cellular turnover are especially vulnerable to ARS. One of the most sensitive biological systems to radiation exposure is the hematopoietic system. The hematopoietic system is responsible for maintenance of peripheral blood and immune cell homeostasis, and as such, produces approximately $4x10^{11}$ cells in an average adult human daily (Stewart, Akleyev et al. 2012). These are made in privileged areas of the body located within bone marrow and the thymus by stem- and progenitor-cells undergoing lineage commitment and differentiation (Ladi, Yin et al. 2006) (Scadden 2006). Data suggest that a lethal dose in 50% of the population 60 days post-exposure falls within the ranges of 3.3-4.5 Gy without medical intervention or 6-7 Gy with medical intervention (Guskova, Barabanova et al. 1988). Clinically relevant symptoms can be seen from 2-10 Gy (Stewart, Akleyev et al. 2012). Irradiated active hematopoietic progenitor cells have a compromised ability to divide after doses greater than 3 Gy, resulting in pancytopenia due to an inability to replenish peripheral cells (Hall and Giaccia 2005) (Harfouche and Martin 2010). There exists a sub-set of radio-resistant G_0 progenitor cells which may play an important role in hematopoietic recovery (Wagemaker 1995) (Fliedner, Graessle et al. 2012). Upon irradiation, humans display

severe lymphopenia within 24-48 hours and then display severe neutropenia and thrombocytopenia in a dose and dose-rate dependant manner (Dainiak and Sorba 1997). After irradiation, bone marrow displays hypoplasia or aplasia and this may be a permanent morphological effect at high doses (Fajardo 2005). In the context of radiation-induced immuno-compromisation or hindered coagulation, death generally occurs within 2-4 weeks post-irradiation via opportunistic infection or haemorrhaging. Medical intervention in this context can be beneficial, and is geared towards the protection and induction of hematopoietic stem cells so as to restore immune function and coagulation; survival requires haematological recovery (Singh, Ducey et al. 2012). The Strategic National Stockpile Radiation Working Group has assembled clinical guidelines for the treatment of ARS (Waselenko, MacVittie et al. 2004). It includes the recommendation of supportive care (antibiotics, antiemetics, antidiarrheals, fluids, nutrition etc.) and acute infection management. Ancillary supplementation with cytokines and the administration of granulocyte-colony stimulating factor (G-CSF), and especially granulocyte macrophage-colony stimulating factor (GM-CSF) have also been shown to positively modulate recovery and neutrophil immune function after irradiation (Liu, Jiang et al. 2008) (Heslet, Bay et al. 2012). Cytokine therapy should begin in suspected radiation exposure, as soon as declining haematological symptoms are present or dosimetry confirms exposure to a dose >3 Gy, as promptness has beneficial patient outcomes (Donnelly, Nemhauser et al. 2010) (Gourmelon, Benderitter et al. 2010). In the event of exposure to high (7-10 Gy) acute doses wherein the endemic stem-cell pool may not be capable of autologous recovery, stem-cell transplantation may be considered (Fliedner 2006). It has been documented in a lethally-exposed radiation worker that allogeneic stem-cell transplantation resulted in successful partial chimeric engraftment with gradual haematological recovery (Asano 2005). Unfortunately, without resolving underlying systemic organ and tissue damage, this patient still succumbed to opportunistic infection and non-haematological tissue failure. Given the

severity of wounds, the usual accompanying trauma and the minimal success rate treating ARS with haematological stem-cell treatment, there is no clear consensus on whether to employ such demanding procedures (Asano 2012). Even with extreme medical intervention there is a possibility of succumbing to ARS at high doses, and there is a need to optimize assets in a resource scarce triage environment.

7.4.2 Treatment of Internal Contamination

Alpha-particles have limiting penetrating power and are thus primarily an inhalation, ingestion or wound absorption concern. There exist several possible ways in which alpha-particles may hit blood cells without radioactive isotopes entering systemic circulation. As the distance from the epithelial lining of the lung to the capillary lumen is on the order of micrometers, it is possible that lymphocytes in the alveolar space, intraepithelial tissue, and the lung lymphatic vessels and pleura can be irradiated (Harley and Robbins 1992). Lymphocytes also co-locate with basal stem cells within the tracheobronchial epithelium, and at a mean distance of 27 micrometers from the mucosal surface, are within the range of being hit by an alpha-particle (Figure 4) (Harley and Robbins 2009). Almost 10% of the cells found in adult bronchial epithelial lining are likely to be lymphocytes (Mercer, Russell et al. 1994).

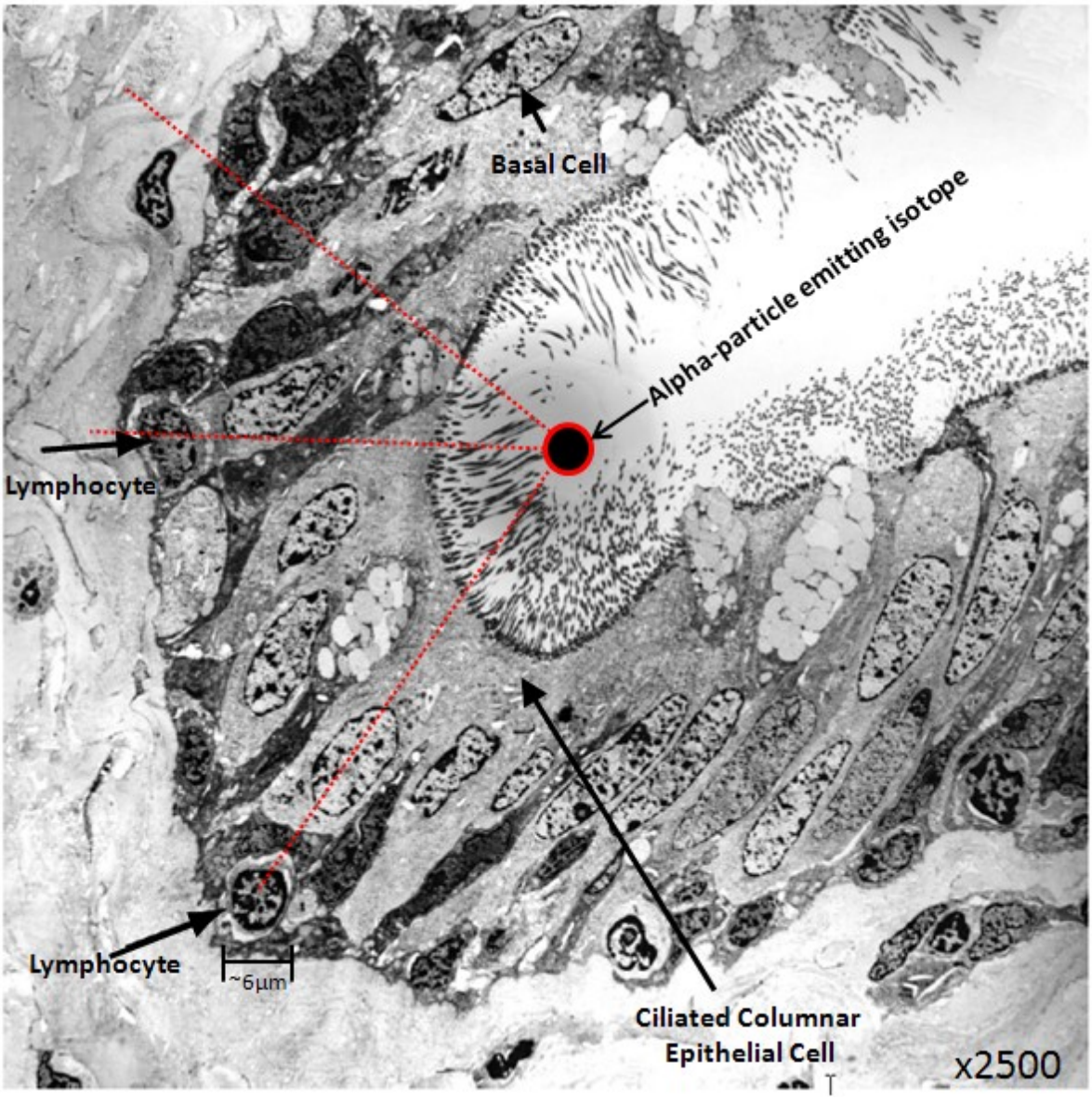

Figure 4: Human small bronchial epithelium magnified x2500. The bronchial tissue is composed of ciliated columnar epithelial cells, basal cells and lymphocytes (shown by arrows). Alpha-particle emitting isotopes can cause irradiation of lymphocytes without entering into systemic circulation when deposited on the epithelial lining via inhalation. Adapted from Harley and Robbins (1992).

If alpha-particle emitting isotopes come to rest on the lining of the lungs, the ICRP has recommended that the use of radionuclide specific bio-kinetic models be employed when there is sufficient data, but to otherwise adopt absorption type M parameters. These parameters equate to a moderate biological absorption (10% in 10 minutes and 90% over the course of 140 days) from the lung to blood (Eckerman, Harrison et al. 2012). The

National Council on Radiation Protection and Measurements (NCRP) has formed bio-kinetic absorption parameters for many isotopes of concern based on available case-reports (NCRP 2008). They conclude that previously listed alpha-particle emitting isotopes of concern (Americium, Plutonium, Radium and Polonium) generally follow type-M solubilisation rates, representing moderate solubility and thus causing blood exposure. This leads to additional treatment concerns as there is a need for a patient to undergo decorporation therapy, usually via the administration of a chelating agent, to remove the nuclide from the body (Wood, Sharp et al. 2000) (Cassatt, Kaminski et al. 2008). There are several parameters that should be considered before engaging in decorporation via chelation therapy (Menetrier, Grappin et al. 2005) as these agents do have the possibility of binding and altering mineral levels in the body.

7.4.3 Long Term Health Risks

There have been several critical atomic events in which many members of the public have become exposed to ionising radiation, but much of the data to date on radiation epidemiology has been founded on the long-term follow up of atomic bomb survivors (Sakata, Grant et al. 2012). The atomic bombings of Japan during World War 2 wrought devastation on an unprecedented scale, and to this day remain the only examples of nuclear detonation over civilian centres. As this was the first mass civilian exposure to ionising radiation, extraordinary effort went into documenting exposure histories, with surveys and contact of over 180,000 individuals (Ishida and Beebe 1959) and remains robust to this day with about 35,000 participants still enrolled (Ozasa, Grant et al. 2013). This mass-exposure has been the longest studied nuclear incident and has led to risk assessment for both acute and delayed radiation effects (Shigematsu 1998) (Stewart, Akleyev et al. 2012). It has been well documented in this cohort that radiation exposure can

lead to higher cancer incidence regardless of age at exposure and for a myriad of cancer types (Kodama, Ozasa et al. 2012). Thus, it is essential from a medical management perspective to know whether an individual has been exposed to radiation to both treat acute-radiation effects and ensure that the victim is enrolled in enhanced cancer screening programs throughout life.

7.5 Biodosimetry

Dosimetry is the ability to calculate a radiation dose, whereas biodosimetry is the ability to determine dosimetric estimations from biological materials. There are currently a number of methods for determining the radiation exposure status of an individual (Amundson, Bittner et al. 2001) (Ainsbury, Bakhanova et al. 2011). To date, many of these assays have been cytogenetic in nature (Lloyd, Edwards et al. 2000) (Pinto, Santos et al. 2010). Although many methods are technically possible, there are several key factors which must be considered in any given methodology of biodosimetry. There are logistical considerations such as the time and expertise required to perform an assay, the scalability or capacity for automation of an assay for the purposes of mass triage, minimal inter-person variation at baseline, the specificity of the response to ionizing radiation, and ideally a dose dependent relationship in an endpoint. One of the most difficult criteria to meet is the ability to discriminate between internal and external exposures as well as differentiate between radiation qualities and dose rates. As previously mentioned, the medical follow-up for internal and external contamination differ, as do the acute and delayed health effects of varying radiation quality and dose rate. Thus, these are important parameters to take into account when conducting biodosimetry assays.

Most current methods of biodosimetry involve the sampling of cells from the hematopoietic system, usually drawn from peripheral vein blood. This gives relatively easy access to some of the most radiation sensitive cells of the body, as well as allowing for the detection of systemic effects (Fliedner, Graessle et al. 2007). The intentional “gold standard” for biodosimetry is the dicentric assay (DCA) (Hoffmann and Schmitz-Feuerhake 1999) (Romm, Oestreicher et al. 2009). In addition to DCA, there is another cytogenetic technique known as the micronucleus analysis (Vral, Fenech et al. 2011), which has had some success in automation (Rossnerova, Spatova et al. 2011). The phosphorylation of histone H2AX is an indicator of DNA strand breaks, and as ionizing radiation is prone to causing DNA damage, DNA damage foci can be counted as a means of biodosimetry (Roch-Lefèvre, Mandina et al. 2010). In addition, there has been attempts to base biodosimetry on changes in gene expression (Paul and Amundson 2008), blood cell counts (Fliedner, Graessle et al. 2007), proteins (Marchetti, Coleman et al. 2006), enzyme activity (Rana, Kumar et al. 2010), miRNA (Jacob, Cooley et al. 2013), metabolites (Coy, Cheema et al. 2011) and multi-parameter approaches (Blakely, Ossetrova et al. 2010) (Fenech 2011). To date, there has been limited success in the ability to rapidly discriminate between exposure to alpha-particle radiation and photon radiation.

7.5.1 H2AX Phosphorylation

Atexia Telangiectasia Mutated (ATM) is a critical protein responsible for coordinating much of the DNA damage response, including p53 activation and responding to genotoxic stress (Shiloh 2003).Upon DNA DSB damage, one of the first cellular DNA damage responses is the phosphorylation of histone H2AX at serine 139 (Riches, Lynch et al. 2008) by ATM kinase (Burma, Chen et al. 2001). This was originally observed by the lab of Rogaku (Rogakou, Pilch et al. 1998). This phosphorylated variant of H2AX, known as gamma-

H2AX, appears within minutes and over a megabase range of DNA adjacent to the site of strand breakage (Rogakou, Boon et al. 1999) and is directly proportional to the amount of DNA damage (Sedelnikova, Rogakou et al. 2002). As such, it is extremely useful as a genotoxicity marker (Garcia-Canton, Anadón et al. 2012), with the appearance of discrete foci which can be measured via immunochemistry and flow cytometry (Sharma, Singh et al. 2012). Furthermore, it has been shown that gamma-H2AX intensity increases until reaching a plateau after 30 minutes (Paull, Rogakou et al. 2000), followed by a subsequent decrease in intensity over the course of hours as foci are resolved and DNA strands are repaired.

A study by Jenner et al. (1993) was one of the first to document LET dependant altered DNA repair kinetics, and subsequent studies have shown this can also be seen with the H2AX assay. Leatherbarrow et al. (2006) demonstrated that there is a difference in the repair kinetics of 1Gy gamma-ray and alpha-particle radiation as measured by foci resolution. The majority (~80%) of gamma-ray induced gamma-H2AX foci are resolved 2h post irradiation whereas only ~40% are resolved in the case of alpha-particle irradiations. Not only does increasing LET cause delays in repair kinetics, but the fidelity of repair is also affected. In a study by Khune et al. (2002), it was shown that the percentage of DNA DSBs which are mis-repaired is dose dependant for gamma-rays between doses of 5-80 Gy whereas alpha-particles had a consistently elevated mis-repair rate across the same doses. Furthermore, low, continuous doses of gamma-rays resulted in minimal mis-repair. This suggests that the spatial-temporal nature of strand breakages elicits distinct cellular effects and responses in terms of DNA repair, likely due to aforementioned strand break complexity. H2AX phosphorylation was measured in the current study as a biological control, serving as a DNA double strand break damage proxy-marker from exposure to the radiation sources.

7.5.2 Transcriptional Profiling and Gene Signatures

Development of biomarker-based biodosimetry have been put forth as one of the key priority development areas for nuclear threat countermeasures (Pellmar and Rockwell 2005) and microarray data / gene based profiling can serve as timely and minimally invasive procedures (Chaudhry 2008). Benefits of gene-expression based biodosimetry include the combinatorial co-expression of gene-signatures which can help grant specificity, and the natural binding chemistry of RNA allows for complimentary hybridization. This can be done using small blood volumes (Brengues, Paap et al. 2010), in the field (Huang, Paul et al. 2011) and can predict the exposure status of a person (Paul, Barker et al. 2011). There have been several studies examining the gene expression profiles of human cells using functional genomics platforms to create signatures of expression with utility in photon biodosimetry (Paul and Amundson 2008). In this study by Paul and Amundson (2009), total blood irradiation was performed on extracted whole blood from 5 donors to gamma-rays from a cobalt sources at doses of 0.5, 2, 5 and 8 Gy at a dose rate of 0.82 Gy/h. Both 6 and 24 hours post-exposure, RNA was extracted from the whole white blood cell population and hybridized using the Agilent platform. There were 338 significant, dose responsive genes identified 6h post exposure and 101 genes identified 24h post-exposure. Using multi-dimensional scaling, it was determined that there was a 74-gene consensus panel that could be used to predict exposure status over time. Some of these genes were validated using qPCR and validated in different sample sets and experimental set-ups. However, similar availability of gene tools for high LET radiation types, such as alpha-particles, remains far more limited.

To date, the majority of alpha-particle transcriptional studies have been performed in lung or fibroblast cells and several cancerous cell types (Ghandhi, Yaghoubian et al. 2008)

(Kalanxhi and Dahle 2012) (Chauhan, Howland et al. 2012a). There have also been few studies comparing the transcriptional effects of two radiation types in the same experimental set-up (Danielsson, Claesson et al. 2012) (Chauhan, Howland et al. 2012b). In a study by Danielsson et al. (2012), normal human fibroblasts were exposed to alpha-particles or gamma-rays for 1 hour at varying dose rates. Alpha-particle irradiations were performed using Astanine-211 conjugated antibodies at initial dose rates of 0.4, 0.83 and 1.7 cGy/min totalling a mean absorbed dose of 0.25, 0.5 and 1.0 Gy respectively. Gamma-irradiations were performed using a Cobalt-60 source at a dose rate of 1.6, 3.3 and 5 cGy/min totaling doses of 1, 2 and 3 Gy respectively. Global gene expression was assessed 5h post-irradiation using the Illumina bead chip platform and statistically significant gene modulations with a fold-change greater than 1.5 were included in analysis. Results were not validated via alternative technology. It was found that 548 (158 up-regulated and 390 down-regulated) dose-responsive genes were modulated in response to alpha-particle radiation and 414 (222 up-regulated and 192 down-regulated) in response to gamma-rays, with only 70 genes being found differentially modulated in both sets. Within these 70 genes, 15 showed opposite directionality in terms of expression between radiation types. Illumina platform microarray studies in our own lab using epidermal keratinocytes and alpha-particle and X-ray radiation in a dose and dose rate matched fashion also demonstrated transcriptional differences (Chauhan, Howland et al. 2012b). Using a dose rate of 0.98 Gy/h and doses of 0.5, 1.0 and 1.5 Gy it was shown that 24h post alpha-particle exposure, there were 5 dose-dependent genes and 67 differentially expressed transcripts at the highest dose. These dose-dependent genes were validated via qPCR. There were no differentially modulated genes identified by microarray post X-ray irradiation using stringent statistical analysis. Although there were relatively few genes identified as being modified in this study, there was a difference in expression between low and high LET radiation types. These two data sets lend credence to the hypothesis that cells activate different transcriptional

responses to high and low LET radiation, and that it is possible to distinguish between dose and radiation type via gene expression signatures. Though interesting, these studies are not useful for blood-based biodosimetry as work in our own lab group has shown the variety of responses which can be seen between different cell and radiation types as measured by protein modulation (Chauhan, Howland et al. 2012c), gene-expression (Chauhan, Howland et al. 2011) and miRNA regulation (Chauhan, Howland et al. 2012d).

There have been few studies examining transcriptional changes in blood cell types, but those that have been performed include transformed monocyte cultures (Chauhan and Howland 2012e) and isolated lymphocytes (Turtoi and Schneeweiss 2009) (Turtoi, Brown et al. 2010), though none of these studies compare the effects of alpha-particle and photon radiation in the same experimental set-up. In our lab's genomic profiling of cultured monocytes using the Illumina platform, cells were exposed to 0.5, 1.0 and 1.5 Gy of alpha-particle radiation and analysed both 24h and 72h post-exposure (Chauhan and Howland 2012e). Statistically significant genes displaying a fold-change greater than 1.5 fold were included for analysis. In order of increasing dose, there were 38,184, and 163 transcripts differentially expressed after 24h and 143, 152 and 190 transcripts after 72h. Furthermore, some of these genes displayed dose- and time- dependant up-regulated expression patterns. Thus, this experimental set-up demonstrated the plausibility in gauging alpha-particle exposure status while factoring in temporal parameters. Turtoi et al., (2010) are, thus far, the only group to examine the alpha-particle radiation induced genomic-wide transcriptional effects on an isolated normal white blood cell type. They employed the Agilent platform to analyse isolated lymphocytes exposed to 0.05, 0.1, 0.2, 0.4, 0.8 or 1.6 Gy of alpha-particle radiation. It is important to note that this study only performed microarray analysis on one individual and did only three technical-replicate microarrays, seriously compromising the usefulness of the work in terms of biomarker discovery, as there

is no account of biological variability. It was found that 338 genes were differentially modulated 1h post-exposure at one of the given doses. In an earlier study (2009), Turtoi conducted a similar experimental set-up with two donors and looked at gene expression via Taq-man qPCR (Turtoi and Schneeweiss 2009). Both of these Turtoi studies are extremely weak, especially as data useful for the purpose of biodosimetry, as there are insufficient biological replicates to conduct any meaningful biological statistical analysis. Furthermore, a 1-hour harvest point post-irradiation is an extremely short follow-up time in terms of triage. To date there have been no functional genomics scale studies examining the total white blood cell population response to alpha-particle radiation. Genomic technology allows the simultaneous evaluation of thousands of end-points whose combinatorial expression can serve as a suitable biomarker as well as granting subtle mechanistic insights into the cellular response. The work described in this thesis is the first transcriptomics work that examines a variety of doses and radiation types with a sufficient number of biological replicates (n=12 donors) 24h post irradiation so as to be applicable for triage.

The technology which will be employed to screen transcriptional modulations in this current study is the Illumina Universal Bead Array system (Fan, Gunderson et al. 2006). Conventional microarrays are synthesized by spotting probe sequences onto a two-dimensional array (Schena, Shalon et al. 1995), whereas the Illumina platform is manufactured by using a pool of beads randomly strewn into wells (Kuhn, Baker et al. 2004). This allows for an approximately 40,000-fold increase in probe density compared to conventional technology (Michael, Taylor et al. 1998). Each bead contains approximately 700,000 covalently attached oligonucleotide sequences, consisting of both a species-non-homologous address sequence and a complimentary gene sequence. The address sequence allows for dye-labelled oligonucleotide hybridization, which determines the probe location via a decoding algorithm (Gunderson, Kruglyak et al. 2004). This process results

with each bead/probe combination being replicated approximately 40 times per array (Barbosa-Morais, Dunning et al. 2010).

7.5.3 miRNA Profiling

In addition to mRNA profiling, there has been interest in using microRNA (miRNA) modulations as biomarkers of radiation exposure. miRNAs are short (<22 nucleotides) RNA sequences capable of modifying networks of transcriptional activity. They do so by joining a protein complex and binding with imperfect complementary to mRNA sequences (Lhakhang and Chaudhry 2012). Once bound, the mRNA can be targeted for degradation or prevented from undergoing translation (Sontheimer 2005). First discovered in 1993 (Wightman, Ha et al. 1993) and originally consigned solely to *C. Elegans*, there was renewed interested in miRNA when homologs were found in many species including humans (Pasquinelli, Reinhart et al. 2000). Since then, there has been extensive interest in miRNA profiling due to their ability to regulate gene networks (Ambros 2004). Due to their ability to regulate gene-networks and cell fate, miRNA profiling has been a recent focus of oncologists and many miRNA studies have been undertaken in the context of radiotherapy (Metheetrairut and Slack 2013). There have been efforts to use miRNA expression changes taken from blood as a biodosimetry tool (Jacob, Cooley et al. 2013), as miRNA are secreted via microvesicles and found in plasma (Hunter, Ismail et al. 2008). To date, there have been only two studies examining alpha-particle induced miRNA expression changes (Kovalchuk, Zemp et al. 2010) (Chauhan, Howland et al. 2012d). In a study by Kovalchuk and Zemp (2010), an airway model three-dimensional cell construct was irradiated at 1 dose (~5.4 Gy to the first layer of cells) and analysed either 8 h, 3, or 7 days post-irradiation. It was determined that 4, 6 and 2 miRNAs were significantly modulated at these time points respectively with all but one miRNA showing < 2 fold change. In our own laboratory's work,

three cell lines were examined (transformed monocyte, transformed epithelial lung cell and a normal human fibroblast) after doses of 0.5, 1.0 and 1.5 Gy of alpha-particle radiation (Chauhan, Howland et al. 2012d). miRNA profiling was performed 24 h post exposure and it was determined that at least 1 miRNA was differentially modulated at all three doses and there was no overlap in expression between cell lines. Select miRNA were validated via qPCR. Given the absence of overlap in miRNA expression profiles, it is important to derive data from the cell-type of interest. There have been no studies examining alpha-particle induced miRNA changes in whole white blood cell populations.

The technology which will be employed to screen miRNA transcriptional modulations in this current study is the NanoString nCounter system. The nCounter system is designed for detection or screening of up to 800 RNA targets, and does so using a novel digital detection system (Kulkarni 2011). This is done by using a pair of capture and reporter probes which bind to the RNA sequence of interest. The reporter probe carries a colour code at one end, which serves as a bar-code allowing for the identification of the target sequence. Each colour code is comprised of four non-spectrally overlapping colours in six positions, with each combination potentially identifying a different target sequence (Geiss, Bumgarner et al. 2008). This allows for direct hybridization of the probe pair, omitting the need for mRNA to cDNA conversion or cDNA amplification through PCR. The expression level of each gene is instead determined by the number of times the colour code sequence is counted. This is well suited to miRNA screening as the majority of well characterized miRNA sequences can be screened in one experiment, and the technology allows for quantification to a level of 1 transcript copy per cell.

7.5.4 Protein Profiling

There has been significant interest in the use of protein biomarkers for biodosimetry, and a thorough review on the subject has been conducted by Marchetti et al. (2006). In this review, the authors examined intracellular protein modulations and modifications from a variety of cellular sources, including *in-vivo and in-vitro* human and animal work, and applied a grading system to create a 20 protein consensus sequence that would theoretically be able to distinguish dose- and time- information from an exposure. The authors highlight that further studies are required to validate this model. In addition, intracellular proteins were examined which, for the purposes of biodosimetry, may not be detectable in systemic circulation. There have been comparatively fewer studies examining the effects of alpha-particle radiation on secreted proteins, especially in the blood. A study by Narayanan et al. (1999) showed that alpha-particles could induce expression of interleukin (IL)-8 in normal human lung fibroblasts at low (0.03-0.2 Gy) doses of alpha-particle radiation as quickly as 30 minutes post-irradiation. Results from our own laboratory (Chauhan, Howland et al. 2012c) have shown the modulated expression of secreted cytokine profiles from both transformed epithelial lung and transformed monocyte cultures. This study employed multiplexed analysis of 27 inflammatory cytokines from cells exposed to 1.5 Gy of alpha-particle and X-ray radiation at ~1 Gy/hr dose rate. Analysis resulted in differential expression of a number of cytokines, including similarities and differences between radiation types and between cell lines. This included dose-response validation of some targets via enzyme-linked immunosorbent assay (ELISA). This study showed that under matched dose and dose-rate exposure conditions, alpha-particles and X-rays induce differential cytokine expression, and that this response is cell-type specific. Further studies from our laboratory have also shown that alpha-particles and X-rays will induce similar and differential cytokine expression in normal epidermal keratinocytes (Chauhan, Howland et al. 2012b). This was shown over a four-day time-course at doses of 0, 0.5, 1.0 and 1.5 Gy of alpha-particle radiation using multiplexed cytokine analysis. Alpha-particle radiation has the

ability to induce cytokine secretion and these responses differ from photon radiation and could thus serve as a means of biodosimetry. In the current experimental set-up, multiplexed protein analysis was employed for the purposes of identifying possible protein biomarkers of alpha-particle radiation exposure.

7.5.5 Plasma Profiling and Clinical Chemistry

Plasma is one the most complex human proteomes, with protein and metabolite quantities extending over 12 orders of magnitude, containing subsets of other proteomes and leakages from tissues entering systemic circulations (Anderson and Anderson 2002). Clinical biochemistry is an important and common-place diagnostic factor for many diseased states, and valuable information can be derived from examining the plasma component of blood including protein levels and enzyme function (Marshall and Bangert 2008). There are two ways radiation can affect plasma proteins, either through direct ionisation of bonds in the protein structure or through the much more common (>99.9%) damage via free radical generation and intermediaries (Kempner 2001). As such, it is plausible that the proteins and metabolites in plasma may be degraded, damaged due to alpha-particle radiation as it delivers high localized energy. To date, no studies have examined the effects of alpha-particle radiation on isolated plasma and protein function. There was an interest in irradiating plasma, at kGy photon radiation doses, as a means of sterilization of blood-borne pathogens (Miekka, Busby et al. 1998), but this resulted in damage to plasma components (Hiemstra, Tersmette et al. 1991).

7.6 Rationale

Since the advent of the atomic age there have been nuclear escalations between states, attempts at development or acquisition of nuclear technologies by terrorist organizations, nuclear accidents as well as intentional nuclear poisonings. Given these circumstances, it is important that preparations are undertaken to ensure emergency preparedness planners and first responders have the necessary tools to effectively manage a radiological emergency. In the event of either a nuclear detonation or dispersal of radioactive materials, the ability to triage those who have been exposed to radiation is critical for effective casualty management, (Dumont, Roux et al. 2010) (Valentin 2005) and to reassure the public (Blakely, Salter et al. 2005). Although numerous methods have been put forth, there is no ideal biomarker that is yet able to meet all these triage needs (Alexander, Swartz et al. 2007).

A biomarker is defined by the Biomarkers Definitions Work Group as “A characteristic that is objectively measured and evaluated as an indicator of normal biological processes, pathogenic processes, or pharmacologic responses to a therapeutic intervention” (BDWG 2001). A good biomarker should be testable from a peripheral, non-invasive tissue, it should be quantifiable using affordable and robust technologies, and it should be as specific and quantifiable as possible to a given pathological state (NPG 2010). Blood has been highlighted as one of the most clinically useful tissues from which to derive minimally invasive biomarkers, especially gene-based profiling studies, which result in patterns of expression changes acting as gene signature (Frank and Hargreaves 2003). Thus, multiple biological endpoints were examined from blood-isolated leukocytes to potentially identify strong alpha-particle radiation specific biomarkers in the blood.

7.7 Hypothesis and Objective

It has been well documented that ionising radiation exposure can induce changes in a number of end-points that may be detectable in the form of DNA damage, clinical chemistry end points, cell counts, gene expression modulations at the mRNA and miRNA level as well as inter- and intra-cellular protein expression, but this has not been well studied using whole leukocyte populations exposed to alpha-particle radiation. Alpha-particle exposure, either through inhalation or absorption, will result in irradiation of leukocytes. Due to the differing dose deposition patterns between alpha-particle and X-ray radiation and previous studies showing modified chromosomal damage and DNA repair kinetics, it is possible that alpha-particle exposure may elicit distinct cellular effects from photon radiation. The goal of the present work is to build upon the foundation of genomics-based gene-signature expression developed for photon radiation and develop a comparable capacity for alpha-particle exposure. It is hypothesised that alpha-particle exposure will results in significant DNA damage, triggering transcriptional responses centered along cell-cycle arrest, DNA repair and apoptosis. Though there will be significant overlap with the gene networks induced by photon radiation, there may be subtle differences due to inequalities in energy deposition and cellular effects. Differences in either degree of modulation or a select few genes may be useful in distinguishing radiation type for the purposes of triage. Furthermore, even in the absence of differences, this work will confirm the suitability of gene-based triage for alpha-particles. By examining multiple end points and contrasting the effects elicited by the different radiation types, significant contributions have been made to alpha-particle radiation biodosimetry.

8 Methodology

8.1 Experimental Plan and Flow Chart

The experimental plan was broken into two stages, a preliminary phase examining fewer end points in *ex-vivo* isolated peripheral blood mononuclear cells and a more in-depth phase using *ex-vivo* isolated leukocytes after attaining positive results (Figure 5). The primary phase consisted of a transcriptomics screen and validation via qPCR. The follow-up experiments examined additional endpoints including complete blood cell counts, clinical chemistry markers, miRNa modulations, altered secretomic profiles, gamma-H2AX induction as well as gene modulations.

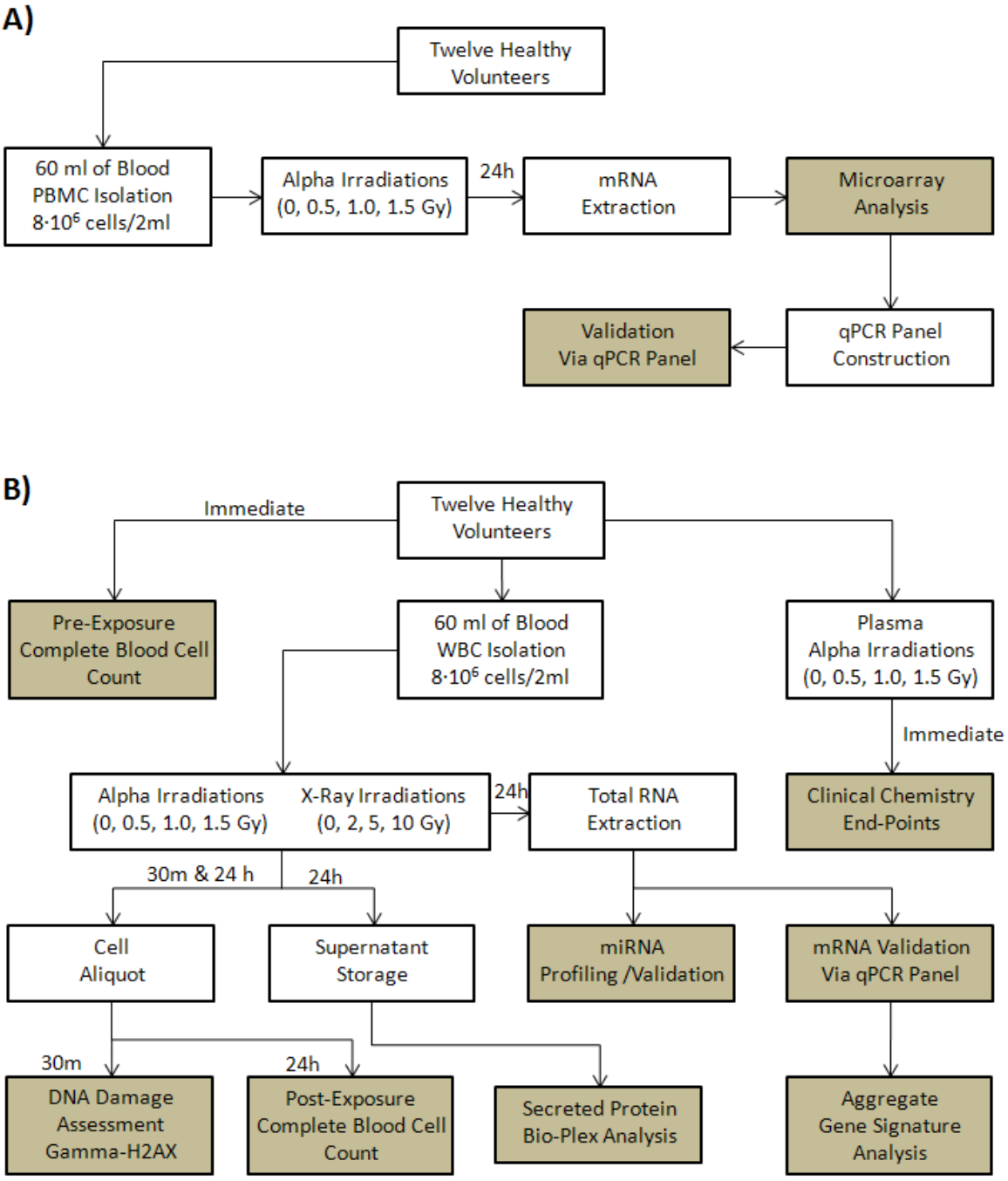

Figure 5: Flow chart demonstrating the experimental process, assays and endpoints (those yielding data are shaded) for the A) peripheral blood mononuclear cell and B) the white blood cell populations

8.2 Blood Draws

All procedures were approved by Health Canada's Research Ethics Committee. Peripheral blood from healthy, non-smoking volunteers was drawn via periphery venipuncture with informed consent from all subjects and was drawn into either 5 x 10 ml EDTA (for gene analysis) or 2 x 4 ml lithium heparin (for plasma analysis) vacutainer tubes (Becton Dickinson and Company, Franklin Lakes, NJ). A total of 6 male and 6 female donors participated. Before any further processing, a 100 µl whole blood sample was drawn to perform a complete blood count (CBC) via automatic haemocytometer (Beckman Coutler, Mississauga, ON).

8.3 Peripheral Blood Mononuclear Cells and White Blood Cells Isolation

Peripheral blood mononuclear cells (PBMCs) were employed as a representative cell-type for an initial global screening of gene transcripts using microarray technology. A similar isolation procedure was employed as described by Boyum (Boyum 1968). Briefly, a 15 ml of Histopaque-1077 sucrose gradient (Sigma-Aldrich, MO, USA) was pipetted into the upper chamber of an Accuspin Tube (Sigma-Aldrich). The tube was centrifuged (800 x g) for 30 seconds to ensure that the Histopaque was below the frit layer. Freshly drawn whole blood was pipetted into the upper chamber of tube. The tube was then centrifuged 800 x g for 15 minutes. The band of mononuclear cells was transferred to an alternate centrifuge tube and washed with 10 ml of isotonic phosphate buffered saline (PBS) three times. Pelleted cells were then resuspended in RPMI-1640 media supplemented with 10% fetal bovine serum (FBS), 2mM L-glutamine and 100U penicillin & 100µg streptomycin/ml.

8.4 Total White blood Cell Isolation

Following initial experiments on microarray analysis of PBMC, further validation studies using qPCR were conducted on the complete white blood cell (WBC) population. WBCs were isolated from whole blood using Histopaque-1119 (Sigma-Aldrich). Twenty-five milliliters of whole blood was gently poured over 15 ml of Histopaque-1119 and spun at 1000 x g for 10 minutes. This resulted in erythrocyte sedimentation below the Histopaque gradient and a total white blood cell population above the gradient. This volume (~15 ml) was then transferred to a new 50 ml falcon tube and diluted 1:2 with phosphate buffered saline (PBS). The resulting WBC pellet was then washed twice more with 10 ml PBS and resuspended in RPMI-1640 media supplemented with 10% FBS, 2mM L-glutamine and 100U penicillin&100µg streptomycin/ml.

8.5 PBMCs and WBC Irradiations

Either Isolated PBMCs or WBCs were seeded at total cell density of 8-10 $X10^6$ cells in 2ml of media and were cultured on thin Mylar based plastic dishes (MD) (Chemplex Industries, Palm City, FL, USA), which allowed for penetration of alpha-particles (Figure 6: Mylar dishes capable of being assembled within a sterile culture hood. A) The unassembled dish consisting of, from left to right, an outer sleeve, an inner sleeve and a pierced ventilated cap. B) A sheet of 2.5 µm Mylar held in white cardboard. C) An assembled MD placed upside down showing the Mylar stretched taunt across the bottom of the dish. D) MDs without caps assembled in a sterile culture hood placed on 60mm dishes to protect the Mylar during transit. Reproduced from Beaton, Burn et al. (2011)Figure 6).

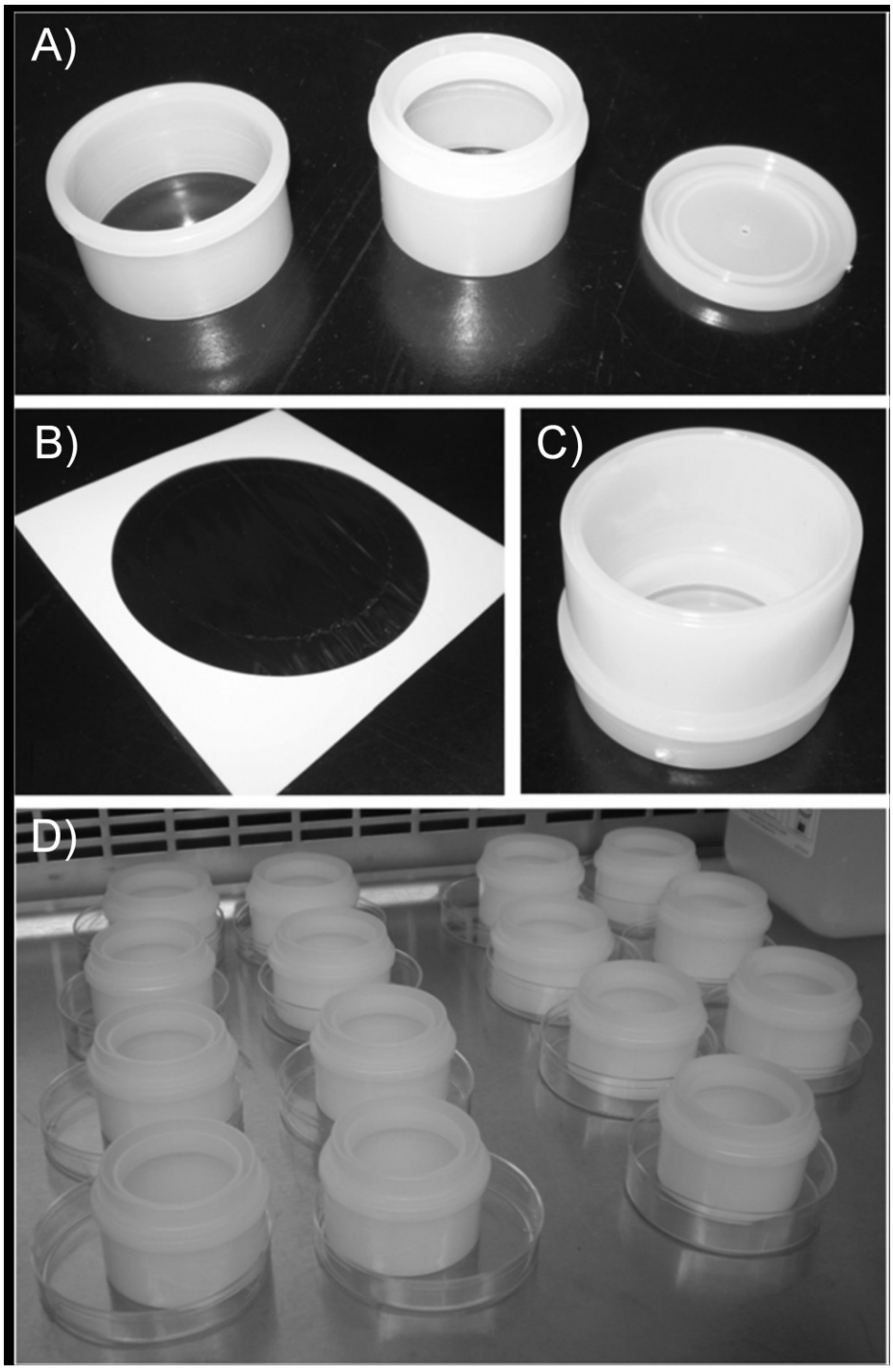

Figure 6: Mylar dishes capable of being assembled within a sterile culture hood. A) The unassembled dish consisting of, from left to right, an outer sleeve, an inner sleeve and a pierced ventilated cap. B) A sheet of 2.5 µm Mylar held in white cardboard. C) An assembled MD placed upside down showing the Mylar stretched taunt across the bottom of the dish. D) MDs without caps assembled in a sterile culture hood placed on 60mm dishes to protect the Mylar during transit. Reproduced from Beaton, Burn et al. (2011)

Cells were allowed to settle for 10 minutes before performing the irradiations. Irradiations were performed at doses of 0 (control), 0.5, 1.0 or 1.5 Gy using Americium (^{241}Am) electroplated discs with an activity level of 66.0 kBq ± 3% (dose rate of 0.98 ± 0.01 Gy/h, LET of 127.4±0.4 keV/µm) (Figure 7) (Figure 8).

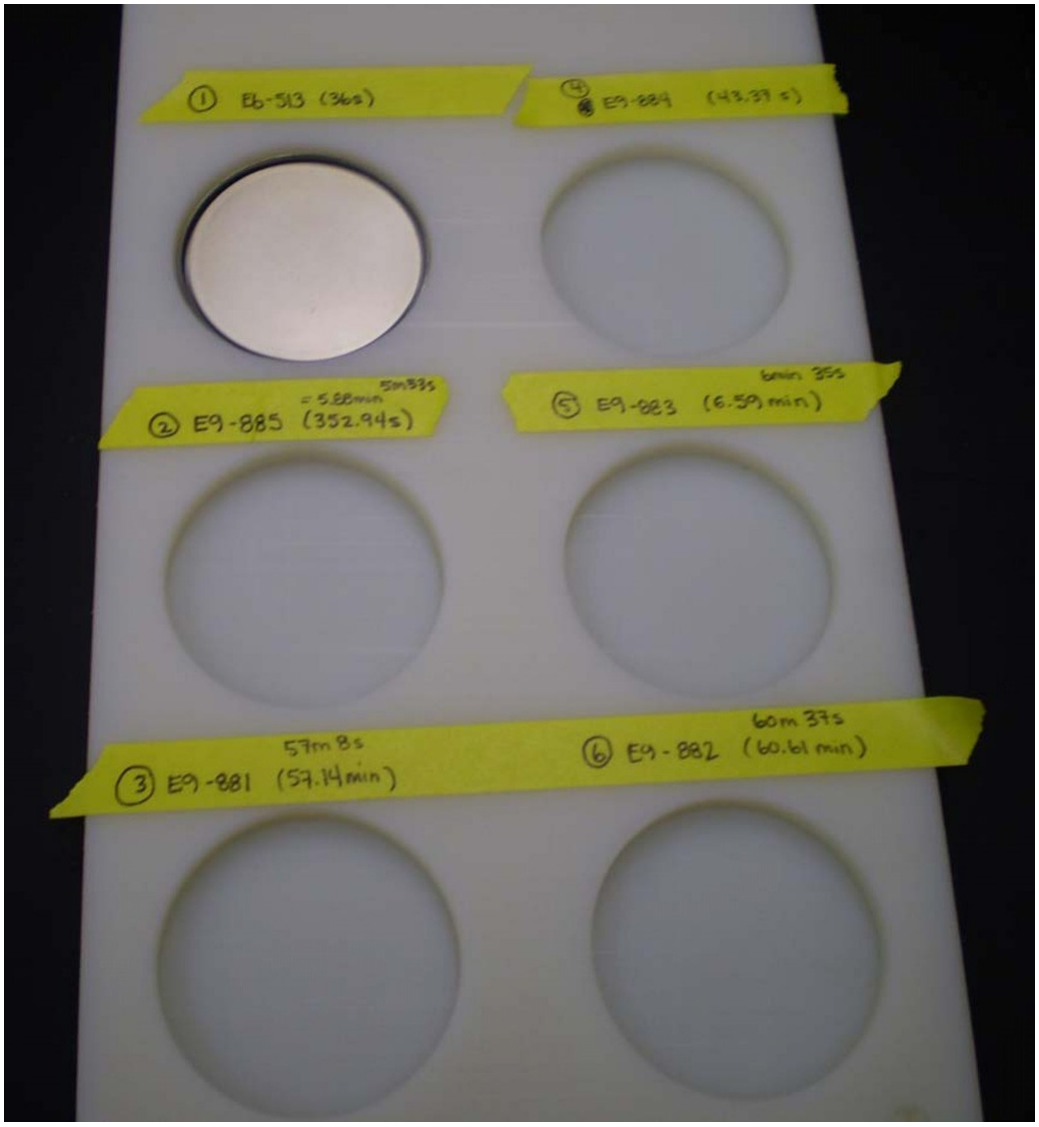

Figure 7 : Nylon holder meant to house Am-241 electroplated disks. Each of the 6 cut-outs measures 5.2 cm in diameter and is sunken 0.6 cm into the base. An Am-241 disk is place in the top left hole for demonstration purposes. Reproduced from Beaton, Burn et al. (2011)

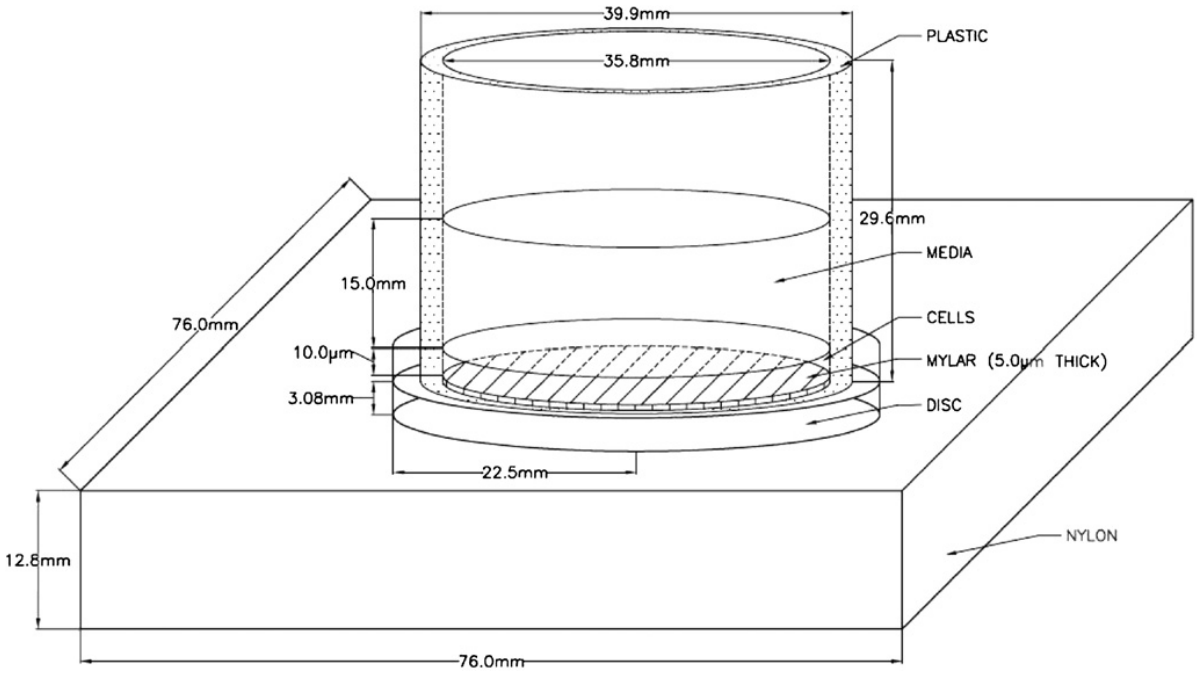

Figure 8 : Schematic of an MD containing cells and media sitting on an Am-241 source dish set inside the nylon holder. Reproduced from Beaton, Burn et al. (2011)

The absorbed dose of alpha-particle radiation to which the cells were exposed was calculated using the GEANT4 v.9.1 Monte Carlo tool-kit (Beaton, Burn et al. 2011). Cells destined for X-ray radiation at doses of 0 (control) 2, 5 or 10 Gy were exposed using the X-RAD 320 X-ray irradiation system (Precision X-ray, Inc., North Branford, CT, USA) at a high dose rate of 0.98 ± 0.05 Gy/min. Exposures were performed in duplicate and pooled. Thirty minutes post-exposure, 100 µl aliquots of cells were analysed for DNA damage response via H2AX phosphorylation assay. Twenty-four hours following irradiation, a 50 µl aliquot of cells was assessed for cellular viability using the Trypan Blue viability assay (Bio-Rad, Hercules, CA), and a 100 µl aliquot was used for a CBC via automatic haemocytometer. The remainder of the cells were spun down and the media frozen for protein analysis and the cell pellets destined for RNA extraction.

8.6 H2AX Phosphorylation Assay

H2AX phosphorylation was assessed using flow cytometry following a modified protocol by MacPhail et al. (MacPhail, Banath et al. 2003). Thirty minutes after exposure, cell suspensions (5×10^5 cells per sample) fixed with 10% formaldehyde (Fisher Scientific, USA) and incubated for 10 min at room temperature. The cells were then washed and re-suspended in 1 mL cold (−40 °C), 70% methanol (Fisher Scientific) in 1x PBS and stored at -40 °C overnight or up to two weeks. One mL of cold TBS (tris-phosphate buffered saline, 0.0154 M Trizma Hydrochloride (Sigma–Aldrich Canada), 0.5 M NaCl (Fisher Scientific), pH 7.4) was then added to each sample, mixed well, centrifuged (8 min, 400 × g, 4 °C) and re-suspended in 1 mL of cold TST (TBS serum triton, 96% TBS, 4% FBS (Sigma–Aldrich), 0.1% Triton X-100 (Sigma–Aldrich)). The samples were incubated on ice for 10 min, centrifuged (5 min, 400 × g, 4°C) and re-suspended in 200 µL of anti-gamma-H2AX-fluorescein isothiocyanate (FITC) antibody (Millipore, USA) diluted 1:500 in TST. After a 2 h incubation on ice in the dark, 1 mL of TBS with 2% FBS was added. The samples were then centrifuged (5 min, 400 × g, 4°C), re-suspended in 250 µL TBS with 2% FBS. Immediately prior to analysis by flow cytometry, 2 µL of 1 mg/mL propidium iodide (PI) was added to each sample. For flow cytometry analysis, data acquisition was set to analyze 2×10^4 cells from the whole cell population as identified by a forward scatter (FSC) vs. side scatter (SSC) dot plot. All debris under the FSC and SSC threshold were excluded from the analysis. The gamma-H2AX response was measured by assessing the increased level of intracellular fluorescence characterized in the cells, as determined by the geometric mean of the intensity peak of the anti-gamma-H2AX-FITC (channel number) of the gamma-H2AX positive cells. All samples were analyzed on a BD FACSCalibur flow cytometer (BD Biosciences, San Jose, CA, USA).

8.7 Plasma Irradiation and Clinical Chemistry Analysis

Blood drawn into lithium heparin containers was spun down at 1000 x g for 5 minutes and then the top layer consisting of plasma was removed for experimentation. Aliquots of 1 ml were placed on Mylar dishes for exposure and were irradiated at 0.0, 0.5, 1.0, 1.5 Gy of alpha-particle radiation. Samples were frozen after exposure and stored at -40°C before being processed next day. Plasma was analysed using the Piccolo Express Chemistry Analyser (Fisher Scientific, Ottawa, ON) for *in-vitro* diagnostics according to manufacturer's instructions.

8.8 Multiplexed Supernatant Immuno-Assays

Supernatants from exposed WBCs was collected and frozen at -40°C until processing. Samples supernatants were assayed for 22 proteins on 3 panels using an assortment of multiplexed immuno-assays prepared according to manufacturer's instructions (Millipore). This included a cardiovascular panel containing the proteins: a disintegrin and metalloproteinase with a thrombospondin type 1 motif, member 13 (ADAMTS13), D-Dimer, growth differentiation factor 15 (GDF-15), Lipocalin-2/ neutrophil gelatinase-associated lipocalin (LCN2/ NGAL), Myeloperoxidase (MPO), Myoglobin, P-selectin, Serum amyloid A (SAA), soluble intercellular Adhesion Molecule 1 (sICAM-1), Vascular cell adhesion protein 1 (sVCAM-1), an apoptosis panel containing Active Caspase 8 (Asp384), Active Caspase 9 (Asp315), Protein Kinase B (Akt (Ser473)), Bcl-2-associated death promoter (BAD (Ser112)), B-cell lymphoma 2 (Bcl-2 (Ser70)), c-Jun N-terminal kinases (JNK (Thr183/Tyr185)), tumor protein 53 (p53 (Ser46)), and an anti-oxidant panel containing Catalase, Peroxiredoxin-2 (PRDX2), Superoxide dismutase [Cu-Zn] (SOD1), Superoxide dismutase 2 (SOD2), Thioredoxin (TXN1). Briefly, conjugated beads were allowed to react with a sample containing a known (standard) or unknown amount of protein overnight at

4°C. Some kits did not contain standardized concentrations of proteins, necessitating the measurement of background-corrected fluorescence intensity (BFI). Conjugated beads with bound target were then washed and incubated with biotinylated detection antibodies that were directed against specific epitopes. The resulting complexes were then incubated further with streptavidin-phycoerythrin and excess reagent was washed off. Magnetic beads were suspended in assay buffer and analysed for bound cytokine using a Biorad luminex 200 instrument (Bio-Rad). Bio-Plex Manager v6.1 (BioRad) was used to construct optimized standard curves for the individual analytes and the concentration of proteins in the supernatants was then assessed from the generated standard curves for each protein. This data was then imported into Bio-Plex Data Pro software v1.1.0.05 (Bio-Rad) which allowed the data to be interpreted.

8.9 RNA extractions

Twenty-four hours post ionising radiation exposure or negative control conditions, RNA extractions were performed on either PBMCs or WBCs. In the case of PBMCs, the cells were resuspended in 350 µL of Buffer RLT containing 1% β-Mercaptoethanol (Qiagen's RNeasy Mini kit; Qiagen Inc, Mississauga, ON) then frozen at -80^{o}C until processed. Frozen lysates were thawed on ice and mixed well by pipetting. The lysate was transferred directly onto a QIAshredder spin column (Qiagen Inc), placed in a 2 mL collection tube and centrifuged for 2 min at ~12,000 g. A volume of 350 µL of 70% ethanol was added. Total RNA was then extracted using the RNeasy Mini kit according to the manufacturer's instructions (Qiagen Inc), with the addition of Qiagen's On-Column RNase-free DNase (Qiagen Inc) to eliminate any remaining DNA contamination. In the case of the WBCs, RNA extractions were performed using QIAzol reagent (Qiagen) and following manufacturer's instructions. Briefly, 700 µl of QIAzol reagent was added to the cell pellet and then

homogenized via up-and-down pipetting of the mixture 50 times. After room temperature incubation for 15 minutes, 140 µl of chloroform was added for phase separation. The aqueous layer containing RNA was then removed and precipitated with 100% ethanol. Total RNA was then isolated using the miRNeasy column purification kit. All total RNA sample concentrations and RNA quality were determined using both an Agilent 2100 Bioanalyzer and RNA Nanochips (Agilent Technologies Canada Inc., Mississauga, ON) and spectrophotometrically using a Nanodrop (Fisher Scientific, Ottawa, ON) (OD ratio of A260:A280). All extracted PBMC RNA samples were determined to be of good quality (RNA Integrity Number ≥ 7.7 except one sample – Annex I) with minimal degradation and stored at -80^{o}C until further analysis. WBC RNA from alpha-particle exposed samples were determined to be of good quality (RNA Integrity Number ≥ 9.2 – Annex II) with three samples being excluded from sample analysis due to insufficient RNA yield.

8.10 Genomic Profiling

An input of 200 ng of PBMC m RNA was used for whole genome analysis following the Illumina(r) Whole Genome Expression Profiling Assay Guide (11317302 Rev. A). Samples were hybridized on Illumina human-12 v2 RNA BeadChips. BeadChips were imaged and quantified with the Illumina iScan scanner and data was processed with Illumina GenomeStudio v2010.2.

8.11 miRNA Profiling

An input of 100 ng of WBC miRNA expression was profiled using the nCounter system (NanoString Technologies, Seattle, WA) which profiles the expression levels of 800 miRNAs. This was performed using the human miRNA expression assay (version 2) according to manufactures instructions and read using the nCounter digital analyser

8.12 Quantitative real time-polymerase chain reaction (qPCR) validation

Selected genes deemed significant by microarray analysis or nCounter system were further assessed by qPCR. Total RNA (400 ng mRNA 200 ng miRNA) isolated from cells were reverse transcribed into complementary DNA using the RT2 First Strand Kit (Qiagen). Gene profiling was performed according to the manufacturer's instructions using custom RT2-profiler PCR arrays (Qiagen). Reactions were prepared in 96-well plates and performed using a spectrofluorometric thermal cycler (Biorad iCycler; Hercules, CA). The relative expression of each gene was determined by using the comparative threshold (Ct) method (Schmittgen and Livak 2008). Analysis of qPCR expression profiles of data was performed using the super array biosciences web portal for data analysis of their products (SABiosciences http://www.sabiosciences.com/pcr/arrayanalysis.php).

8.13 Pathway Analysis

Significantly expressed genes at the high (1.5 Gy) dose of alpha-particle radiation were further explored by assessing their interactivity in terms of pathways, functions and networks. Gene lists were uploaded into Ingenuity Pathway Analysis (IPA) software, version 11904312 with corresponding fold change data. Analysis was performed using Ingenuity Expert Information core analysis. Functional Analysis identified the biological functions and/or diseases that were most significant to the given gene list. Canonical pathways analysis identified the pathways from the IPA library of canonical pathways that were most significant to the gene list. The significance of the association between the gene list and the canonical pathway was measured in two ways. Firstly, a ratio of the number of molecules from the gene list that map to the pathway divided by the total number of molecules that map to the canonical pathway and secondly, a Fisher's exact test was used to calculate a

p-value determining the probability that the association between the genes in the list and the canonical pathway is explained by chance alone. Networks were constructed to demonstrate the interactivity and molecular relationships between induced genes. Molecules are represented as nodes, and the biological relationship between two nodes is represented as an edge (line). All edges are supported by at least one reference from literature, or from canonical information stored in the Ingenuity Knowledge Base.

8.14 Customized Gene Array Panel

A total of 96 genes were used for the development of a customized 384 well format gene array panel (Figure 9). This panel was comprised of genes that were shown by microarray technology to be dose-responsive and also expressed at the medium and high dose. This panel also included negative control genes, housekeeping gene and some genes derived from the work of Paul and Amundson (Paul and Amundson 2008). SABiosciences (Qiagen) designed the primers and provided a 384 well-format platform that was compatible for use on the LightCycler 480 real-time PCR system (Roche, Mississauga, ON). A high-throughput PCR platform, comprising the Caliper Zephyr Compact Liquid Handling Station, the Caliper Twister II plate handler (PerkinElmer , Woodbridge, ON) and the Lightcycler 480 was employed with custom protocols developed in the Inhalation Toxicology Laboratory of Health Canada. This system allowed for the screening of 144 samples in a one-week time-span.

	1	2	3	4	5	6	7	8	9	10	11	12	13	14	15	16	17	18	19	20	21	22	23	24
A	ACTA2 1	ACTA2 1	AEN 2	AEN 2	ANKRA2 3	ANKRA2 3	ANXA4 4	ANXA4 4	APOBEC3H 5	APOBEC3H 5	ARHGEF3 6	ARHGEF3 6	ASCC3 7	ASCC3 7	ASTN2 8	ASTN2 8	BAX 9	BAX 9	BBC3 10	BBC3 10	BTG3 11	BTG3 11	CCDC90B 12	CCDC90B 12
B	ACTA2 1	ACTA2 1	AEN 2	AEN 2	ANKRA2 3	ANKRA2 3	ANXA4 4	ANXA4 4	APOBEC3H 5	APOBEC3H 5	ARHGEF3 6	ARHGEF3 6	ASCC3 7	ASCC3 7	ASTN2 8	ASTN2 8	BAX 9	BAX 9	BBC3 10	BBC3 10	BTG3 11	BTG3 11	CCDC90B 12	CCDC90B 12
C	CCNG1 13	CCNG1 13	CD70 14	CD70 14	CDKN1A 15	CDKN1A 15	CMBL 16	CMBL 16	DCP1B 17	DCP1B 17	DDB2 18	DDB2 18	DRAM1 19	DRAM1 19	E2F7 20	E2F7 20	EDA2R 21	EDA2R 21	EI24 22	EI24 22	FAM127B 23	FAM127B 23	FAM20B 24	FAM20B 24
D	CCNG1 13	CCNG1 13	CD70 14	CD70 14	CDKN1A 15	CDKN1A 15	CMBL 16	CMBL 16	DCP1B 17	DCP1B 17	DDB2 18	DDB2 18	DRAM1 19	DRAM1 19	E2F7 20	E2F7 20	EDA2R 21	EDA2R 21	EI24 22	EI24 22	FAM127B 23	FAM127B 23	FAM20B 24	FAM20B 24
E	FAS 25	FAS 25	FBXO22 26	FBXO22 26	FDXR 27	FDXR 27	FHL2 28	FHL2 28	GADD45A 29	GADD45A 29	GDF15 30	GDF15 30	GLS2 31	GLS2 31	GNG7 32	GNG7 32	GSS 33	GSS 33	HIST1H4B 34	HIST1H4B 34	IER5 35	IER5 35	IGFBP4 36	IGFBP4 36
F	FAS 25	FAS 25	FBXO22 26	FBXO22 26	FDXR 27	FDXR 27	FHL2 28	FHL2 28	GADD45A 29	GADD45A 29	GDF15 30	GDF15 30	GLS2 31	GLS2 31	GNG7 32	GNG7 32	GSS 33	GSS 33	HIST1H4B 34	HIST1H4B 34	IER5 35	IER5 35	IGFBP4 36	IGFBP4 36
G	IL21R 37	IL21R 37	ISCU 38	ISCU 38	ISG20 39	ISG20 39	AEN 40	AEN 40	LAMC3 41	LAMC3 41	LIG1 42	LIG1 42	LY9 43	LY9 43	MAMDC4 44	MAMDC4 44	MAP4K4 45	MAP4K4 45	MDM2 46	MDM2 46	METTL7A 47	METTL7A 47	METTL7A 48	METTL7A 48
H	IL21R 37	IL21R 37	ISCU 38	ISCU 38	ISG20 39	ISG20 39	AEN 40	AEN 40	LAMC3 41	LAMC3 41	LIG1 42	LIG1 42	LY9 43	LY9 43	MAMDC4 44	MAMDC4 44	MAP4K4 45	MAP4K4 45	MDM2 46	MDM2 46	METTL7A 47	METTL7A 47	METTL7A 48	METTL7A 48
I	MYC 49	MYC 49	NUDT15 50	NUDT15 50	PCNA 51	PCNA 51	PCNXL2 52	PCNXL2 52	PHLDA3 53	PHLDA3 53	PHPT1 54	PHPT1 54	PLK2 55	PLK2 55	PLK3 56	PLK3 56	POLH 57	POLH 57	PPM1D 58	PPM1D 58	PRKAB1 59	PRKAB1 59	PTP4A1 60	PTP4A1 60
J	MYC 49	MYC 49	NUDT15 50	NUDT15 50	PCNA 51	PCNA 51	PCNXL2 52	PCNXL2 52	PHLDA3 53	PHLDA3 53	PHPT1 54	PHPT1 54	PLK2 55	PLK2 55	PLK3 56	PLK3 56	POLH 57	POLH 57	PPM1D 58	PPM1D 58	PRKAB1 59	PRKAB1 59	PTP4A1 60	PTP4A1 60
K	PVT1 61	PVT1 61	RASGRP2 62	RASGRP2 62	RetSat 63	RetSat 63	RPS27L 64	RPS27L 64	SAC3D1 65	SAC3D1 65	SESN1 66	SESN1 66	SLC4A11 67	SLC4A11 67	SLC4A11 68	SLC4A11 68	SLC7A6 69	SLC7A6 69	TCF3 70	TCF3 70	TMEM30A 71	TMEM30A 71	TMPRSS7 72	TMPRSS7 72
L	PVT1 61	PVT1 61	RASGRP2 62	RASGRP2 62	RetSat 63	RetSat 63	RPS27L 64	RPS27L 64	SAC3D1 65	SAC3D1 65	SESN1 66	SESN1 66	SLC4A11 67	SLC4A11 67	SLC4A11 68	SLC4A11 68	SLC7A6 69	SLC7A6 69	TCF3 70	TCF3 70	TMEM30A 71	TMEM30A 71	TMPRSS7 72	TMPRSS7 72
M	TNFRSF10B 73	TNFRSF10B 73	TNFRSF10D 74	TNFRSF10D 74	TNFSF4 75	TNFSF4 75	TNFSF8 76	TNFSF8 76	TOB1 77	TOB1 77	TP53 78	TP53 78	TP53TG1 79	TP53TG1 79	TP53INP1 80	TP53INP1 80	TP53TG1 81	TP53TG1 81	TRIAP1 82	TRIAP1 82	TRIM22 83	TRIM22 83	TRIM32 84	TRIM32 84
N	TNFRSF10B 73	TNFRSF10B 73	TNFRSF10D 74	TNFRSF10D 74	TNFSF4 75	TNFSF4 75	TNFSF8 76	TNFSF8 76	TOB1 77	TOB1 77	TP53 78	TP53 78	TP53TG1 79	TP53TG1 79	TP53INP1 80	TP53INP1 80	TP53TG1 81	TP53TG1 81	TRIAP1 82	TRIAP1 82	TRIM22 83	TRIM22 83	TRIM32 84	TRIM32 84
O	UROD 85	UROD 85	VWCE 86	VWCE 86	XPC 87	XPC 87	ZNF337 88	ZNF337 88	ZNF79 89	ZNF79 89	ACTB 90	ACTB 90	GAPDH 91	GAPDH 91	GUSB 92	GUSB 92	B2M 93	B2M 93	HGDC 94	HGDC 94	RTC 95	RTC 95	PPC 96	PPC 96
P	UROD 85	UROD 85	VWCE 86	VWCE 86	XPC 87	XPC 87	ZNF337 88	ZNF337 88	ZNF79 89	ZNF79 89	ACTB 90	ACTB 90	GAPDH 91	GAPDH 91	GUSB 92	GUSB 92	B2M 93	B2M 93	HGDC 94	HGDC 94	RTC 95	RTC 95	PPC 96	PPC 96

Figure 9: Schematic representation of the 384-well gene array that was developed for use in high-throughput qPCR validation and screening

8.15 Statistical analysis

Microarrays statistical analysis was performed as follows. Data background correction was done within GenomeStudio (Illumina), and then exported to the lumi R package (Du, Kibbe et al. 2008). Data was then normalized via quantile method, rendering the distribution of probe intensities of each array in a set of arrays equivalent (Bolstad, Irizarry et al. 2003). Normalized data was then log2 transformed for statistical comparisons. Linear models for microarray data (LIMMA) was employed to identify differentially expressed gene signatures between the different exposure conditions (Smyth 2004) (Smyth 2005). In brief, this method involves fitting a linear model for each gene in the data and moderating the standard error via an empirical Bayes method. An empirical Bayes method is a procedure which estimates the distribution of data without the prior specifications a full Bayesian analysis would require (Efron and Tibshirani 2002). This is used to estimate the moderated t-statistics/F-statistics for each gene, shrinking the standard error towards a common value. This test is similar to an ANOVA for each gene with the exception that standard deviations are moderated across genes, allowing more stable inference for each gene. Moderated standard deviations are a compromise between individual gene-wise standard deviations and overall pooled standard deviations. Multiple comparison false discovery rate (FDR) was evaluated using the Benjamini-Hochberg (BH) method (Benjamini and Hochberg 1995).

Statistical analysis for clinical chemistry endpoints, gamma-H2AX and WBC population sub-sets were conducted using a standard ANOVA with a Dunnett's post-test (Dunnett 1955) to account for multiple testing. This was done using GraphPad InStat version 3.00 (Graphpad.com). Though these end-points could be treated as repeated measures, it was decided that statistical stringency was more important for biomarker discovery than statistical power. Mulitplexed supernatant data was flagged as being significant within the

Data-Pro software via ANOVA analysis but without accounting for multiple comparisons. Data that was identified as significant was imported into the GraphPad software to conduct ANOVA tests with a Dunnett's post-test. PBMC qPCR data was analysed for statistical significance without multiple correction comparison using gene-wise ANOVA as there was *a-priori* reason for gene analysis. WBC qPCR data and nCounter data was analysed for statistical significance via LIMMA as described above.

8.16 Hierarchical Clustering and Principal Component Analysis

Hierarchical clustering was performed using the WBC qPCR data using dChip (http://www.hsph.harvard.edu/cli/complab/dchip). This software was used to cluster the different exposure conditions by gene signature and group genes by similarity of expression patterns. The distance between genes is measured as 1- r (Pearson correlation coefficient). Principal component analysis (PCA) was performed using the pca function in labdsv R package (http://cran.r-project.org/web/packages/labdsv/index.html) and, data was confined to a projectable 3-dimensinonal PCA.

9 Results

9.1 Clinical Chemistry End-Points of Exposed Human Plasma

Clinical chemistry markers were assessed from irradiated plasma post-irradiation. Table 1 provides a representative table of typical values that were obtained from the *ex-vivo* irradiation of plasma with alpha-particles from each of the individuals (all results can be found in Appendix – VI). Overall no significant effects, as determined by ANOVA, were observed in each of the tested clinical biomarkers post-irradiation.

Table 1: A typical representation of clinical chemistry biomarkers from plasma obtained from healthy individuals. Plasma was ex-vivo irradiated with alpha-particles (0-1.5 Gy) and assessed for changes in various metabolites and enzyme activities following irradiation.

Analyte	0 Gy	0.5 Gy	1.0 Gy	1.5 Gy
Alanine Aminotransferase (ALT) U/L	30	27	30	27
Albumin (ALB) g/dL	4	4	3.9	4
Alkaline Phosphatase (ALP) U/L	39	32	33	37
Amylase (AMY) U/L	46	43	43	45
Aspartate Aminotransferase (AST) U/L	44	41	39	42
Blood Urea Nitrogen (BUN) mg/dL	18	19	18	18
Calcium (CA) mg/dL	9.6	9.8	9.6	9.6
Chloride (CL-) mmol/L	101	103	100	100
C-Reactive Protein (CRP) mg/L	< 5.0	< 5.0	< 5.0	< 5.0
Creatinine (CRE) mg/dL	1.1	1.1	1.1	1.2
Direct Bilirubin (DBIL) mg/dL	0.3	0.2	0.2	0.2
Gamma Glutamyltransferase (GGT) U/L	28	26	26	28
Glucose (GLU) mg/dL	108	110	106	106
High Density Lipoprotein mg/dL	68	68	66	64
Low Density Lipoprotein mg/dL	172	164	170	167
Potassium (K+) mmol/L	4.5	4.6	4.5	4.4
Sodium (NA+) mmol/L	134	138	133	134
Total Bilirubin (TBIL) mg/dL	0.8	0.8	0.7	0.7
Total Carbon Dioxide (tCO2) mmol/L	29	29	31	30
Total Cholesterol (CHOL) mg/dL	280	272	276	270
Total Protein (TP) g/dL	7.3	7.2	7	7.1
TRIG mg/dL	203	198	203	194
Uric Acid (UA) mg/dL	4	4.1	4.1	4.1
VLDL mg/dL	41	40	41	39

9.2 Complete Blood Count

Isolated WBC's from whole blood was analyzed for cell type, cell number and viability post-exposure (Table 2) Total white blood cell counts were typically in the range of 5-10 x 10^6 cells/mL. The viability of the cells was assessed using the Trypan Blue Viability Assay pre- and post-irradiation. The cells remained viable (above 98%) and no significant changes in blood cell counts or populations subsets, as assessed by ANOVA, were observed post-irradiation relative to un-irradiated cells. There was a relative enrichment of lymphocytes relative to neutrophils in isolated cells compared to whole blood due to the isolation procedure.

Table 2: A typical representation of complete blood counts from isolated white blood cells obtained from healthy individuals pre- and post-exposure.

Exposure Condition (Gy)	Viability (%)	WBC Total (cell/ml X10^6)	Neutrophils (% indicates the relative contribution of each cell-type to the total count)	Lymphocytes	Monocytes	Eosonophils	Basophils
Pre-Exposure							
Control	99.0	5.2	3.43(66.3%)	0.96 (18.6%)	0.52 (10.1%)	0.24 (4.7%)	0.02 (0.3%)
Post-Exposoure							
Alpha 0.0	98.0	4.0	1.78 (45%)	1.86 (47.1%)	0.26 (6.7%)	0.04 (1.1%)	0.00 (0.1%)
Alpha 0.5	99.0	3.8	1.69 (44.4%)	1.86 (48.9%)	0.22 (5.9%)	0.02 (0.6%)	0.01 (0.2%)
Alpha 1.0	99.0	3.8	1.73 (45.1%	1.86 (48.4%)	0.2 (5.3%)	0.04 (1.0%)	0.01 (0.2%)
Alpha 1.5	99.0	3.7	1.69 (48%)	1.76 (48%)	0.19 (5.1%)	0.03 (0.8%)	0.00 (0.00%)
X-Ray 0.0	99.0	3.8	1.76 (45.8%)	1.88 (48.9%)	0.17 (4.4%)	0.03 (0.8%)	0.00 (0.1%)
X-Ray 2.0	99.0	3.8	1.74 (46.3%)	1.82 (48.4%)	0.16 (4.2%)	0.03 (0.9%)	0.01 (0.2%)
X-Ray 5.0	99.0	3.7	1.70 (46%)	1.80 (48.9%)	0.13 (3.6%)	0.05 (1.4%)	0.00 (0.1%)
X-Ray 10.0	99.0	4.0	1.85 (45.7%)	2.03 (50.4%)	0.11 (2.8%)	0.04 (1.0%)	0.00 (0.1%)

9.3 DNA Double Strand Breaks

Thirty minutes post-exposure, cells were assessed for the expression of gamma-H2AX, a marker indicative of DNA double strand breaks. A dose-dependent increase in the gamma-H2AX signal was observed following exposure to alpha-particle radiation as seen by the pronounced shift in the curve and a plot of the geometric mean of this signal as a function of dose (Figure 10). Statistically significant responses, as determined by ANOVA, were obtained at the medium and high doses of alpha-particle radiation tested ($p<0.01$) relative to the non-irradiated control treatment group. A bi-modal shaped curve was observed at the lowest dose of alpha-particle radiation and becomes mono-modal with increasing dose. At the highest dose (1.5 Gy) an approximate 3-fold increase in gamma-H2AX signal was observed relative to the control sample. As a positive control, isolated leukocytes were irradiated with X-rays at a high dose rate (1 Gy/min) and a dose range of 2-10 Gy. A plot of this response indicated X-rays to be significantly more damaging as seen by the marked increase in gamma-H2AX signal with dose of radiation relative to alpha-particle treated cells. Alpha-particle irradiated cells displayed less gamma-H2AX expression relative to the X-ray irradiated cells.

9.4 Multiplexed Antibody Supernatant Analysis

Supernatants from control (0 Gy unirradiated) and exposed (0.5, 1.0 and 1.5 Gy alpha-particle and 2, 5, 10 Gy X-rays) were analyzed for the expression of 22 proteins. Analysis was performed using a variety of multiplex suspension arrays assay according to the manufacturer's instructions (Milipore). Results are summarized in Table 3 and proteins found to be statistically significant are depicted in Figure 11.

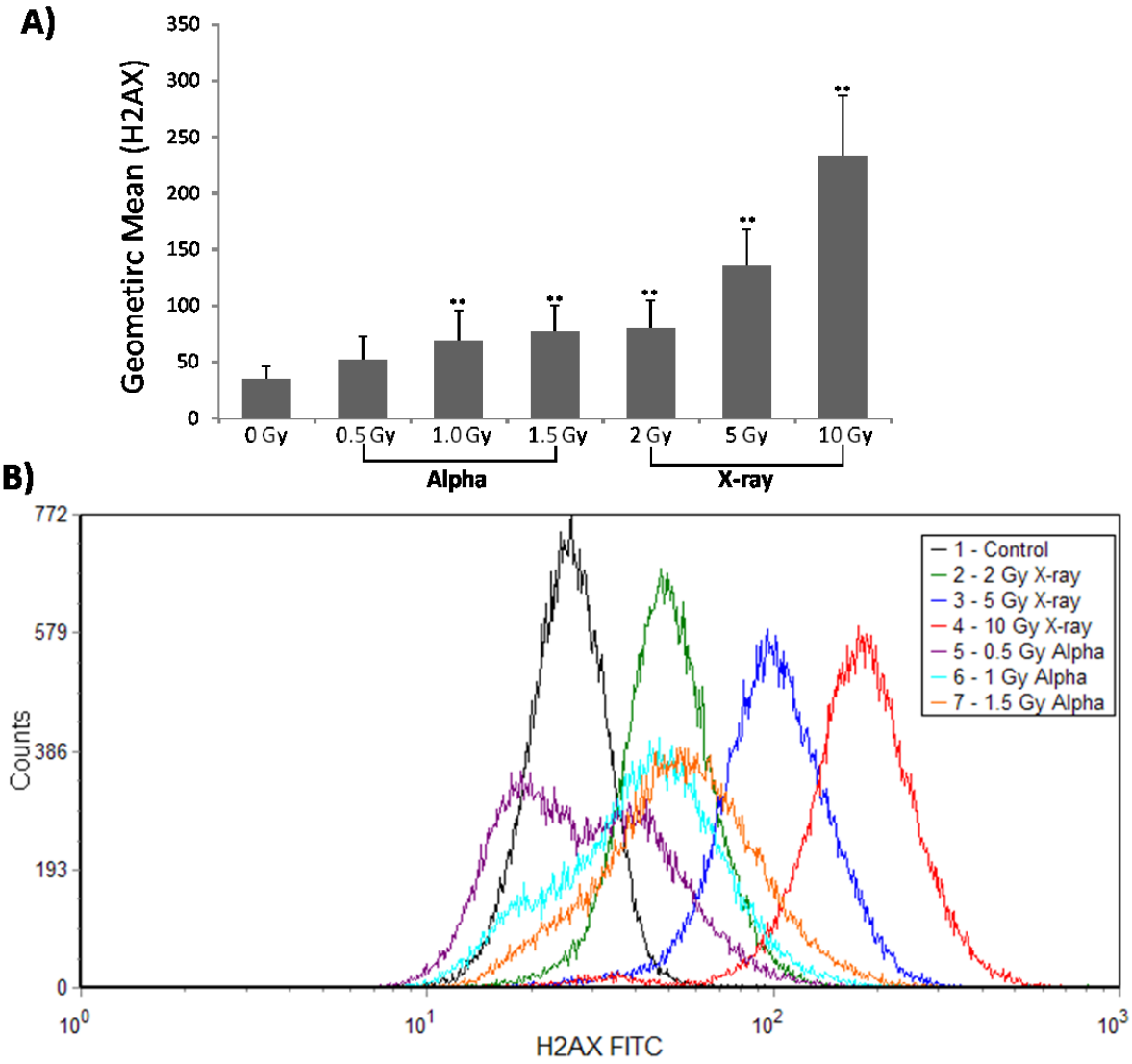

*Figure 10: WBC H2AX phosphorylation expression after exposure to alpha-particle or X-ray radiation. A) Geometric mean of signal intensity (indicative of gamma-H2AX expression) for each of the doses and radiation types. Data is presented as means ± SD with n= 12 biological replicates. ** represents p<0.01 B) Representative flow cytometric histogram overlay of gamma-H2AX expression in WBC cells at various doses of alpha-particle and X-ray exposure measured 30 min post-exposure.*

Table 3: Tabulated results for the various multiplex immune-assay panels examining the supernatants of WBCs exposed to alpha-particle or X-ray radiation. Data is presented as either concentration (ng/ml) or background-corrected fluorescence intensity (BFI) ± standard deviation (SD).

Radiation Type	Alpha								X-Ray							
Dose (Gy)	0		0.5		1		1.5		0		2		5		10	
Protein	Value	SD	Value	SD	Value	SD	Value	SD	Value	SD	Value	SD	Value	SD	Value	SD
Cardiovascular Disease																
ADAMTS13 (ng/ml)	8.86	3.81	7.81	3.45	7.47	3.15	7.04	2.77	7.93	3.32	15.36	23.09	8.16	2.95	8.02	3.36
D-Dimer (ng/ml)	217	84	174	92	173	81	188	127	187	316	258	299	246	314	208	185
GDF-15 (ng/ml)	0.0097	0.0045	0.0130	0.0057	0.0180	0.0089	0.0187	0.0093	0.0065	0.0026	0.0226	0.0319	0.0175	0.0117	0.0251	0.0191
Lipocalin-2/NGAL (ng/ml)	15.6	3.8	16.5	4.4	15.2	3.4	14.2	3.1	17.4	8.0	16.8	2.2	15.9	4.0	17.3	7.8
MPO (ng/ml)	73.6	19.8	62.3	22.8	56.6	21.9	53.5	17.7	67.3	37.9	64.6	20.6	64.8	24.2	73.0	36.4
Myoglobin (ng/ml)	0.169	0.182	0.136	0.157	0.149	0.155	0.145	0.151	0.109	0.065	0.190	0.200	0.138	0.129	0.139	0.146
P-Selectin (ng/ml)	74.8	17.2	55.2	29.7	58.3	16.6	60.6	17.7	43.6	17.0	71.3	21.6	58.7	15.3	56.6	13.9
SAA (ng/ml)	48.7	2.5	39.5	2.4	39.0	1.7	40.7	2.0	40.4	6.9	53.6	18.9	49.8	14.7	46.6	2.1
sICAM-1 (ng/ml)	0.214	0.133	0.241	0.104	0.250	0.089	0.272	0.129	0.455	0.591	0.500	0.771	0.404	0.491	0.257	0.116
sVCAM-1 (ng/ml)	4.32	1.98	3.54	1.64	3.51	1.74	3.74	1.76	2.96	1.03	4.24	1.93	3.80	1.52	3.29	2.19
Early Apoptosis																
Akt (Ser473) (BFI)	162	66	214	185	204	153	268	257	198	169	220	197	210	165	222	229
Active Caspase 8 (Asp384) (BFI)	270	131	369	463	357	371	384	478	431	559	358	423	355	420	346	414
Active Caspase 9 (Asp315) (BFI)	657	368	710	527	631	440	738	488	674	619	642	469	681	558	662	497
BAD (Ser112) (BFI)	471	377	496	411	438	345	475	367	462	380	447	348	473	390	453	388
Bcl-2 (Ser70) (BFI)	318	208	371	278	345	249	355	252	387	324	338	231	356	292	335	250
JNK (Thr183/Tyr185) (BFI)	704	350	940	836	855	652	907	686	1142	980	852	686	881	793	857	757
p53 (Ser46) (BFI)	847	641	1071	1075	946	831	922	891	1210	1317	1003	984	1005	1023	1077	1183
Oxidative Stress																
Catalase (BFI)	13550	3446	12649	2940	12621	2847	12575	2940	12599	3021	12927	3147	13357	3266	13184	2955
PRX2 (BFI)	154	27	206	48	261	89	244	69	145	26	210	53	272	101	298	110
SOD1 (BFI)	293	133	281	149	287	134	269	111	251	89	312	158	354	204	318	156
SOD2 (BFI)	17112	4640	17534	3238	17693	3387	17089	3800	17791	2910	17081	3819	17730	3703	17233	3676
TRX1 (BFI)	2179	866	2169	727	2202	707	2195	634	2070	541	2280	1033	2290	1015	2115	819

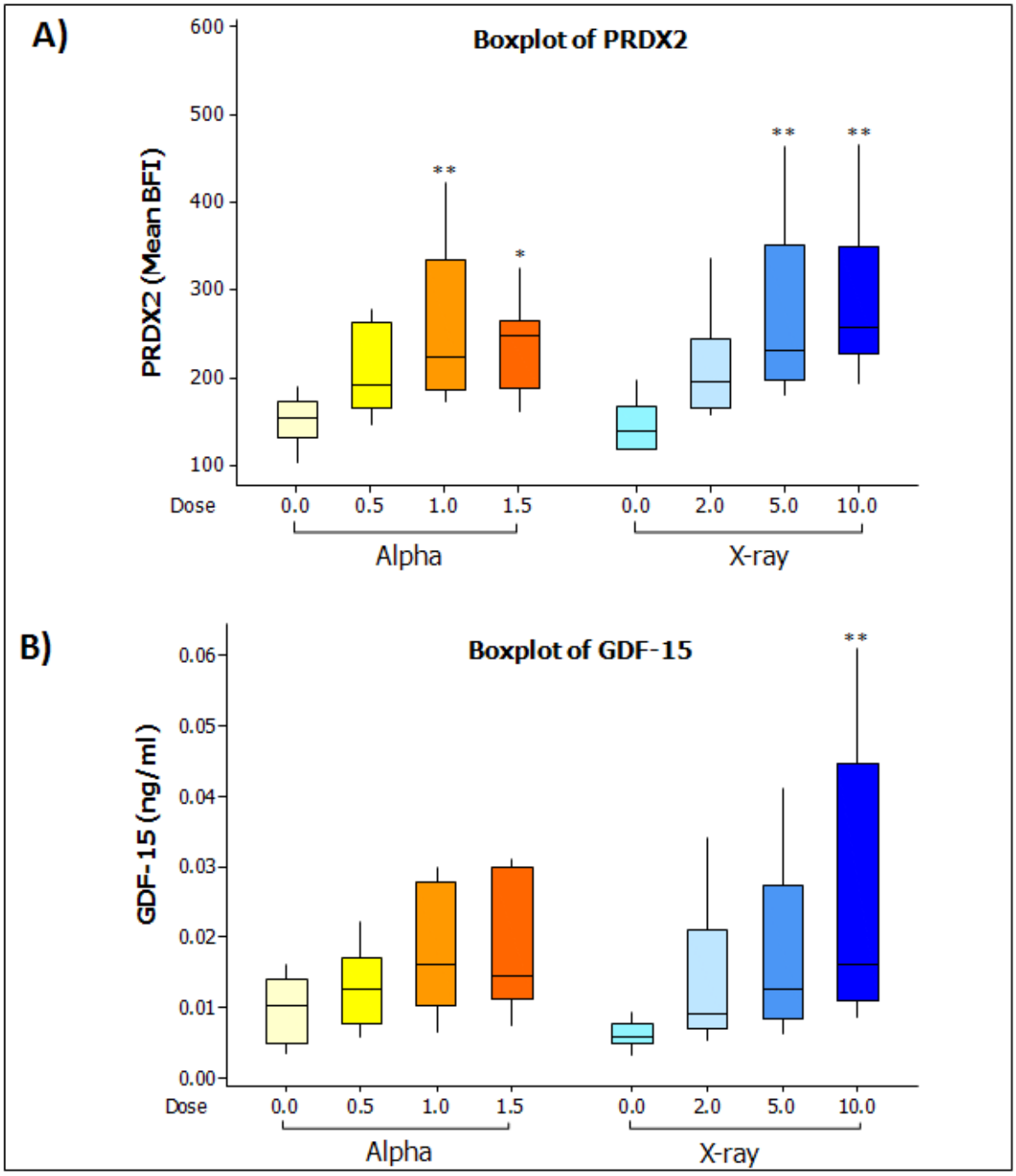

*Figure 11: Box-plot representation of statistically significant, differentially expressed proteins found in the supernatants of WBCs following alpha-particle or X-ray radiation exposure. The central line represents the median of the data and the box edges represent the upper (75th) and lower (25th) percentile. Whiskers denote the highest and lowest values from the data set within the upper and lower limits. Limits are defined as 1.5*50 percentile spread.* represents p<0.05, ** represents p<0.01*

9.5 Genomic Profiling

Genomic profiling using the Illumina Bead array platform was performed on RNA extracted from isolated PBMN cells 24 h post-exposure. In order to mine for reliable biomarkers, statistical stringency was prioritized over ambiguous inclusion, thus Benjamini Hochberg (BH) false discovery rate (FDR) correction was employed to mine for reliable genes. All differentially expressed genes were filtered on a BH FDR corrected p-value <0.05. A summary of the gene responses at each of the doses is provided in Table 4 (full gene lists can be found in Annex IV). Overall, there was a pronounced induction of transcriptional response, with the majority of genes being up-regulated in the presence of the radiation insult. Escalating doses induced an increasing number of transcripts with 33, 77 and 154 genes differentially modified at 0.5, 1.0 and 1.5 Gy respectively. A Venn diagram was constructed to provide a quantitative representation of the similarities and differences in expression profiles at each of the doses (Figure 12). Thirty-one genes were shown to be expressed at all three doses with expression levels ranging from 2-10 fold. Forty-four genes were expressed at both the medium and high dose. The range in expression levels of these genes is summarized as a heat map, which delineates the genes by degree of fold change, and is comprised of high, medium and low expressers (Figure 13). The 31 dose responsive genes as well as the 44 genes expressed at the medium and high dose were further validated using quantitative reverse-transcription polymerase chain reaction (qPCR).

Table 4: Numeric summary of differentially expressed transcripts that were obtained from exposure of isolated PBMC to alpha-particle radiation and categorized by dose. Bracketed numbers indicate the percentage of transcripts that were expressed in each of the categories from the total number of genes responding at each dose.

	0.5 Gy	1.0 Gy	1.5 Gy
Number of Transcripts	**33**	**77**	**154**
Common Amongst Doses *(%)*	**31** (94)	**31** *(40)*	**31** *(20)*
Exclusive *(%)*	2 (6)	2 *(3)*	79 *(51)*
Up Regulated *(%)*	**31** (94)	**74** *(96)*	**135** *(88)*
Common Amongst Doses *(%)*	31 (100)	31 *(46)*	31 *(23)*
Exclusive *(%)*	0 (0)	1 *(1)*	62 *(46)*
Down Regulated *(%)*	**2** (6)	**3** *(4)*	**19** *(12)*
Common Amongst All Doses *(%)*	0 (0)	0 *(0)*	0 *(0)*
Exclusive *(%)*	2 (100)	1 *(33)*	17 *(89)*

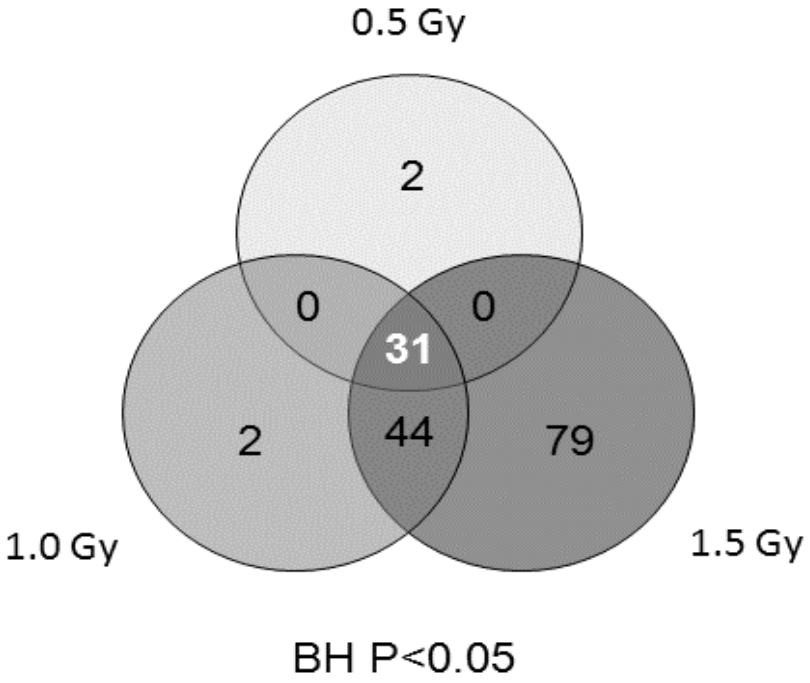

Figure 12: Venn diagram depicting the exclusive and common genes which were shown to be significantly modulated via microarray in PBMCs following various doses of alpha-particle radiation. Based on an n=12 human donors.

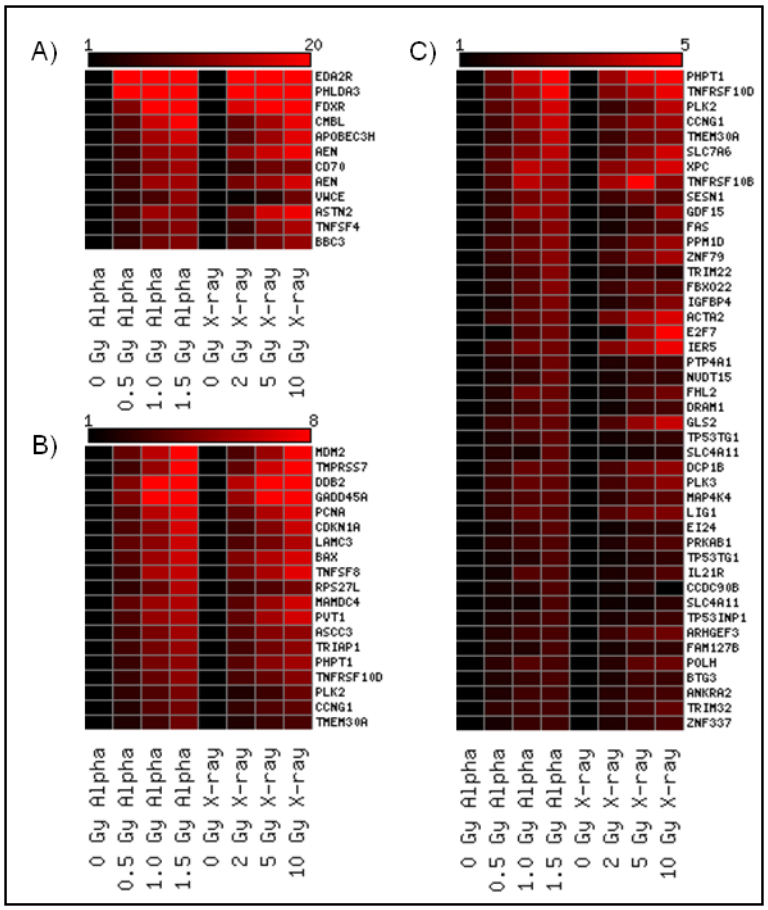

Figure 13: Heat map depicting the microarray fold change expression values of the genes which were found to be statistically significant at the medium and high doses and at all three doses of alpha-particle radiation exposure using microarray technology. Red colouring signifies up-regulation based on an n=12 biological replicates. The heat map is divided into three profiles based on high (A) medium (B) and low (C) fold change induction

9.6 qPCR Validation

The 44 transcripts observed to be expressed at the medium and high dose and the 31 genes expressed at all three doses were further validated using qPCR (Table 5). Of these genes four were omitted, either due to name duplication from the microarray, or could not be validated due to the unavailability of effective primers. A comparison of the responses using the two technologies showed a similar trend in expression levels. As shown in Table 4, all 70 genes that exhibited a significant response across the 3 doses using microarray

analysis were also observed to exhibit a similar trend using qPCR. Genes that were expressed at both the medium and high dose also displayed similar fold expression changes between the two methodologies, however, there was occasionally a discrepancy in assigning statistical significance. Approximately 20 of the total validated targets were shown to be non-significant using qPCR, potentially due to the low expression levels of these transcripts. In contrast, there were also a sub-set of 10 genes which showed statistical significance at the 0.5 Gy dose via qPCR but not microarray analysis.

Table 5: Validation of PBMC gene responses identified by microarray via qPCR. A comparison of the gene expression fold change (FC) responses obtained using microarray technology (MA) and qPCR at the three doses of alpha-particle radiation examined. Transcripts that were shown to differentially expressed at the medium and high dose and at all three dose were validated using qPCR . PV indicates the p-value obtained using either ANOVA or microarray statistics. The table is divided into two sections; the first section is comprised of genes that were shown to be significant using MA technology at all three doses and the second section are those genes that were shown to be significant using MA technology at the medium and high dose.

Radiation Type	**0.5 Gy Alpha**				**1.0 Gy Alpha**				**1.5 Gy Alpha**			
Technology	**qPCR**		**MA**		**qPCR**		**MA**		**qPCR**		**MA**	
Symbol	**FC**	**PV**	**FC**	**PV**	**FC**	**PV**	**FC**	**PV**	**FC**	**PV**	**FC**	**PV**
All Doses												
TRIAP1	2.15	0.00	1.81	0.00	3.32	0.00	2.14	0.00	3.78	0.00	2.57	0.00
GADD45A	2.94	0.00	2.27	0.01	4.43	0.00	2.77	0.00	4.70	0.00	3.38	0.00
RPS27L	2.01	0.00	1.67	0.01	2.59	0.00	1.90	0.00	3.57	0.00	2.04	0.00
MAP4K4	1.51	0.01	1.40	0.05	1.79	0.00	1.54	0.00	1.90	0.00	1.69	0.00
TNFRSF10D	2.15	0.01	1.81	0.01	2.94	0.00	2.08	0.00	3.08	0.00	2.39	0.00
ASTN2	6.18	0.01	2.07	0.01	8.02	0.00	2.67	0.00	8.98	0.00	3.15	0.00
TNFRSF10B	2.28	0.01	2.02	0.01	3.06	0.00	2.32	0.00	3.13	0.00	2.72	0.00
TMEM30A	1.92	0.01	1.72	0.01	2.67	0.00	2.13	0.00	2.76	0.00	2.45	0.00
TP53INP1	1.56	0.01	1.53	0.04	1.83	0.00	1.81	0.00	1.88	0.00	2.02	0.00
BAX	2.42	0.01	2.31	0.00	3.17	0.00	2.88	0.00	3.89	0.00	3.23	0.00
FAS	1.89	0.01	1.79	0.00	2.61	0.00	2.06	0.00	2.94	0.00	2.23	0.00
DDB2	2.96	0.01	3.56	0.00	5.15	0.00	4.41	0.00	5.26	0.00	5.49	0.00
AEN	4.24	0.01	2.16	0.01	7.09	0.00	2.80	0.00	7.46	0.00	3.14	0.00
GLS2	1.94	0.01	1.87	0.01	2.30	0.00	2.37	0.00	2.46	0.00	2.62	0.00
CMBL	3.99	0.01	2.52	0.01	6.79	0.00	2.90	0.00	7.41	0.00	3.57	0.00
PHPT1	2.28	0.02	2.23	0.00	3.50	0.00	2.57	0.00	4.17	0.00	3.03	0.00
PCNA	2.49	0.02	2.02	0.00	3.64	0.00	2.44	0.00	4.09	0.00	2.88	0.00
ASCC3	2.14	0.03	1.84	0.00	3.18	0.00	2.22	0.00	3.28	0.00	2.37	0.00
PPM1D	1.58	0.05	1.63	0.01	2.14	0.00	1.81	0.00	2.17	0.00	2.11	0.00
XPC	1.62	0.05	1.81	0.01	2.20	0.00	2.12	0.00	2.00	0.01	2.31	0.00
IER5	2.09	0.05	1.82	0.01	2.71	0.00	2.10	0.00	3.09	0.00	2.41	0.00
TNFSF4	2.91	0.06	2.93	0.00	4.98	0.00	3.69	0.00	5.34	0.00	4.67	0.00
SESN1	1.40	0.06	1.90	0.00	2.25	0.00	2.14	0.00	1.98	0.01	2.44	0.00
FBXO22	1.40	0.08	1.39	0.03	1.97	0.01	1.56	0.00	2.17	0.00	1.65	0.00
PHLDA3	9.91	0.09	3.18	0.00	22.89	0.00	3.96	0.00	28.82	0.00	4.89	0.00
ACTA2	2.12	0.09	2.54	0.01	2.72	0.01	3.07	0.00	2.74	0.01	3.60	0.00
CCNG1	0.91	0.10	1.80	0.00	2.49	0.00	1.97	0.00	2.56	0.00	2.14	0.00
MAMDC4	2.54	0.14	2.06	0.04	3.18	0.02	2.82	0.00	3.52	0.01	3.23	0.00
APOBEC3H	2.38	0.55	2.52	0.04	3.68	0.08	3.20	0.00	4.49	0.02	3.91	0.00

Radiation Type	0.5 Gy Alpha				1.0 Gy Alpha				1.5 Gy Alpha			
Technology	qPCR		MA		qPCR		MA		qPCR		MA	
Symbol	FC	PV	FC	PV	FC	PV	FC	PV	FC	PV	FC	PV
Med/High Doses												
SAC3D1	1.47	0.01	1.26	0.24	1.74	0.00	1.29	0.04	1.91	0.01	1.33	0.01
PVT1	2.02	0.01	1.42	1.00	2.76	0.00	1.68	0.02	3.45	0.00	1.85	0.00
TP53TG1	1.42	0.01	1.20	1.00	1.60	0.00	1.39	0.03	1.92	0.01	1.45	0.01
TNFSF8	2.40	0.01	1.92	0.08	4.01	0.00	2.33	0.00	3.80	0.00	2.61	0.00
TMPRSS7	4.04	0.01	1.24	1.00	4.85	0.01	1.53	0.00	6.74	0.00	1.52	0.00
ZNF79	1.74	0.02	1.39	0.47	2.07	0.00	1.74	0.00	2.34	0.00	1.95	0.00
SLC7A6	1.64	0.03	1.62	0.15	1.98	0.01	1.89	0.00	2.22	0.00	2.15	0.00
CDKN1A	2.41	0.03	2.30	0.11	3.87	0.00	2.94	0.00	5.05	0.00	3.58	0.00
LIG1	1.66	0.04	1.27	1.00	1.77	0.01	1.53	0.01	1.88	0.01	1.57	0.00
MDM2	2.93	0.04	1.24	0.31	4.44	0.00	1.30	0.02	5.17	0.00	1.45	0.00
FDXR	6.46	0.06	1.47	0.85	13.07	0.00	1.76	0.01	14.43	0.00	1.88	0.00
DCP1B	1.68	0.06	1.17	1.00	2.00	0.00	1.45	0.01	2.33	0.00	1.51	0.00
BBC3	4.10	0.06	1.40	0.66	6.75	0.00	1.65	0.01	7.25	0.00	1.83	0.00
ISG20	0.75	0.06	-1.44	1.00	0.46	0.00	-1.92	0.00	0.46	0.00	-2.30	0.00
SESN1	1.40	0.06	1.29	1.00	2.25	0.00	1.57	0.03	1.98	0.01	1.81	0.00
FAM20B	1.49	0.07	1.08	1.00	1.45	0.01	1.25	0.03	1.55	0.01	1.35	0.00
DRAM1	1.41	0.07	1.32	1.00	1.70	0.00	1.55	0.03	1.91	0.00	1.66	0.00
CCDC90B	2.18	0.07	1.20	0.64	1.54	0.07	1.29	0.02	2.89	0.00	1.35	0.00
POLH	1.72	0.08	1.39	0.24	2.37	0.00	1.60	0.00	2.10	0.01	1.92	0.00
GSS	1.19	0.08	1.15	1.00	1.34	0.01	1.29	0.03	1.60	0.00	1.34	0.00
PRKAB1	1.40	0.08	1.29	0.59	1.62	0.01	1.49	0.00	1.85	0.00	1.60	0.00
ARHGEF3	1.37	0.09	1.32	0.59	1.74	0.01	1.51	0.00	1.68	0.02	1.55	0.00
ZNF337	1.23	0.11	1.34	0.25	1.53	0.02	1.44	0.01	1.61	0.02	1.52	0.00
HIST1H4B	1.34	0.11	1.83	0.75	1.62	0.02	2.21	0.03	1.79	0.01	2.59	0.00
LAMC3	2.76	0.12	1.54	1.00	3.63	0.00	1.93	0.02	4.50	0.00	2.13	0.00
GDF15	1.84	0.14	1.49	1.00	2.40	0.01	1.98	0.03	2.96	0.05	2.26	0.00
ISCU	1.15	0.15	1.18	0.98	1.29	0.01	1.24	0.05	1.47	0.00	1.26	0.01
TRIM22	1.28	0.15	1.69	0.25	1.96	0.02	2.06	0.00	1.63	0.02	2.16	0.00
BTG3	1.11	0.23	1.30	0.21	1.69	0.00	1.41	0.00	1.70	0.01	1.54	0.00
NUDT15	1.22	0.23	1.21	0.24	1.48	0.02	1.31	0.00	1.47	0.03	1.38	0.00
RetSat	1.25	0.27	1.21	1.00	1.16	0.56	1.38	0.03	1.19	0.29	1.45	0.00
TRIM32	1.32	0.27	1.25	0.45	1.10	0.15	1.34	0.02	1.58	0.04	1.37	0.00
FHL2	1.74	0.30	1.50	0.44	2.47	0.02	1.82	0.00	2.65	0.01	2.20	0.00
FAM127B	1.14	0.30	1.21	0.54	1.53	0.01	1.31	0.00	1.58	0.05	1.38	0.00
PCNXL2	1.23	0.37	1.19	1.00	1.18	0.52	1.33	0.01	1.34	0.15	1.40	0.00
E2F7	2.23	0.37	1.33	1.00	3.19	0.39	1.49	0.05	4.08	0.43	1.72	0.00
TOB1	1.02	0.40	1.23	0.69	1.40	0.02	1.38	0.00	1.40	0.03	1.47	0.00
ANKRA2	1.07	0.44	1.39	0.27	1.63	0.01	1.48	0.02	1.60	0.02	1.60	0.00
CD70	2.45	0.55	2.04	0.75	4.44	0.04	2.50	0.04	5.05	0.03	3.01	0.00
EDA2R	8.96	0.61	1.31	1.00	19.58	0.87	1.57	0.02	31.64	0.29	1.67	0.00
IGFBP4	1.19	0.68	1.19	1.00	1.61	0.06	1.45	0.01	1.63	0.05	1.52	0.00

9.7 Pathway Analysis

Statistically significant genes expressed at the 1.5 Gy alpha-particle dose were entered into the IPA analysis tool to determine interconnectivity of the genes and associated canonical pathways. The top networks associated with this gene set included apoptosis, cell-to-cell signaling interaction, cell death and delay in cell cycle progression. The top canonical pathways associated with these genes were p53 signaling and GADD45. Several high expressing genes associated with these pathways included *CCNG1*, *PCNA*, *PMAIP1*,*TP53INP1*, *GADD45A*, *BBC3*, *CDKN1A*, *TNFRSF10B*, *MDM2*, *BAX*, *FAS*, *LRP5*, *GS5*, *RPMID*, *PRKAB1*, *RPS276*, *SPATA18*, *SRA1*, *RNU6-1*, *LDA3, PHLDA3* and *DRAM1*. All were up-regulated in expression with the exception of *PACS1N1* which was down-regulated by ~2 fold following alpha-particle irradiation. Networks showing the interconnectivity of expressed genes are shown in Figure 14 and Figure 15.

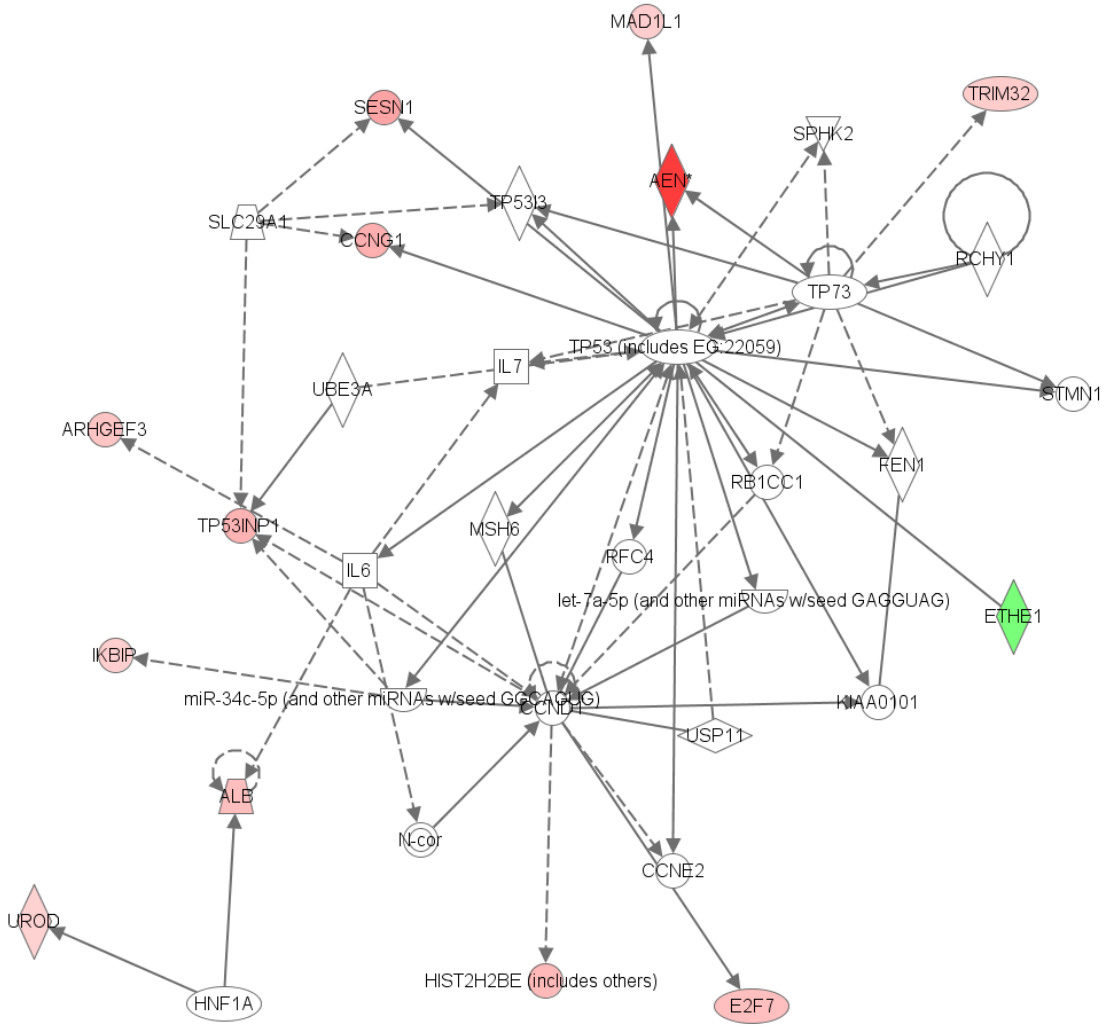

Figure 14: Network assembled from the genes responsive at the high dose and clustered around TP-53 signalling. Red represents up-regulated genes and green represents down-regulated genes. The intensity of the node color indicates the degree of up- (red) or down- (green) regulation.

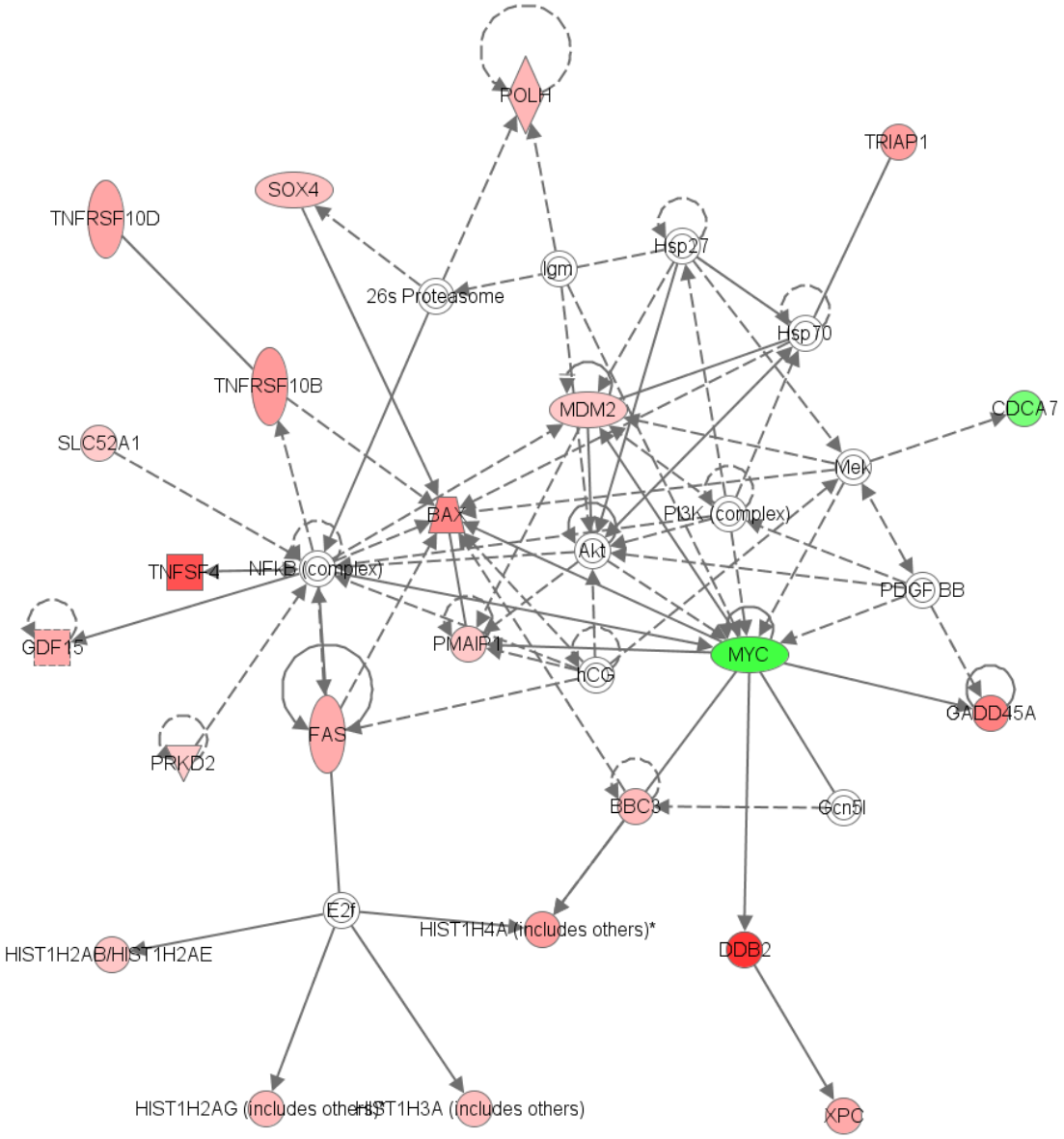

Figure 15: Network assembled from the genes responsive at the alpha-particle high dose and related to GADD45.A Red represents up-regulated genes and green represents down-regulated genes. The intensity of the node color indicates the degree of up- (red) or down- (green) regulation.

9.8 MicroRNA Validation

The screening of 800 miRNA transcripts using NanoString profiling resulted in minimal responding targets. Only one miRNA (miR-34a) was observed to be differentially modulated ($p<0.05$) at all doses examined following alpha-particle radiation exposure (All significant results can be seen in Appendix-V). This target was dose-responsive and subsequently validated using qPCR (Table 6). miR-34a was up-regulated over 2.5 fold in all exposed samples and had a similar 3 fold induction in the 1.0 and 1.5 Gy alpha-particle doses. This target was not specific to alpha-particle exposure as expression was also observed with X-ray irradiation at all three doses tested.

Table 6: qPCR validation of miRNA profiling results. Total isolated RNA from irradiated leukocytes was profiled with the nCounter system and subsequently validated via qPCR. Results are presented from n=12 donors. FC=fold change, PV=p-value.

Radiation Type	**Alpha**						**X-Ray**					
Dose (Gy)	**0.5**		**1.0**		**1.5**		**2.0**		**5.0**		**10.0**	
miRNA	**FC**	**PV**	**FC**	**PV**	**FC**	**PV**	**FC**	**PV**	**FC**	**PV**	**FC**	**PV**
miR-34a	2.67	0.00	3.05	0.00	3.14	0.00	3.14	0.00	3.30	0.00	3.05	0.00

9.9 WBC Transcriptional Profiling Using Custom qPCR Panel

RNA extracted from WBCs was profiled for differential gene expression utilizing the custom qPCR panel developed using the PBMC microarray results. This panel was used to verify the validity, specificity and overall integrity of alpha-particle responsive genes in a new population of cells. Leukocytes were isolated from 12 healthy individuals and exposed to alpha-particle and X-ray radiation. Twenty-four hours post-exposure, RNA was extracted and converted to cDNA for assessment of gene expression modulations using qPCR. All dose-responsive alpha-particle-responsive genes were observed to be significantly expressed at the three doses in the total WBC population. Among the 41 genes observed at the medium and high dose, 15 were shown to be un-responsive at the medium dose,

however the majority of these were observed at high dose of radiation (Table 7). Box-plots of the responding genes allowed for a comparative assessment of the two radiation types and for an assessment of the range in inter-individual variability between transcripts Figure 16-19. A comparison is with some of the genes from the consensus panel identified by Paul and Amundson (2008) are presented in Table 8.

Table 7: WBC transcriptional profiling post alpha-particle and X-ray radiation via custom qPCR array. The table is divided into two sections; the first section is comprised of genes that were shown to be significant at all three alpha-particle doses in the PBMC data sets via microarray technology, the second are those genes which were shown to be significant using microarray technology at the medium and high dose. FC=fold change; PV=p-value.

Radiation Type	**Alpha**						**X-Ray**					
Dose (Gy)	**0.5**		**1.0**		**1.5**		**2.0**		**5.0**		**10.0**	
GeneID	**FC**	**PV**	**FC**	**PV**	**FC**	**PV**	**FC**	**PV**	**FC**	**PV**	**FC**	**PV**
All Doses												
DDB2	4.65	0.00	8.45	0.00	8.76	0.00	5.37	0.00	8.59	0.00	9.12	0.00
PCNA	3.30	0.00	6.05	0.00	7.27	0.00	3.80	0.00	5.76	0.00	7.47	0.00
AEN	6.02	0.01	12.22	0.00	13.86	0.00	12.67	0.00	15.88	0.00	18.58	0.00
TNFSF4	4.71	0.03	9.04	0.00	11.01	0.00	5.56	0.00	10.64	0.00	14.46	0.00
PHPT1	2.65	0.03	4.22	0.00	4.96	0.00	3.68	0.00	4.73	0.00	5.70	0.00
TNFRSF10B	2.29	0.03	3.94	0.00	3.52	0.00	3.66	0.00	5.27	0.00	5.47	0.00
MAP4K4	1.90	0.05	2.29	0.00	2.49	0.00	2.03	0.00	2.28	0.00	2.50	0.00
GLS2	2.00	0.06	2.45	0.00	2.62	0.00	2.66	0.00	3.73	0.00	4.37	0.00
ACTA2	1.99	0.07	2.48	0.00	2.90	0.00	1.95	0.01	2.35	0.00	2.82	0.00
TRIAP1	2.88	0.07	4.27	0.00	5.18	0.00	2.87	0.00	4.11	0.00	5.03	0.00
IER5	2.02	0.09	2.82	0.00	2.79	0.00	2.75	0.00	3.85	0.00	4.47	0.00
APOBEC3H	7.03	0.10	13.35	0.00	16.63	0.00	7.82	0.00	12.59	0.00	17.99	0.00
TNFRSF10D	2.64	0.10	3.83	0.00	4.91	0.00	3.49	0.00	3.81	0.00	4.66	0.00
XPC	2.43	0.13	4.00	0.00	2.99	0.00	3.76	0.00	3.89	0.00	4.28	0.00
PPM1D	2.21	0.13	2.65	0.02	3.18	0.00	2.17	0.00	2.81	0.00	3.55	0.00
BAX	3.35	0.15	5.35	0.00	6.56	0.00	5.21	0.00	5.83	0.00	7.19	0.00
PHLDA3	19.38	0.23	50.31	0.00	46.15	0.00	26.63	0.00	37.99	0.00	47.11	0.00
ASTN2	5.85	0.24	10.73	0.01	10.09	0.01	10.41	0.00	15.76	0.00	16.68	0.00
GADD45A	4.76	0.30	8.33	0.01	8.07	0.00	7.35	0.00	10.87	0.00	14.02	0.00
MAMDC4	3.32	0.36	4.77	0.03	4.98	0.01	3.86	0.00	5.09	0.00	5.68	0.00
CMBL	7.34	0.43	16.13	0.01	19.65	0.00	10.40	0.00	13.33	0.00	18.53	0.00
ASCC3	2.82	0.53	4.35	0.08	5.48	0.01	4.06	0.00	4.63	0.02	5.45	0.00
CCNG1	2.12	0.55	3.35	0.05	4.22	0.00	2.88	0.02	3.23	0.03	3.80	0.00
FBXO22	1.70	0.66	2.41	0.16	3.10	0.02	2.39	0.01	2.63	0.06	2.93	0.01
TP53INP1	1.46	0.66	1.80	0.28	2.20	0.04	1.73	0.05	1.74	0.33	2.10	0.06
FAS	1.72	0.72	2.28	0.30	3.19	0.02	1.80	0.07	2.07	0.46	2.41	0.20
RPS27L	2.34	0.99	3.76	0.89	5.96	0.61	3.83	0.05	3.23	0.90	4.57	0.67
TMEM30A	1.91	0.99	2.82	0.87	4.04	0.56	2.82	0.06	2.70	0.90	3.42	0.67

Radiation Type	Alpha						X-Ray					
Dose (Gy)	0.5		1.0		1.5		2.0		5.0		10.0	
GeneID	FC	PV	FC	PV	FC	PV	FC	PV	FC	PV	FC	PV
Med/High dose												
BBC3	5.15	0.03	9.60	0.00	10.83	0.00	6.80	0.00	9.67	0.00	11.92	0.00
TNFSF8	2.98	0.03	5.64	0.00	6.38	0.00	4.57	0.00	5.65	0.00	7.34	0.00
PVT1	3.20	0.04	5.09	0.00	5.76	0.00	3.76	0.00	5.58	0.00	6.89	0.00
FDXR	10.88	0.05	24.04	0.00	27.24	0.00	17.01	0.00	27.84	0.00	37.91	0.00
TRIM32	1.80	0.05	1.96	0.01	2.01	0.01	1.71	0.01	2.11	0.00	2.48	0.00
ANKRA2	1.54	0.05	2.07	0.00	2.15	0.00	1.73	0.00	2.01	0.00	2.12	0.00
GSS	1.44	0.05	1.67	0.00	1.69	0.00	1.44	0.01	1.72	0.00	2.01	0.00
LIG1	1.89	0.05	2.61	0.00	2.44	0.00	2.27	0.00	2.83	0.00	2.98	0.00
HIST1H4B	1.79	0.07	2.06	0.00	1.96	0.01	1.67	0.04	2.09	0.00	2.59	0.00
ARHGEF3	1.62	0.07	2.03	0.00	2.20	0.00	1.98	0.00	2.47	0.00	2.83	0.00
SLC7A6	2.37	0.09	3.19	0.00	3.94	0.00	2.42	0.00	3.25	0.00	4.28	0.00
CD70	5.76	0.13	10.08	0.00	12.92	0.00	6.14	0.00	9.06	0.00	9.89	0.00
ZNF79	1.96	0.13	2.58	0.00	3.17	0.00	2.18	0.00	2.95	0.00	3.68	0.00
TOB1	1.39	0.13	1.61	0.00	1.74	0.00	1.26	0.13	1.63	0.00	1.78	0.00
ZNF337	1.42	0.37	1.88	0.00	2.08	0.00	1.66	0.01	1.92	0.00	2.30	0.00
PRKAB1	1.67	0.38	2.06	0.05	2.32	0.02	1.81	0.01	2.06	0.01	2.38	0.00
BTG3	1.58	0.38	1.87	0.04	2.15	0.01	1.66	0.02	1.94	0.01	2.06	0.00
TP53	-1.19	0.38	-1.42	0.02	-1.45	0.01	-1.33	0.07	-1.40	0.01	-1.53	0.00
POLH	1.74	0.42	2.34	0.07	2.16	0.13	2.01	0.02	2.44	0.02	2.92	0.00
MDM2	3.83	0.43	6.10	0.05	8.91	0.00	3.76	0.01	5.24	0.01	8.33	0.00
DCP1B	1.84	0.46	2.59	0.04	2.37	0.07	2.47	0.00	2.98	0.00	3.39	0.00
FAM20B	1.41	0.53	1.54	0.23	1.60	0.17	1.50	0.02	1.73	0.01	1.91	0.00
SESN1	1.83	0.55	2.86	0.04	3.45	0.00	2.41	0.02	2.72	0.04	2.54	0.02
PCNXL2	1.26	0.55	1.44	0.09	1.45	0.11	1.23	0.21	1.51	0.02	1.76	0.00
ISG20	-1.18	0.58	-1.53	0.11	-1.36	0.28	-1.55	0.49	-1.67	0.11	-1.61	0.18
CDKN1A	3.12	0.62	4.70	0.20	6.97	0.02	3.67	0.01	4.52	0.13	6.84	0.00
LAMC3	3.76	0.66	4.94	0.47	6.68	0.21	4.42	0.02	4.42	0.33	5.89	0.12
DRAM1	1.54	0.66	2.00	0.19	2.62	0.02	1.56	0.12	1.92	0.25	2.17	0.08
RetSat	1.27	0.66	1.42	0.28	1.19	0.35	1.82	0.02	2.09	0.01	2.35	0.00
ISCU	1.25	0.66	1.43	0.22	1.86	0.01	1.45	0.03	1.53	0.11	1.62	0.02
EDA2R	13.97	0.73	30.23	0.36	39.14	0.15	11.63	0.02	14.28	0.27	13.00	0.20
NUDT15	1.48	0.74	1.85	0.23	2.66	0.03	1.73	0.03	1.84	0.25	1.91	0.14
FHL2	1.66	0.74	2.77	0.16	2.56	0.20	1.69	0.05	2.23	0.13	2.84	0.01
CCDC90B	1.42	0.88	1.68	0.53	2.28	0.04	1.56	0.22	1.57	0.83	1.82	0.42
IGFBP4	1.51	0.92	2.54	0.55	2.81	0.40	2.45	0.02	2.77	0.37	3.23	0.15
SAC3D1	1.46	0.94	1.69	0.77	2.01	0.56	2.04	0.04	2.12	0.51	2.85	0.17
E2F7	-1.98	0.94	-1.26	0.87	1.26	0.92	-1.00	0.31	1.56	0.51	2.61	0.50
FAM127B	1.57	0.98	1.56	0.90	2.18	0.52	1.94	0.06	1.74	0.90	1.96	0.76
TMPRSS7	1.66	0.99	1.55	0.73	2.56	0.76	4.16	0.13	5.92	0.34	8.32	0.05
GDF15	2.98	0.99	5.21	0.87	4.54	0.78	2.90	0.05	2.37	0.94	4.61	0.62
TRIM22	1.67	0.99	2.27	0.89	3.15	0.56	2.20	0.06	1.91	0.96	1.89	0.85
TP53TG1	1.37	0.99	1.62	0.90	2.32	0.49	1.73	0.07	1.53	0.97	1.95	0.77
Negative Control												
GNG7	-1.16	0.99	-1.30	0.55	-1.44	0.49	1.27	0.10	-1.07	0.87	-1.19	0.63

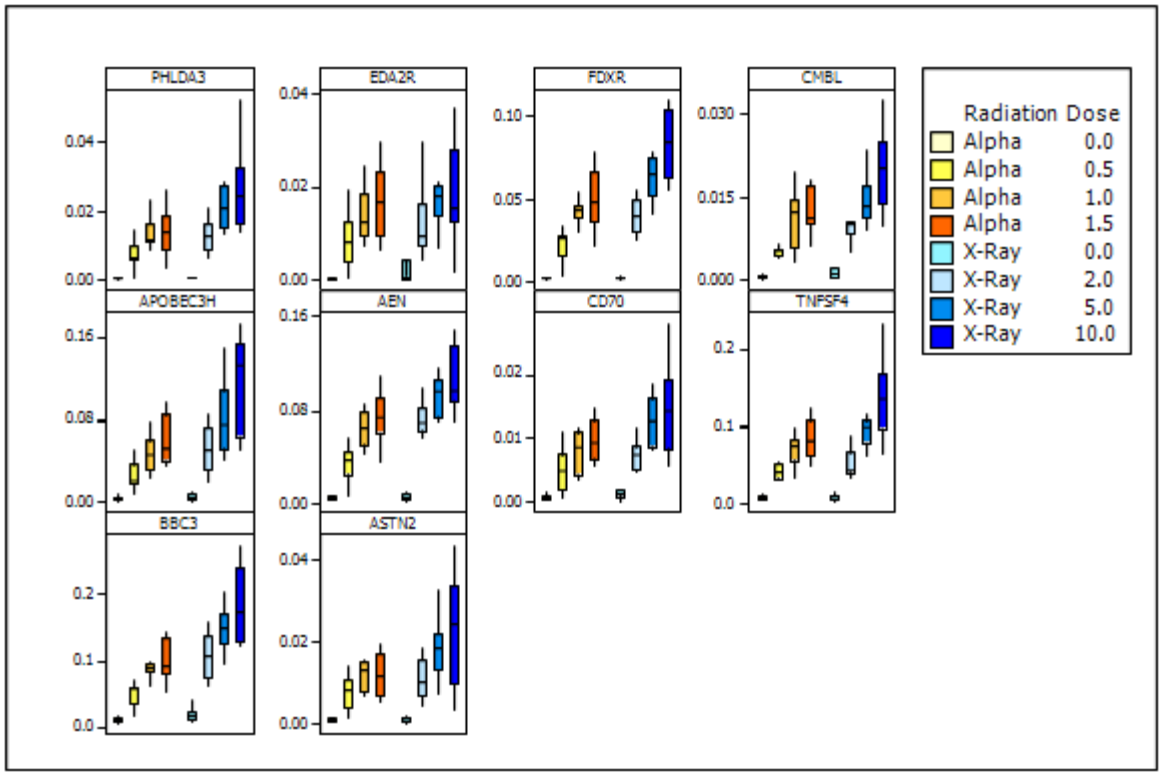

*Figure 16: Box-plot representation of genes responding with fold changes ranging from 5-100 fold via qPCR in isolated leukocytes exposed to alpha-particle and X-ray radiation. The high responding genes that corresponded to the heat-map are plotted with $2^{-\Delta CT}$ values along the Y-axis. The central line represents the median of the data and the box edges represent the upper (75th) and lower (25th) percentile. Whiskers denote the highest and lowest values from the data set within the upper and lower limits. Limits are defined as 1.5*50 percentile spread.*

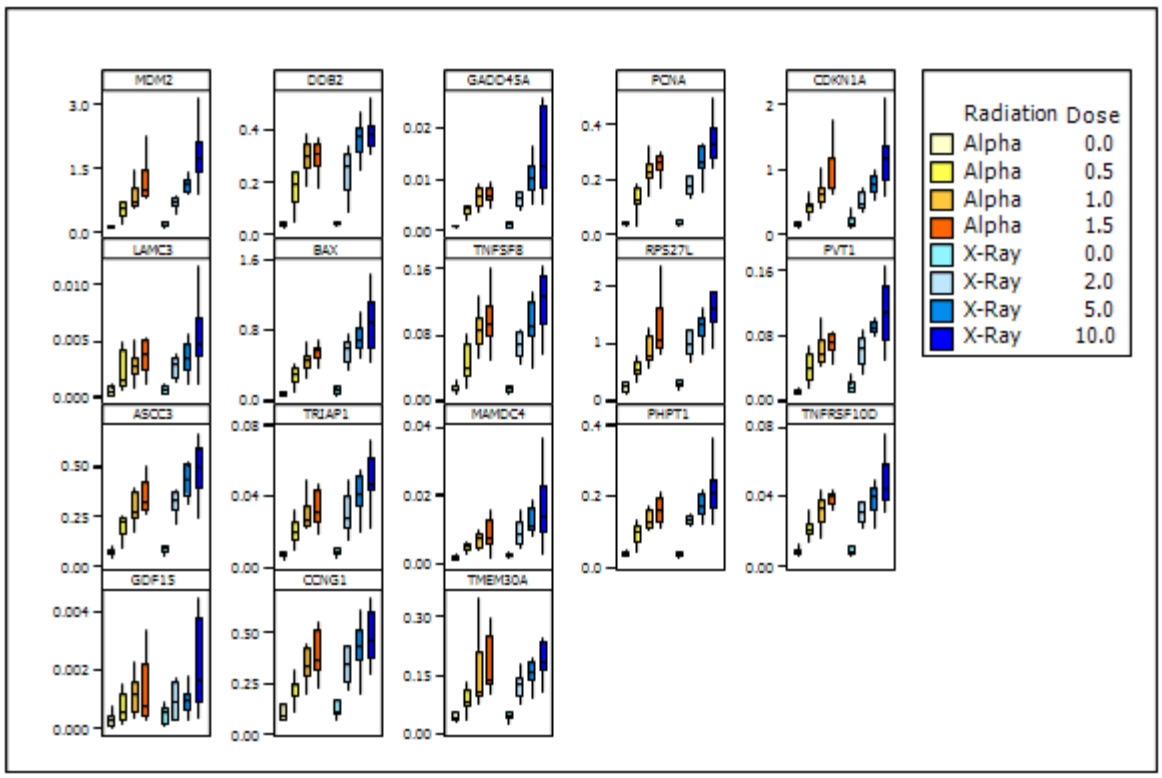

*Figure 17: Box-plot representation of genes responding with fold changes ranging from 2-9 fold via qPCR in isolated leukocytes exposed to alpha-particle and X-ray radiation. The medium responding genes that corresponded to the heat-map are plotted with $2^{-\Delta CT}$ values along the Y-axis. The central line represents the median of the data and the box edges represent the upper (75th) and lower (25th) percentile. Whiskers denote the highest and lowest values from the data set within the upper and lower limits. Limits are defined as 1.5*50 percentile spread.*

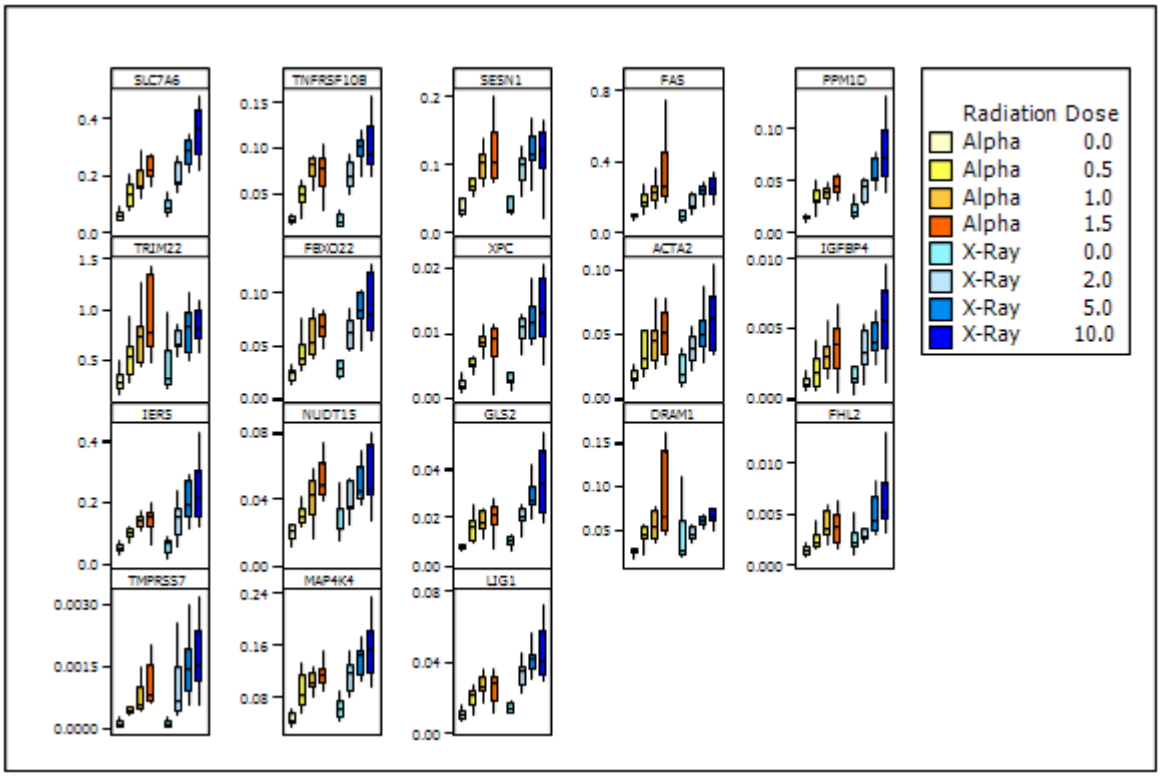

*Figure 18: Box-plot representation of genes responding with fold changes ranging from 1-4 fold via qPCR in isolated leukocytes exposed to alpha-particle and X-ray radiation. The low responding genes that corresponded to the heat-map are plotted with $2^{-\Delta CT}$ values along the Y-axis. The central line represents the median of the data and the box edges represent the upper (75th) and lower (25th) percentile. Whiskers denote the highest and lowest values from the data set within the upper and lower limits. Limits are defined as 1.5*50 percentile spread*

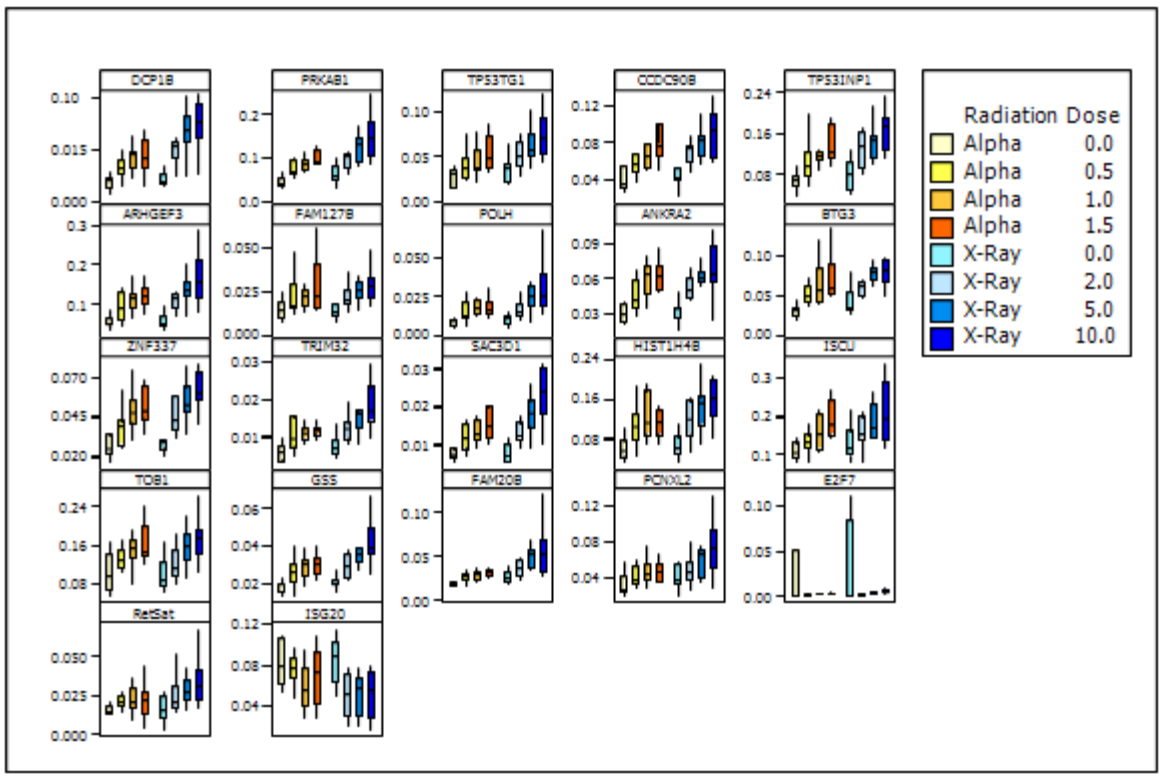

*Figure 19: Box-plot representation of genes responding with fold changes ranging from 1-2 fold via qPCR in isolated leukocytes exposed to alpha-particle and X-ray radiation. The low responding genes that corresponded to the heat-map are plotted with $2^{-\Delta CT}$ values along the Y-axis. The central line represents the median of the data and the box edges represent the upper (75th) and lower (25th) percentile. Whiskers denote the highest and lowest values from the data set within the upper and lower limits. Limits are defined as 1.5*50 percentile spread*

Table 8: Comparison of the qPCR fold-change results from the WBC mRNA experiments from this study compared with the gene consensus panel microarray fold-change results from the study by Paul and Amundson (2008). Only genes with data from both sets are presented. Microarray results were assigned a fold change by taking a ratio of the x-ray dose and the control.

	Paul and Amundson				Present Study					
	X-Ray Dose (Gy)				Alpha Dose (Gy)			X-Ray Dose (Gy)		
Gene	**0.5**	**2**	**5**	**8**	**0.5**	**1**	**1.5**	**2**	**5**	**10**
ACTA2	2.02	3.49	4.01	4.64	1.99	2.48	2.9	1.95	2.35	2.82
ANKRA2	1.18	1.47	1.58	1.85	1.54	2.07	2.15	1.73	2.01	2.12
APOBEC3C	1.61	1.99	2.78	2.35	7.03	13.35	16.63	7.82	12.59	17.99
ARHGEF3	1.20	1.51	1.83	1.76	1.62	2.03	2.2	1.98	2.47	2.83
ASCC3	2.04	3.00	4.31	4.06	2.82	4.35	5.48	4.06	4.63	5.45
ASTN2	2.73	6.90	11.78	13.51	5.85	10.73	10.09	10.41	15.76	16.68
BAX	2.66	4.05	4.14	4.28	3.35	5.35	6.56	5.21	5.83	7.19
BBC3	1.73	3.16	3.84	3.97	5.15	9.6	10.83	6.8	9.67	11.92
BTG3	1.28	1.67	1.93	1.81	1.58	1.87	2.15	1.66	1.94	2.06
CCNG1	1.90	3.34	3.83	3.22	2.12	3.35	4.22	2.88	3.23	3.8
CDKN1A	1.92	4.05	4.92	7.09	3.12	4.70	6.97	3.67	4.52	6.84
DCP1B	1.26	1.76	2.10	2.08	1.84	2.59	2.37	2.47	2.98	3.39
DDB2	3.11	6.02	7.58	9.16	4.65	8.45	8.76	5.37	8.59	9.12
FBXO22	1.61	2.34	3.08	3.01	1.7	2.41	3.1	2.39	2.63	2.93
FDXR	4.43	11.72	19.66	23.23	10.88	24.04	27.24	17.01	27.84	37.91
GADD45A	1.85	4.08	6.31	6.86	4.76	8.33	8.07	7.35	10.87	14.02
GDF15	1.64	2.37	4.76	7.57	2.98	5.21	4.54	2.9	2.37	4.61
GLS2	2.17	4.02	6.79	9.96	2.00	2.45	2.62	2.66	3.73	4.37
GNG7	0.92	0.74	0.53	0.41	-1.16	-1.3	-1.44	1.27	-1.07	-1.19
IER5	1.43	2.05	2.63	2.50	2.02	2.82	2.79	2.75	3.85	4.47
LIG1	1.33	1.90	2.30	2.75	1.89	2.61	2.44	2.27	2.83	2.98
MAMDC4	1.96	3.30	4.09	5.45	3.32	4.77	4.98	3.86	5.09	5.68
MDM2	1.95	2.88	5.95	8.58	3.83	6.1	8.91	3.76	5.24	8.33
PCNA	2.21	4.17	6.43	7.21	3.3	6.05	7.27	3.8	5.76	7.47
PHPT1	1.61	2.36	2.96	3.41	2.65	4.22	4.96	3.68	4.73	5.7
POLH	2.49	4.06	5.78	7.47	1.74	2.34	2.16	2.01	2.44	2.92
PPM1D	1.08	1.46	2.04	2.16	2.21	2.65	3.18	2.17	2.81	3.55
RPS27L	2.04	3.07	3.52	3.36	2.34	3.76	5.96	3.83	3.23	4.57
SESN1	1.54	2.32	2.71	2.86	1.83	2.86	3.45	2.41	2.72	2.54
SLC7A6	1.64	2.34	2.94	4.56	2.37	3.19	3.94	2.42	3.25	4.28
TNFRSF10B	2.05	2.81	3.38	3.77	2.29	3.94	3.52	3.66	5.27	5.47
TNFSF4	2.37	6.73	14.82	14.34	4.71	9.04	11.01	5.56	10.64	14.46
TRIAP1	1.94	2.90	4.75	4.56	2.88	4.27	5.18	2.87	4.11	5.03
TRIM22	2.00	2.65	2.56	2.86	1.67	2.27	3.15	2.2	1.91	1.89
XPC	1.49	2.37	2.92	3.45	2.43	4.00	2.99	3.76	3.89	4.28

9.10 Hierarchical Clustering and PCA Analysis

In order to better stratify expression patterns from the gene expression data derived from the WBC qPCR, further analysis was conducted through hierarchical clustering and principal component analysis. Figure 20 shows gene expression data clustered by gene and exposure group. Inputting all qPCR data resulted in classification of exposure groups in escalating doses categories. In order to better visualise the data and inter-person variability, a 3-dimensional principal component analysis was conducted (Figure 21). This figure plots each qPCR data set (n=96, 12 individuals x 2 radiation types x 4 doses) within coordinates defined by the first three principal components.

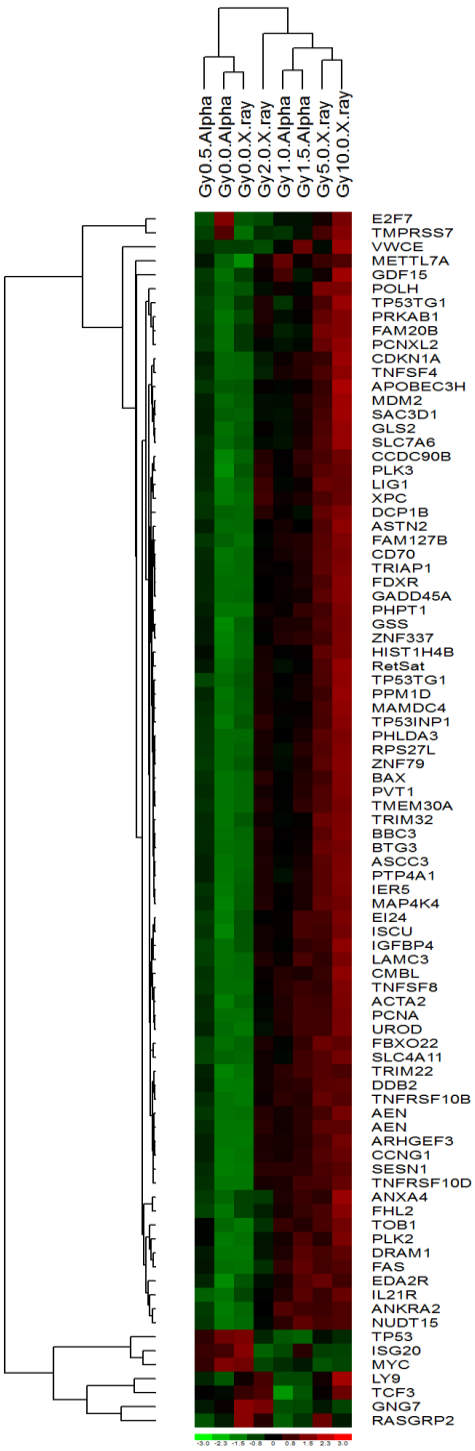

Figure 20: Median based hierarchical clustering dataset to determine common groupings of samples and genes

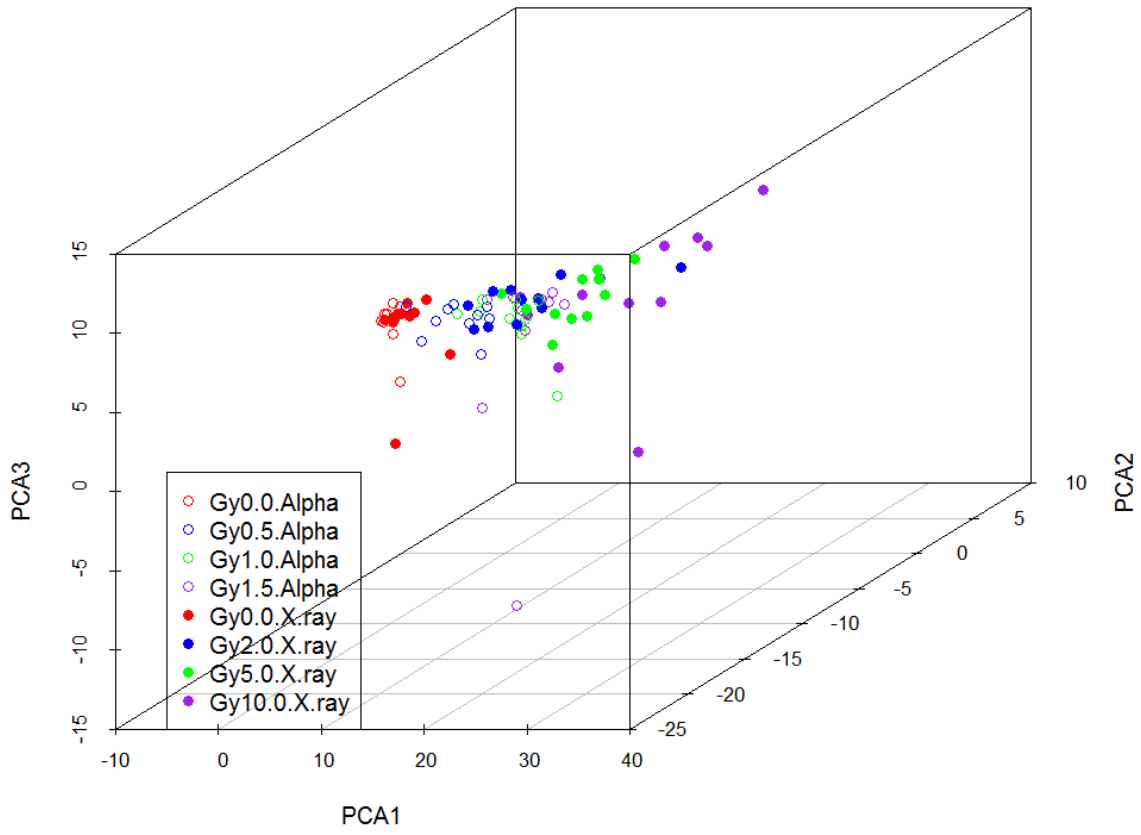

*Figure 21: Three dimensional PCA plot of WBC qPCR data. All 96 (n=12 donors * 2 radiation types * 4 doses) data sets are displayed, with red, blue, green and purple representing the control, low, medium and high doses respectively. Alpha particle data sets are represented by open-circle symbols and X-ray data sets by closed circle symbols.*

10 Discussion

10.1 Overview

The overarching goal of this research was to identify biomarkers of alpha-particle radiation exposure for the purposes of developing effective triage tools for use in a population exposure scenario. The first step towards developing such a biological assessment tool is to identify biological markers of exposure. A biomarker may be defined as a biological response to an insult which significantly differs from the normal status. In general, the biological response should be quantifiably specific, robust and sensitive to the insult with minimal inter-person variability. To date, the majority of biomarker-based radiation triage has been developed using photon radiation. Although there is a large body of work concerning radiation exposure and cytogenetic end-points, it was postulated that alpha-particle radiation may elicit differential cellular response due to its characteristic physical properties, which differ from photon radiation. This may potentially provide more accurate dose estimates for exposures and differentiate between radiation types. To mine for these biomarkers, a comprehensive approach was employed using a multiplicity of biological endpoints to potentially identify strong alpha-particle radiation specific biomarkers in the blood. Circulating blood cells represent a sensitive target for early radiation damage and are easily accessible in a cost-effective manner.

10.2 Dose and Dose Rate Comparisons

Isolated leukocytes from healthy individuals were ex-vivo irradiated at a dose range of 0-1.5 Gy at a slow dose-rate (0.98 Gy/h). These doses were selected based on their relevance to what would be expected from an actual radiological dispersal device scenario (Durante and

Manti 2002), where the dose deposition is approximately 0.5 Gy per alpha-particle track (Lorimore, Goodhead et al. 1993). Furthermore, previous studies from our laboratory have shown considerable biological damage at this dose-range. X-ray exposure doses and dose rates were selected on the work by Paul and Amundson (Paul and Amundson 2008), which was the first proof-of-concept gene-signature study for photon biodosimetry. In this experiment, blood was exposed to doses of 0.5, 2, 5 and 8 Gy at a dose rate of 0.82 Gy/min. This was the first study to demonstrate the ability of gene signatures to correctly classify photon-radiation exposures by dose and time and has subsequently been validated *in-vivo* (Paul, Barker et al. 2011). The research described here will build on this work, and is the first to date to examine global gene transcripts elicited by alpha-particle and X-ray radiation in *ex-vivo* blood from healthy donors.

10.3 Cell Counts

Due to the limitations of the alpha-particle exposure system employed in this study, it would be difficult to mimic whole blood irradiation, as the dosimetry of the system would be greatly altered from what has previously been published. As a preliminary assessment, pilot studies were conducted using both whole blood and isolated leukocytes. Erythrocyte sedimentation in whole blood during the exposure blocked alpha-particle passage as assessed by measuring DNA DSBs via gamma-H2AX. Contrasting the profiles of the irradiated and un-irradiated whole blood showed no difference in H2AX phosphorylation (Appendix III). Thus, experimental limitations necessitated using isolated leukocyte populations.

Lymphopenia and neutropenia is an early indicator of acute radiation exposure (Waselenko, MacVittie et al. 2004). In this study, complete blood counts were measured pre- and post-alpha-particle radiation exposure, in order to determine if a radiation insult altered CBC

under *ex-vivo* conditions. No significant changes in cell counts were observed at the doses tested. The cells remained viable, with no significant changes on absolute leukocyte numbers or differences within subpopulations. This lack of leukopenia may be due to the *ex-vivo* nature of exposure, as organs such as the spleen and liver are not present to actively filter the blood (Mebius and Kraal 2005) (Knolle and Gerken 2000).

10.4 H2AX Phosphorylation

To ensure that cells were undergoing irradiation and sustaining DNA damage, a biological assay indicative of DNA strand breaks, the phosphorylation of H2AX, was employed. As can be seen in Figure 2A, the geometric mean of signal intensity is increased for all exposures relative to the control. Although there is no statistical significance ascribed to the lowest dose of alpha-particle radiation tested (0.5 Gy), this may be due to the stochastic nature of the alpha-particle exposure system. As can be seen in Figure 2B, the 0.5 Gy (purple trace) histogram shows evidence of a bimodal distribution with two distinct intensity peaks. This suggests that only a sub-set of cells were traversed by an alpha-particle, and the remaining cell were un-irradiated. This is further corroborated by the emergence of a single peak in the higher (1.0 and 1.5 Gy) doses of alpha-particle radiation and the minimizing of the left shoulder of the curve. All of the X-ray exposed cells showed clear peaks and dose-dependent increases in signal intensity. It was seen that the alpha-particle exposed samples displayed lower gamma-H2AX intensities than the X-ray exposed samples and this may be due to several factors. Firstly, the X-rays were exposed to higher overall doses which will increase the probability of inducing DNA double strand breaks (DSBs). Secondly, the dose rates of exposure were markedly different. The alpha-particle exposure system is limited to a dose rate of ~1 Gy/hr and the X-ray exposure was performed at a dose rate of ~1 Gy/minute. This means the alpha-particle doses were

delivered over a protracted amount of time relative to the X-rays. It has been previously documented that gamma-H2AX foci reach a peak 30 minutes after exposure and then are resolved as repair is induced (Paull, Rogakou et al. 2000). The time-scale of the higher doses (1.0, 1.5 Gy) of alpha-particle radiation exposure is between ~1-1.5 hours. Thus, there is a degree of repair occurring whilst the cells are undergoing irradiation, and the measured signal is lowered due to resolved H2AX foci. There is an eventual equilibrium between induction and repair; it would be expected that the signal intensity would be higher for an acute exposure of equivalent dose. All of the X-ray exposures were conducted on the order of minutes, with the highest (10 Gy) dose taking ~ 10 minutes.

10.5 Clinical Chemistry

Alpha-particle irradiations of isolated plasma were performed in order to gauge the feasibility of using clinical chemistry markers as indicators of exposure. Clinical chemistry markers are routinely analysed in medical institutions and thus would be a simple and valuable triage tool. Multiple commercially available kits were tested after irradiation of isolated plasma at doses equivalent to the white blood cell alpha-particle experiments (0-1.5Gy). Table 1 shows a representative profile of one of the donors including control and exposure results. There were no statistically significant alterations in any of the profiles. It was expected that alpha-particle radiation would cause either direct molecular damage or free-radical induced damaged to plasma constituents, resulting in lower observed rates on enzyme activity. The radiation doses were likely of an order of magnitude that no protein or bimolecular damage occurred on an observable scale. Previous studies using ionising radiation for sterilization of plasma products used photon radiation doses in the kGy range (Miekka, Busby et al. 1998), well outside what was employed in this study. Previous studies that have shown modulations in clinical chemistry markers, such as serum amylase

(Blakely, Ossetrova et al. 2010), are based on *in-vivo* studies in which tissue damage can result in systemic effects (Marshall and Bangert 2008).

10.6 Protein Secretion

Post- WBC irradiation, cell culture supernatants were stored and analysed for protein secretion via multiplexed protein immuno-assay. It was determined that only two of the profiled proteins, PRDX2 and GDF15 were differentially expressed at statistically significant levels. Ionising radiation induces reactive oxygen species (ROS) and these damaging molecules can be scavenged by specific antioxidant proteins (Winterbourn 2008). Peroxiredoxins are a subset of these antioxidant proteins and account for 0.1%-1.0% of the soluble protein fraction in various mammalian cells (Chae, Kim et al. 1999). After WBC exposure to ionising radiation only Peroxiredoxin 2 (PRDX2) protein levels were found to be elevated in a dose responsive manner, with statistically significant changes observed in the medium and high doses tested. Fold changes ranged from 1.3 at the lowest dose to approximately 2 fold in the highest dose tested. Peroxiredoxins are a family of enzyme capable of catalysing the reduction of hydrogen peroxide and scavenging organic hydroperoxides (Nystrom, Yang et al. 2012). PRDX2 has been shown to be displayed on the exofacial surface of human lymphocytes (Szabo-Taylor, Eggleton et al. 2012), can be seen in serum, serving as a prognostic marker (Ji, Li et al. 2013) and is responsive to ionising radiation (Zhang, Wang et al. 2009). Furthermore, PRDX2 has been shown to have a higher affinity for peroxidation substrates than other peroxidoxins (Jarvis, Hughes et al. 2012). PRDX2 has also been found secreted via exosomes (Mathivanan, Ji et al. 2010). The display of PRDX2 on the exofacial surface of lymphocytes and secretion into circulation may allow the protein to regulate the peroxide concentration of extracellular fluids such as plasma. Detection of elevated PRDX2 protein levels in plasma may serve as a

corroborating criterion in assessing *in-vivo* exposure status, but it is not specific to radiation exposure.

GDF-15 was also shown to be dose-dependently secreted following radiation exposure. By using stringent statistical methods, as a way of discovering potentially strong biomarkers of exposure, only the highest (10 Gy) dose of X-ray radiation was statistically significant. Fold changes ranged from 1.3-3.8 fold. The physiological significance of this remains to be determined, however, GDF15 is a divergent member of the transforming growth factor beta (TGF-β) family of cytokines, found primarily in the placenta (Fairlie, Moore et al. 1999). Of particular interest is that GDF-15 has been found to have functions tied to inflammation, apoptosis and differentiation (Shi and Massague 2003), with elevated expression levels upon various types of injury to the liver, kidney and lung in a murine model (Zimmers, Jin et al. 2005). Furthermore, GDF15 has been shown to play a role in the radio-sensitivity of various cell types (Chang, Chan et al. 2007), and its mRNA expression serving as an indicator of radiation exposure (Joiner, Thomas et al. 2011). GDF15 induction appears to be responsive to general mechanical stress, genotoxicity and injury, thus limiting its usefulness in being a singular indicator of radiation exposure. Furthermore, there is currently much interest in the use of GDF15 as a marker for cardiovascular disease (Kehl, Iqbal et al. 2012, Stratz, Amann et al. 2012), suggesting that detection of GDF15 may be consigned to an ancillary biodosimetry role. In conclusion, though dose-dependent trends in various protein expressions were observed, their potential to serve as biomarkers of radiation exposure remains to be determined through future in-vivo based studies. Preliminary data has shown modulations in protein levels, but it remains to be seen if this holds true in a physiological environment. Furthermore, the specificity of these would not serve as suitable primary indicators of exposure as they are induced upon general oxidative stress and cardiovascular events. They may be of value in a confirmatory role.

10.7 Genomic Analysis

Peripheral blood mononuclear cells isolated from healthy individuals were exposed to alpha-particle radiation (0-1.5 Gy) and assessed for transcriptional modulations using genomic technology. It was found that radiation induced dose-dependent expression in 31 transcripts across all doses tested and a further 44 at the medium and high dose. This data was validated further using qPCR and the results were shown to be comparable between the two technologies in terms of fold change and statistical significance, with the exception that qPCR results of the 44 genes not shown to be statistically significant at the low dose using microarray technology, were shown to be significant by using qPCR. This is not unexpected as in comparison to microarrays, qPCR has been shown to exhibit higher relative fold changes, demonstrate a lower coefficient of variation (Skrzypski 2008) and may report different statistical assignments. (Wang, Barbacioru et al. 2006). To confirm the robustness of these responses in a more physiologically relevant population of cells, the complete white blood cell population was used for further validation studies. Furthermore, the ability of this gene panel to discriminate between radiation qualities was concurrently assessed. All dose-responsive alpha-particle induced genes that were identified in PBMC were also observed to be significantly expressed at the three doses in the total WBC population. Among the 44 medium and high dose genes, 15 were shown to lack statistical significance, most likely due to the use of stringent statistical analysis. When less stringent statistical methods not accounting for multiple comparisons were employed, the qPCR dataset was more comparable to the PBMC microarray data. Nevertheless, for biomarker discovery, stringent statistical analysis may potentially identify more robust gene biomarkers (Oh, Wong et al. 2012). It was also observed that the magnitude of transcript expression was higher in the WBCs compared to PBMCs, highlighting the cell-type specific nature of the response and further emphasising the need for rigorous statistical analysis of the WBC

data. Figures 6-9 depicts box plots of the WBC qPCR data and better illustrates the spread of data including inter-person variability. Of particular note is the relatively muted variability observed in control samples for the majority of genes, even between radiation types. For blood-based genomic biomarkers of exposure it is important to have a sense of the inter-person variability in basal gene expression (Whitney, Diehn et al. 2003). This data displayed minimal variability between control treatment groups under varied radiation exposure conditions, highlighting the potential for these transcript modulations to act as strong biomarkers. Furthermore, the majority of genes displayed strong dose-response trends for both alpha-particle and X-ray radiation. Within the WBC alpha-particle expression patterns, there exists a subset of genes which are only significant at the medium and high dose, suggesting the ability to discriminate dose with unique gene expression signatures potentially rendering these subsets useful for biodosimetry.

10.8 Aggregate Gene Signature Analysis

Although the ability to clearly discriminate between the two radiation types was not obtained from the gene transcript data, the degree of response was shown to be variable, highlighted in the hierarchical clustering of the dataset (Figure 17). Gene expression clustering has proven useful for displaying trends in an intuitive graphical form from microarray data (Eisen, Spellman et al. 1998) and making class distinctions (Golub, Slonim et al. 1999). Figure 16 shows gene expression data clustered by gene and exposure group. Inputting all qPCR data resulted in classification of exposure groups in escalating doses categories. The two control groups clustered together as expected and showed a distinct trend relative to the other exposed groups. The lowest dose of radiation (0.5 Gy alpha-particle) also clustered with the unexposed groups. This is interesting, as the H2AX data suggests that only a subset of cells were being irradiated, and gene expression values seem to be a

combination of irradiated and un-irradiated cells, classifying in a distinct grouping. The next largest classification comprised the remaining exposure groups, in which the 2 Gy X-ray, 1.0 and 1.5 Gy alpha-particle and 5 and 10 Gy X-ray were classified further from the controls in order of descending similarity respectively. The 2 Gy X-ray dose clustered alone, suggesting that the gene signature expressed at this dose of radiation is of intermediate value, somewhat dissimilar to any higher doses. The subsequent clustering of the 1.0 and 1.5 Gy alpha-particle exposure together and the 5 and 10 Gy X-ray exposure together suggests that it is possible to make distinctions between high X-ray radiation doses and alpha-particle doses using this clustering algorithm. In addition, exposure conditions were clustered in escalating dose, reaffirming the dose responsiveness of the genes analysed, even when modelled using clustering.

In order to better visualise the data and the inter-person variability, a 3-dimensional principal component analysis was conducted (Figure 18). PCA allows for an n-dimensional data set to be projected in ≤ n-dimensional space (Jolliffe 2002). PCA identifies new variables, the principal components, which are linear combinations of the original variables (Ringnér 2008). PCA is constructed in such a way that the first component accounts for as much of the variability in the data as possible and each subsequent component accounting for the next largest segment (Abdi and Williams 2010). This figure plots each qPCR data set within coordinates defined by the first three principal components. Principal component analysis has found use in previous microarray and large gene-set studies (Ospina and Lopez-Kleine 2013). As can be seen, the controls cluster relatively closely. There appears to be a distinct separation between increasing X-ray doses. The alpha-particle radiation responses were not as clearly demarcated. Both of these data analyses suggest that there may be distinct alpha-particle and X-ray effects when gene expression data is analysed in an aggregate

fashion and that although no distinct gene responses could discriminate between radiation qualities, the degree of response may be a factor that could be used to distinguish them.

The genes which were used to construct the qPCR validation panel were derived from alpha-particle exposed cells analysed via microarray technology. Had the resources to conduct microarray analysis with X-ray exposed samples been available, differentially responding photon radiation genes may have been identified. It has been shown that the alpha-particle responsive genes are induced by X-rays, but not that all X-ray responsive genes are induced by alpha-particles. Although all genes modulated in the alpha-particle exposed cells were also seen in the X-ray exposed cells, there were differing degrees of induction. Also, it remains to be seen if radiation type can be delineated on the basis of combinatorial analysis of gene expression magnitude changes. One of the confounding factors in trying to discriminate radiation type is the difference in linear energy transfer, meaning doses of alpha-particle radiation are more potent and this can be seen by similar levels of gene induction in this study. Alpha-particle doses of 1.0 Gy at a dose rate of ~1 Gy/hr were able to elicit the same response as a 10 Gy X-ray dose at ~ 1 Gy/min in some genes. Thus, despite being an order of magnitude different in dose and more than fifty times the dose rate, a similar cellular response was observed. Irrespective of the inherent differences in linear energy transfer, matching the dose and dose-rate between the two radiation-types would likely result in different gene expression profiles. Completely different transcriptional responses and induction of dose-responsive alpha-particle genes have been seen in our laboratory using normal human lung fibroblasts (manuscript submitted). In addition, it has been previously established that the lesions caused by alpha-particle tracks display different repair kinetics and fidelity (Leatherbarrow, Harper et al. 2006). Only a 24-h time point was examined in this study and there may be pronounced temporal differences in gene expression resulting from the differing degrees of damage between radiation types.

Thus, future studies should explore the effects of modifying exposure parameters (dose, dose-rate, harvest time) in order to elucidate more complete gene expression signatures.

10.9 Pathways Analysis

Significantly expressed genes at the high (1.5 Gy) dose of alpha-particle radiation were further explored by assessing their interactivity in terms of pathways, functions, and networks. This was undertaken to assess the canonical pathways induced by alpha-particle radiation. Though not strictly necessary for biomarker discovery, this mechanistic data helps assess the nature of any biomarker signatures. It was found that induced genes clustered around p53 and GADD45A signalling, with functions relating to cell-cycle arrest, apoptosis and cell-to-cell signalling. P53 is a transcription factor, termed the guardian of the genome, which can be activated in response to DNA damage (Vousden and Lane 2007). Upon induction, p53 regulates a plethora of genes, centered along the axes of cell cycle arrest, DNA repair and apoptosis (Riley, Sontag et al. 2008). P53 is coordinated by ataxia–telangiectasia mutated (ATM) protein (Shiloh 2003), a kinase which is also responsible for the phosphorylation of H2AX (Burma, Chen et al. 2001). Photon radiation is a known inducer of p53 (Eriksson and Stigbrand 2010) and this is equally the case for alpha-particle radiation (Prise, Folkard et al. 2006). Similarly, growth arrest and DNA damage (GADD) family proteins are induced upon DNA damage (Rosemary Siafakas and Richardson 2009) and can be transcriptionally activated in a p53 dependant manner (Zhan 2005) upon exposure to gamma-ray radiation (Zhan, Bae et al. 1994). GADD45A has been cited as playing roles in signal transduction, DNA repair and cell-cycle checkpoint (Liebermann, Tront et al. 2011). Given that alpha-particle radiation induces DNA DSBs as well as produces free-radicals, the transcriptional induction of networks associated with p53 and GADD45A cell-cycle arrest, DNA repair and apoptosis is expected. *p53* mRNA levels were

significantly altered at the medium and high doses for both alpha-particle and X-ray radiation and the associated transcriptional networks also show p53 activation including elevated (~3-4 fold) GADD45A levels. Furthermore, there was one miRNA (miR-34a) which was shown to be significantly up-regulated across all doses tested. miR-34a is an important direct interaction partner of p53 and the p53 tumour-suppressor network (Chang, Wentzel et al. 2007). The up-regulation of miR-34a has been shown to induce cell-cycle arrest (Tarasov, Jung et al. 2007), apoptosis (Raver-Shapira, Marciano et al. 2007) and has influence over the transcription of many cell-cycle and apoptosis related genes (Chen and Hu 2012). Extracellular p53 protein levels were assessed via the early apoptosis immune-assay kit but there was minimal detection and large variation, suggesting that this protein was not leaking into the supernatant. GDF15, which was identified as being up-regulated in this study, is a known down-stream mediator of p53 function (Li, Wong et al. 2000) (Yang, Filipovic et al. 2003) and PRDX2 relies on p53 induced proteins to maintain their antioxidant potential (Budanov, Sablina et al. 2004). Thus there is evidence that p53 activation is relevant to the effects which were seen at the secretomic level. Intracellular p53 levels were not assessed, but this would be important future mechanistic work.

10.10 Gene Expression Comparison with Literature

10.10.1 Photon Radiation

The photon biodosimetry gene expression panel identified by Paul and Amundson (Paul and Amundson 2008) had a number of p53 regulated transcripts as well as modified GADD45A transcription levels. When our 96-gene panel was initially constructed, comparisons were made to the findings of this study. Based on this comparative assessment, our “in-house” gene panel comprised transcripts that were not present on the panel proposed by Paul and Amundson, and therefore potentially alpha-particle radiation

specific. For example, the transcript *CMBL* was identified in this study as being a high expressing alpha-particle specific gene, and not present in the Paul and Amundson panel. It was observed however, that *CMBL* was found to be induced by X-rays. This discrepancy may be the result of the advancement in microarray technology and probe availability. The panel developed by Paul and Amundson in 2008, was based on the Agilent platform. For instance, in the case of *CMBL*, the Agilent array (Agilent-012391 Whole Human Genome Oligo Microarray G4112A) did not have a CMBL identified probe. Alternatively, these differences could also be attributed to exposure and harvesting conditions. These two differences may account for the discrepancies in genes originally exhibiting alpha-particle exclusive responses but then responding to both radiation types. Table 8 provides a fold-change comparison between the data obtained in this study and that of Paul and Amundson. Only a partial table could be constructed due to limitations in the data presentation of Paul, including unresolved transcript identities, gene duplication and only the presentation of geometric means. Regardless, the gene responses obtained in this study are comparable to the work of Paul and Amundson.

This work highlights the need to re-assess photon biodosimetry with the novel genes which were identified in this study and not obtained in the screens by the group of Paul and Amundson. Interestingly, there were four genes (*POLH, DCP1B, FAM20B, RetSat*) which were found to be statistically significant in all X-ray doses and not in the highest dose of alpha-particle radiation. *POLH* and *DCP1B* were both statistically significant at the 1.0 Gy alpha-particle dose. Both *FAM20B* and *RetSat* showed no statistical significance at any alpha-particle dose, and in the case of *RetSat*, all alpha-particle fold changes were lower than those induced by X-rays. The box plot of *RetSat* demonstrates a large degree of variability, indicating it may not serve as a suitable biomarker. *FAM20B* however, responded relatively consistently to higher doses of X-ray radiation and not alpha-particles, possibly

serving as a parsing mechanism between radiation types. FAM20 family members are evolutionarily conserved secreted proteins expressed in hematopoietic cells (Nalbant, Youn et al. 2005), and FAM20B has been identified as having kinase activity related to xylose (Koike, Izumikawa et al. 2009). The function of *FAM20B* is not well characterized, and it is not immediately evident why it may be induced upon X-ray exposure but not alpha-particle radiation. In addition, *FAM20B* was present on the gene panel developed by Paul and Amundson so it is unclear as to why it may not have been significantly altered. This may be related to probe sequence or exposure conditions.

10.10.2 Other Relevant Alpha-Particle Studies

Turtoi et al, (2010) are, thus far, the only group to examine the alpha-particle radiation induced genomic-wide transcriptional effects on an isolated normal white blood cell type. They employed the Agilent platform to analyse isolated lymphocytes exposed to 0.05, 0.1, 0.2, 0.4, 0.8 or 1.6 Gy of alpha-particle radiation and harvested cells 1 hour after irradiation. There was no pathway analysis performed in the context of p53, but the study did identify some genes associated with cell growth and signal transduction as well as muted (1.9 FC) GADD45A induction. There were 339 genes identified as being modified at one of the doses, with 54% up-regulated and 46% down-regulated and this general trend was seen over all doses. This is in stark contrast to the data presented herein, in which ~90% of the genes identified as significant were up-regulated. This results in a roughly equivalent number of up-regulated genes between the two studies. There are several important differences between this study and that of Turtoi. Firstly, Turtoi used varying dose-rates spanning an order of magnitude from ~ 0.1 to 3.18 Gy/hr in contrast to our constant dose rate of 0.98 Gy/hr. This confounding variability in dose-rate makes it difficult to delineate dose from dose-rate effects. Another key difference was the time point of harvest post-

irradiation. Our study used a 24-hour time-point so as to be suitable for triage, whereas the Turtoi paper sought to identify early alpha-particle responsive transcripts 1 hour after irradiation. Furthermore, Turtoi et al., performed three technical replicate arrays at each dose, but using RNA derived from one individual and this prevents the study from commenting on baseline variability of expression. No supplemental data was presented and so it was difficult to assess the expression patterns of *FAM20B* and *RetSat*. Only eight genes were validated via qPCR Taqman assay normalized to one housekeeping gene, and this data was only derived from two individuals. In contrast, our study performed arrays for 12 individuals at each dose point of alpha-particle radiation and expression was validated in over 80 genes via qPCR with endogenous controls and 4 housekeeping genes. An array pattern was designed to assay both exposure and control RNA from either radiation type on the same 384-well plate to minimize technical variability. In addition to validation, our qPCR assays provided proof of concept in the scalability of gene-based biodosimetry. Using the liquid handler capacity at Health Canada, it was possible to process 144 samples within a one-week time span. qPCR is a common lab instrument, and with multiple machines this throughput would be even greater.

10.11 Conclusion

10.11.1 Summary

In summary, numerous biological endpoints in isolated leukocytes were assessed after alpha-particle and X-ray radiation exposure in an attempt to improve existing biodosimetry techniques and determine to the plausibility of differentiating the two radiation types. Absolute cell counts and white blood cell subpopulations remained unchanged up to 24 hours post-exposure. In addition, clinical chemistry plasma markers were not altered by

either radiation type. To ensure that cells were undergoing damage, H2AX phosphorylation was assessed and dose-dependent increases were observed. X-rays elicited discrete shifts in mean intensity peaks, whereas the stochastic nature of the alpha-particle exposure system resulted in more distributed expression. Supernatants remaining after cell harvest were analysed for the presence of 22 proteins, of which PRDX2 and GDF15 were up-regulated relative to controls, however the utility of these proteins acting as strong biomarkers remains to be determined through further validation studies. Lastly, genomic strategies were employed for biomarker discovery. Thirty-one dose responsive and forty-four medium and high dose responding genes were induced by alpha-particle radiation. These genes were associated with signalling pathways centred along p53 and GADD45A, consistent with DNA damage literature. Subsequent comparison with high dose-rate X-ray radiation showed that both radiation types elicited similar gene responses. It was expected that there would be alpha-particle exclusive transcript modulation based on a review of literature, but this was not observed. This is potentially due to advancement in microarray technology, resulting in the better sequence coverage compared to probe-sets from earlier years. *FAM20B* was identified as possibly being useful in discriminating between radiation types; however expression levels were low thereby deterring it from being a strong biomarker. Despite the lack of obtaining discriminatory radiation responsive genes, a number of novel findings have been identified. Firstly, the use of global transcription strategies seems feasible for the development of radiation specific biodosimetry assays. Furthermore, with respect to radiation exposure, this data has shown that the degree of expression (fold change) may be a strong parameter for developing computational models for exposure type. These subtle differences, as shown by hierarchical clustering and PCA analysis, may be an avenue for further research.

10.11.2 Future Work

Although radiation responsive genes have been identified, considerable work is needed to further validate these responses. Future work includes time and dose sensitivity assessment exploring the temporal response of the genes identified in this study. Distinctions between alpha-particle radiation and X-ray radiation may become evident over a time-period under matched conditions with respect to dose and dose-rate of exposure. The panel of genes should also be tested in an *in-vivo* environment, using patients undergoing total body irradiations and alpha-particle radiation therapy.

11 References

Ainsbury, E. A., E. Bakhanova, J. F. Barquinero, M. Brai, V. Chumak, V. Correcher, F. Darroudi, P. Fattibene, G. Gruel, I. Guclu, S. Horn, A. Jaworska, U. Kulka, C. Lindholm, D. Lloyd, A. Longo, M. Marrale, O. Monteiro Gil, U. Oestreicher, J. Pajic, B. Rakic, H. Romm, F. Trompier, I. Veronese, P. Voisin, A. Vral, C. A. Whitehouse, A. Wieser, C. Woda, A. Wojcik and K. Rothkamm (2011). "Review of retrospective dosimetry techniques for external ionising radiation exposures." Radiat Prot Dosimetry **147**(4): 573-592.

Alexander, G. A., H. M. Swartz, S. A. Amundson, W. F. Blakely, B. Buddemeier, B. Gallez, N. Dainiak, R. E. Goans, R. B. Hayes and P. C. Lowry (2007). "BiodosEPR-2006 Meeting: Acute dosimetry consensus committee recommendations on biodosimetry applications in events involving uses of radiation by terrorists and radiation accidents." Radiation Measurements **42**(6): 972-996.

Ambros, V. (2004). "The functions of animal microRNAs." Nature **431**(7006): 350-355.

Amundson, S. A., M. Bittner, P. Meltzer, J. Trent and J. Fornance, Albert J (2001). "Biological indicators for the identification of ionizing radiation exposure in humans." Expert review of molecular diagnostics **1**(2): 211-219.

Anderson, N. L. and N. G. Anderson (2002). "The human plasma proteome: history, character, and diagnostic prospects." Mol Cell Proteomics **1**(11): 845-867.

Andreo, P., M. Evans, J. Hendry, J. Horton, J. Izewska, B. Mijnheer, J. Mills, M. Olivares, P. Ortiz López and W. Parker (2005). Radiation oncology physics: a handbook for teachers and students. Vienna, International Atomic Energy Agency

Asaithamby, A. and D. J. Chen (2011). "Mechanism of cluster DNA damage repair in response to high-atomic number and energy particles radiation." Mutat Res **711**(1-2): 87-99.

Asano, S. (2005). "Multi-organ involvement: lessons from the experience of one victim of the Tokai-mura criticality accident." BJR Suppl **27**: 9-12.

Asano, S. (2012). "Current status of hematopoietic stem cell transplantation for acute radiation syndromes." Int J Hematol **95**(3): 227-231.

Ash, D. and T. Bates (1994). "Report on the clinical effects of inadvertent radiation underdosage in 1045 patients." Clinical Oncology **6**(4): 214-226.

Barbosa-Morais, N. L., M. J. Dunning, S. A. Samarajiwa, J. F. Darot, M. E. Ritchie, A. G. Lynch and S. Tavaré (2010). "A re-annotation pipeline for Illumina BeadArrays: improving the interpretation of gene expression data." Nucleic Acids Research **38**(3): e17-e17.

BDWG (2001). "Biomarkers and surrogate endpoints: preferred definitions and conceptual framework." Clin Pharmacol Ther **69**(3): 89-95.

Beaton, L. A., T. A. Burn, T. J. Stocki, V. Chauhan and R. C. Wilkins (2011). "Development and characterization of an in vitro alpha radiation exposure system." Phys Med Biol **56**(12): 3645-3658.

Bechtel, D. (2007). Radioactive Dispersion Devices (RDD): What are the Odds? Technology and Society, 2007. ISTAS 2007. IEEE International Symposium on, IEEE.

Benjamini, Y. and Y. Hochberg (1995). "Controlling the false discovery rate: a practical and powerful approach to multiple testing." Journal of the Royal Statistical Society. Series B (Methodological): 289-300.

Bhattacharjee, Y. (2010). "An unending mission to contain the stuff of nuclear nightmares." Science **328**(5983): 1222-1224.

Blakely, W. F., N. I. Ossetrova, M. H. Whitnall, D. J. Sandgren, V. I. Krivokrysenko, A. Shakhov and E. Feinstein (2010). "Multiple parameter radiation injury assessment using a nonhuman primate radiation model-biodosimetry applications." Health physics **98**(2): 153.

Blakely, W. F., C. A. Salter and P. G. Prasanna (2005). "Early-response biological dosimetry-recommended countermeasure enhancements for mass-casualty radiological incidents and terrorism." Health physics **89**(5): 494-504.

Boag, J. (1975). Twelfth Failla Memorial Lecture The Time Scale in Radiobiology. Radiation research: biomedical, chemical, and physical perspectives: proceedings of the fifth International Congress of Radiation Research held at Seattle, Washington, USA, July 14-20, 1974, Academic Press.
Bolstad, B. M., R. A. Irizarry, M. Astrand and T. P. Speed (2003). "A comparison of normalization methods for high density oligonucleotide array data based on variance and bias." Bioinformatics **19**(2): 185-193.
Boyum, A. (1968). "Isolation of leucocytes from human blood. Further observations. Methylcellulose, dextran, and ficoll as erythrocyteaggregating agents." Scand J Clin Lab Invest Suppl **97**: 31-50.
Brengues, M., B. Paap, M. Bittner, S. Amundson, B. Seligmann, R. Korn, R. Lenigk and F. Zenhausern (2010). "Biodosimetry on small blood volume using gene expression assay." Health physics **98**(2): 179.
Brumfiel, G. (2011). "Nuclear agency faces reform calls." Nature **472**(7344): 397-398.
Budanov, A. V., A. A. Sablina, E. Feinstein, E. V. Koonin and P. M. Chumakov (2004). "Regeneration of peroxiredoxins by p53-regulated sestrins, homologs of bacterial AhpD." Science **304**(5670): 596-600.
Burma, S., B. P. Chen, M. Murphy, A. Kurimasa and D. J. Chen (2001). "ATM phosphorylates histone H2AX in response to DNA double-strand breaks." J Biol Chem **276**(45): 42462-42467.
Cassatt, D. R., J. M. Kaminski, R. J. Hatchett, A. L. DiCarlo, J. M. Benjamin and B. W. Maidment (2008). "Medical countermeasures against nuclear threats: radionuclide decorporation agents." Radiat Res **170**(4): 540-548.
Chae, H. Z., H. J. Kim, S. W. Kang and S. G. Rhee (1999). "Characterization of three isoforms of mammalian peroxiredoxin that reduce peroxides in the presence of thioredoxin." Diabetes Res Clin Pract **45**(2-3): 101-112.
Chang, J. T., S. H. Chan, C. Y. Lin, T. Y. Lin, H. M. Wang, C. T. Liao, T. H. Wang, L. Y. Lee and A. J. Cheng (2007). "Differentially expressed genes in radioresistant nasopharyngeal cancer cells: gp96 and GDF15." Mol Cancer Ther **6**(8): 2271-2279.
Chang, T. C., E. A. Wentzel, O. A. Kent, K. Ramachandran, M. Mullendore, K. H. Lee, G. Feldmann, M. Yamakuchi, M. Ferlito, C. J. Lowenstein, D. E. Arking, M. A. Beer, A. Maitra and J. T. Mendell (2007). "Transactivation of miR-34a by p53 broadly influences gene expression and promotes apoptosis." Mol Cell **26**(5): 745-752.
Chaudhry, M. A. (2008). "Biomarkers for human radiation exposure." Journal of biomedical science **15**(5): 557-563.
Chauhan, V. and M. Howland (2012e). "Genomic Profiling of a Human Leukemic Monocytic Cell-Line (THP-1) Exposed to Alpha Particle Radiation." The Scientific World Journal **2012**.
Chauhan, V., M. Howland, J. Chen, B. Kutzner and R. C. Wilkins (2011). "Differential effects of alpha-particle radiation and X-irradiation on genes associated with apoptosis." Radiology Research and Practice **2011**.
Chauhan, V., M. Howland, H. B. Greene and R. C. Wilkins (2012b). "Transcriptional and Secretomic Profiling of Epidermal Cells Exposed to Alpha Particle Radiation." The Open Biochemistry Journal **6**: 103.
Chauhan, V., M. Howland, A. Mendenhall, S. O'Hara, T. J. Stocki, J. P. McNamee and R. C. Wilkins (2012a). "Effects of alpha particle radiation on gene expression in human pulmonary epithelial cells." International journal of hygiene and environmental health.
Chauhan, V., M. Howland and R. Wilkins (2012c). "A Comparitive Assessement of Cytokine Expression in Human-Derived Cell Lines Exposed to Alpha Particles and X-Rays." The Scientific World Journal **2012**.
Chauhan, V., M. Howland and R. Wilkins (2012d). "Effects of α-Particle Radiation on MicroRNA Responses in Human Cell-Lines." The Open Biochemistry Journal **6**: 16.
Chen, F. and S. J. Hu (2012). "Effect of microRNA-34a in cell cycle, differentiation, and apoptosis: a review." J Biochem Mol Toxicol **26**(2): 79-86.
Cohen, L., T. E. Schultheiss and R. C. Kennaugh (1995). "A radiation overdose incident: initial data." Int J Radiat Oncol Biol Phys **33**(1): 217-224.
Conklin, W. C. and P. L. Liotta (2005). "Radiological threat assessment and the Federal Response Plan--a gap analysis." Health Phys **89**(5): 457-470.

Coy, S. L., A. K. Cheema, J. B. Tyburski, E. C. Laiakis, S. P. Collins and A. J. Fornace Jr (2011). "Radiation metabolomics and its potential in biodosimetry." International Journal of Radiation Biology **87**(8): 802-823.
Dainiak, N. and S. Sorba (1997). "Early identification of radiation accident victims for therapy of bone marrow failure." Stem Cells **15 Suppl 2**: 275-285.
Danielsson, A., K. Claesson, T. Z. Parris, K. Helou, S. Nemes, K. Elmroth, J. Elgqvist, H. Jensen and R. Hultborn (2012). "Differential gene expression in human fibroblasts after alpha-particle emitter 211At compared with 60Co irradiation." International journal of radiation biology(0): 1-9.
Dingfelder, M. (2012). "Track-structure simulations for charged particles." Health Physics **103**(5): 590-595.
Donnelly, E. H., J. B. Nemhauser, J. M. Smith, Z. N. Kazzi, E. B. Farfan, A. S. Chang and S. F. Naeem (2010). "Acute radiation syndrome: assessment and management." South Med J **103**(6): 541-546.
Du, P., W. A. Kibbe and S. M. Lin (2008). "lumi: a pipeline for processing Illumina microarray." Bioinformatics **24**(13): 1547-1548.
Dumont, F., A. L. Roux and P. Bischoff (2010). "Radiation countermeasure agents: an update." Expert opinion on therapeutic patents **20**(1): 73-101.
Dunnett, C. W. (1955). "A multiple comparison procedure for comparing several treatments with a control." Journal of the American Statistical Association **50**(272): 1096-1121.
Durante, M. and L. Manti (2002). "Estimates of radiological risk from a terrorist attack using plutonium." Radiat Environ Biophys **41**(2): 125-130.
Eckerman, K., J. Harrison, H. G. Menzel and C. H. Clement (2012). "ICRP Publication 119: Compendium of dose coefficients based on ICRP Publication 60." Ann ICRP **41 Suppl 1**: 1-130.
Efron, B. and R. Tibshirani (2002). "Empirical Bayes methods and false discovery rates for microarrays." Genetic epidemiology **23**(1): 70-86.
Eriksson, D. and T. Stigbrand (2010). "Radiation-induced cell death mechanisms." Tumour Biol **31**(4): 363-372.
Fairlie, W. D., A. G. Moore, A. R. Bauskin, P. K. Russell, H. P. Zhang and S. N. Breit (1999). "MIC-1 is a novel TGF-beta superfamily cytokine associated with macrophage activation." J Leukoc Biol **65**(1): 2-5.
Fajardo, L. F. (2005). "The pathology of ionizing radiation as defined by morphologic patterns*." Acta Oncologica **44**(1): 13-22.
Fan, J. B., K. L. Gunderson, M. Bibikova, J. M. Yeakley, J. Chen, E. Wickham Garcia, L. L. Lebruska, M. Laurent, R. Shen and D. Barker (2006). "[3] Illumina Universal Bead Arrays." Methods in enzymology **410**: 57-73.
Feinendegen, L., P. Hahnfeldt, E. E. Schadt, M. Stumpf and E. O. Voit (2008). "Systems biology and its potential role in radiobiology." Radiat Environ Biophys **47**(1): 5-23.
Fenech, M. (2011). "Current status, new frontiers and challenges in radiation biodosimetry using cytogenetic, transcriptomic and proteomic technologies." Radiation Measurements **46**(9): 737-741.
Fliedner, T. M. (2006). "Nuclear terrorism: the role of hematology in coping with its health consequences." Curr Opin Hematol **13**(6): 436-444.
Fliedner, T. M., D. Graessle, V. Meineke and H. Dörr (2007). "Pathophysiological principles underlying the blood cell concentration responses used to assess the severity of effect after accidental whole-body radiation exposure: an essential basis for an evidence-based clinical triage." Experimental hematology **35**(4): 8-16.
Fliedner, T. M., D. H. Graessle, V. Meineke and L. E. Feinendegen (2012). "Hemopoietic response to low dose-rates of ionizing radiation shows stem cell tolerance and adaptation." Dose Response **10**(4): 644-663.
Frank, R. and R. Hargreaves (2003). "Clinical biomarkers in drug discovery and development." Nat Rev Drug Discov **2**(7): 566-580.
Franken, N., R. ten Cate, P. Krawczyk, J. Stap, J. Haveman, J. Aten and G. Barendsen (2011). "Comparison of RBE values of high- LET α-particles for the induction of DNA-DSBs, chromosome aberrations and cell reproductive death." Radiation Oncology **6**(1): 64.

Friedrich, T., U. Scholz, T. ElsäSser, M. Durante and M. Scholz (2012). "Systematic analysis of RBE and related quantities using a database of cell survival experiments with ion beam irradiation." Journal of radiation research.
Garcia-Canton, C., A. Anadón and C. Meredith (2012). "γH2AX as a novel endpoint to detect DNA damage: Applications for the assessment of the in vitro genotoxicity of cigarette smoke." Toxicology in Vitro **26**(7): 1075-1086.
Geiss, G. K., R. E. Bumgarner, B. Birditt, T. Dahl, N. Dowidar, D. L. Dunaway, H. P. Fell, S. Ferree, R. D. George and T. Grogan (2008). "Direct multiplexed measurement of gene expression with color-coded probe pairs." Nature biotechnology **26**(3): 317-325.
Ghandhi, S. A., B. Yaghoubian and S. A. Amundson (2008). "Global gene expression analyses of bystander and alpha particle irradiated normal human lung fibroblasts: synchronous and differential responses." BMC Medical Genomics **1**(1): 63.
Goodhead, D. (1994). "Initial events in the cellular effects of ionizing radiations: clustered damage in DNA." International journal of radiation biology **65**(1): 7-17.
Gourmelon, P., M. Benderitter, J. M. Bertho, C. Huet, N. C. Gorin and P. De Revel (2010). "European consensus on the medical management of acute radiation syndrome and analysis of the radiation accidents in Belgium and Senegal." Health Phys **98**(6): 825-832.
Gregory, S. (2011). "Terrorist tactics in Pakistan threaten nuclear weapons safety." West Point CTC Sentinel, June **1**.
Gunderson, K. L., S. Kruglyak, M. S. Graige, F. Garcia, B. G. Kermani, C. Zhao, D. Che, T. Dickinson, E. Wickham and J. Bierle (2004). "Decoding randomly ordered DNA arrays." Genome research **14**(5): 870-877.
Guskova, A., A. Barabanova, A. Baranov, G. Gruszdev, Y. Pyatkin and N. Nadezhina (1988). "UNSCEAR 1988 Report: Acute radiation effects in victims of the Chernobyl accident: Appendix to Annex: Early effects in man of high radiation doses." United Nations Scientific Committee on the Effects of Atomic Radiation, New York.
Hall, E. J. and A. J. Giaccia (2005). Radiobiology for the Radiologist, Lippincott Williams & Wilkins.
Hall, E. J. and T. K. Hei (2003). "Genomic instability and bystander effects induced by high-LET radiation." Oncogene **22**(45): 7034-7042.
Harfouche, G. and M. T. Martin (2010). "Response of normal stem cells to ionizing radiation: a balance between homeostasis and genomic stability." Mutat Res **704**(1-3): 167-174.
Harley, N. H. and E. S. Robbins (1992). "222Rn Alpha Dose to Organs Other than Lung." Radiation Protection Dosimetry **45**(1-4): 619-622.
Harley, N. H. and E. S. Robbins (2009). "Radon and leukemia in the Danish study: another source of dose." Health Phys **97**(4): 343-347.
Harper, F. T., S. V. Musolino and W. B. Wente (2007). "Realistic radiological dispersal device hazard boundaries and ramifications for early consequence management decisions." Health physics **93**(1): 1-16.
Heslet, L., C. Bay and S. Nepper-Christensen (2012). "Acute radiation syndrome (ARS) - treatment of the reduced host defense." Int J Gen Med **5**: 105-115.
Hiemstra, H., M. Tersmette, A. H. Vos, J. Over, M. P. van Berkel and H. de Bree (1991). "Inactivation of human immunodeficiency virus by gamma radiation and its effect on plasma and coagulation factors." Transfusion **31**(1): 32-39.
Hoffmann, W. and I. Schmitz-Feuerhake (1999). "How radiation-specific is the dicentric assay?" Journal of exposure analysis and Environmental Epidemiology **9**(2): 113.
Houee-Levin, C. and K. Bobrowski (2013). "The use of the methods of radiolysis to explore the mechanisms of free radical modifications in proteins." J Proteomics.
Huang, T.-c. D., S. Paul, P. Gong, R. Levicky, J. Kymissis, S. A. Amundson and K. L. Shepard (2011). "Gene expression analysis with an integrated CMOS microarray by time-resolved fluorescence detection." Biosensors and Bioelectronics **26**(5): 2660-2665.
Hunter, M. P., N. Ismail, X. Zhang, B. D. Aguda, E. J. Lee, L. Yu, T. Xiao, J. Schafer, M. L. Lee, T. D. Schmittgen, S. P. Nana-Sinkam, D. Jarjoura and C. B. Marsh (2008). "Detection of microRNA expression in human peripheral blood microvesicles." PLoS One **3**(11): e3694.

IAEA (2008). The international nuclear and radiological event scale, Factsheet.
ICRU (2011). "5. Dosimetry." Journal of the ICRU **11**(1): 23-28.
Ishida, M. and G. W. Beebe (1959). Research Plan for Joint NIH-ABCC Study of Life-span of A-bomb Survivors, Atomic Bomb Casualty Commission.
Jacob, N. K., J. V. Cooley, T. N. Yee, J. Jacob, H. Alder, P. Wickramasinghe, K. H. Maclean and A. Chakravarti (2013). "Identification of Sensitive Serum microRNA Biomarkers for Radiation Biodosimetry." PLOS ONE **8**(2): e57603.
Jarvis, R. M., S. M. Hughes and E. C. Ledgerwood (2012). "Peroxiredoxin 1 Functions as a Signal Peroxidase to Receive, Transduce and Transmit Peroxide Signals in Mammalian Cells." Free Radical Biology and Medicine.
Jenner, T. J., C. M. deLara, P. O'Neill and D. L. Stevens (1993). "Induction and rejoining of DNA double-strand breaks in V79-4 mammalian cells following gamma- and alpha-irradiation." Int J Radiat Biol **64**(3): 265-273.
Ji, D., M. Li, T. Zhan, Y. Yao, J. Shen, H. Tian, Z. Zhang and J. Gu (2013). "Prognostic role of serum AZGP1, PEDF and PRDX2 in colorectal cancer patients." Carcinogenesis.
Johns, H. E. and J. R. Cunningham (1983). The physics of radiology, Charles C. Thomas Publisher.
Joiner, M. and A. Van Der Kogel (2009). Basic clinical radiobiology, CRC Press.
Joiner, M. C., R. A. Thomas, W. E. Grever, J. M. Smolinski, G. W. Divine, A. A. Konski, G. W. Auner and J. D. Tucker (2011). "Developing point of care and high-throughput biological assays for determining absorbed radiation dose." Radiother Oncol **101**(1): 233-236.
Jostes, R. F. (1996). "Genetic, cytogenetic, and carcinogenic effects of radon: a review." Mutat Res **340**(2-3): 125-139.
Kadhim, M., M. Hill and S. Moore (2006). "Genomic instability and the role of radiation quality." Radiation protection dosimetry **122**(1-4): 221-227.
Kalanxhi, E. and J. Dahle (2012). "Transcriptional responses in irradiated and bystander fibroblasts after low dose α-particle radiation." International Journal of Radiation Biology(0): 1-17.
Kazi, R. (2009). "Pakistan's HEU-based Nuclear Weapons Programme and Nuclear Terrorism: A Reality Check." Strategic Analysis **33**(6): 861-876.
Kehl, D. W., N. Iqbal, A. Fard, B. A. Kipper, A. De La Parra Landa and A. S. Maisel (2012). "Biomarkers in acute myocardial injury." Transl Res **159**(4): 252-264.
Kempner, E. S. (2001). "Effects of high-energy electrons and gamma rays directly on protein molecules." J Pharm Sci **90**(10): 1637-1646.
Knolle, P. A. and G. Gerken (2000). "Local control of the immune response in the liver." Immunological Reviews **174**(1): 21-34.
Kodama, K., K. Ozasa, H. Katayama, R. E. Shore and T. Okubo (2012). "Radiation effects on cancer risks in the Life Span Study cohort." Radiat Prot Dosimetry **151**(4): 674-676.
Koike, T., T. Izumikawa, J. Tamura and H. Kitagawa (2009). "FAM20B is a kinase that phosphorylates xylose in the glycosaminoglycan-protein linkage region." Biochem J **421**(2): 157-162.
Kovalchuk, O., F. J. Zemp, J. N. Filkowski, A. M. Altamirano, J. S. Dickey, G. Jenkins-Baker, S. A. Marino, D. J. Brenner, W. M. Bonner and O. A. Sedelnikova (2010). "microRNAome changes in bystander three-dimensional human tissue models suggest priming of apoptotic pathways." Carcinogenesis **31**(10): 1882-1888.
Kuhn, K., S. C. Baker, E. Chudin, M.-H. Lieu, S. Oeser, H. Bennett, P. Rigault, D. Barker, T. K. McDaniel and M. S. Chee (2004). "A novel, high-performance random array platform for quantitative gene expression profiling." Genome Research **14**(11): 2347-2356.
Kuhne, M., K. Rothkamm and M. Lobrich (2002). "Physical and biological parameters affecting DNA double strand break misrejoining in mammalian cells." Radiat Prot Dosimetry **99**(1-4): 129-132.
Kulkarni, M. M. (2011). "Digital multiplexed gene expression analysis using the NanoString nCounter system." Current Protocols in Molecular Biology: 25B. 10.21-25B. 10.17.
Ladi, E., X. Yin, T. Chtanova and E. A. Robey (2006). "Thymic microenvironments for T cell differentiation and selection." Nat Immunol **7**(4): 338-343.

Leatherbarrow, E. L., J. V. Harper, F. A. Cucinotta and P. O'Neill (2006). "Induction and quantification of gamma-H2AX foci following low and high LET-irradiation." Int J Radiat Biol **82**(2): 111-118.
Lhakhang, T. W. and M. A. Chaudhry (2012). "Current approaches to micro-RNA analysis and target gene prediction." J Appl Genet **53**(2): 149-158.
Li, P. X., J. Wong, A. Ayed, D. Ngo, A. M. Brade, C. Arrowsmith, R. C. Austin and H. J. Klamut (2000). "Placental transforming growth factor-beta is a downstream mediator of the growth arrest and apoptotic response of tumor cells to DNA damage and p53 overexpression." J Biol Chem **275**(26): 20127-20135.
Liebermann, D. A., J. S. Tront, X. Sha, K. Mukherjee, A. Mohamed-Hadley and B. Hoffman (2011). "Gadd45 stress sensors in malignancy and leukemia." Crit Rev Oncog **16**(1-2): 129-140.
Liu, Q., B. Jiang, L. P. Jiang, Y. Wu, X. G. Wang, F. L. Zhao, B. H. Fu, T. Istvan and E. Jiang (2008). "Clinical report of three cases of acute radiation sickness from a (60)Co radiation accident in Henan Province in China." J Radiat Res **49**(1): 63-69.
Lloyd, D., A. Edwards, J. Moquet and Y. Guerrero-Carbajal (2000). "The role of cytogenetics in early triage of radiation casualties." Applied Radiation and Isotopes **52**(5): 1107-1112.
Lorimore, S., D. Goodhead and E. Wright (1993). "Inactivation of haemopoietic stem cells by slow α-particles." International journal of radiation biology **63**(5): 655-660.
MacPhail, S. H., J. P. Banath, T. Y. Yu, E. H. Chu, H. Lambur and P. L. Olive (2003). "Expression of phosphorylated histone H2AX in cultured cell lines following exposure to X-rays." Int J Radiat Biol **79**(5): 351-358.
Maguire, H., G. Fraser, J. Croft, M. Bailey, P. Tattersall, M. Morrey, D. Turbitt, R. Ruggles, L. Bishop, I. Giraudon, B. Walsh, B. Evans, O. Morgan, M. Clark, N. Lightfoot, R. Gilmour, R. Gross, R. Cox and P. Troop (2010). "Assessing public health risk in the London polonium-210 incident, 2006." Public Health **124**(6): 313-318.
Marchetti, F., M. A. Coleman, I. M. Jones and A. J. Wyrobek (2006). "Candidate protein biodosimeters of human exposure to ionizing radiation." International journal of radiation biology **82**(9): 605-639.
Marshall, W. J. and S. K. Bangert (2008). Clinical Biochemistry 2e: Metabolic and Clinical Aspects, Churchill Livingstone.
Mathivanan, S., H. Ji and R. J. Simpson (2010). "Exosomes: extracellular organelles important in intercellular communication." J Proteomics **73**(10): 1907-1920.
McFee, R. B. and J. B. Leikin (2009). "Death by polonium-210: lessons learned from the murder of former Soviet spy Alexander Litvinenko." Semin Diagn Pathol **26**(1): 61-67.
Mebius, R. E. and G. Kraal (2005). "Structure and function of the spleen." Nat Rev Immunol **5**(8): 606-616.
Menetrier, F., L. Grappin, P. Raynaud, C. Courtay, R. Wood, S. Joussineau, V. List, G. N. Stradling, D. M. Taylor, P. Berard, M. A. Morcillo and J. Rencova (2005). "Treatment of accidental intakes of plutonium and americium: guidance notes." Appl Radiat Isot **62**(6): 829-846.
Mercer, R. R., M. L. Russell, V. L. Roggli and J. D. Crapo (1994). "Cell number and distribution in human and rat airways." Am J Respir Cell Mol Biol **10**(6): 613-624.
Metheetrairut, C. and F. J. Slack (2013). "MicroRNAs in the ionizing radiation response and in radiotherapy." Curr Opin Genet Dev.
Michael, K. L., L. C. Taylor, S. L. Schultz and D. R. Walt (1998). "Randomly ordered addressable high-density optical sensor arrays." Analytical chemistry **70**(7): 1242-1248.
Miekka, S. I., T. F. Busby, B. Reid, R. Pollock, A. Ralston and W. N. Drohan (1998). "New methods for inactivation of lipid-enveloped and non-enveloped viruses." Haemophilia **4**(4): 402-408.
Nagaishi, R. and Y. Kumagai (2011). "Radiolysis of Water." Nuclear Hydrogen Production Handbook **6**: 177.
Nalbant, D., H. Youn, S. I. Nalbant, S. Sharma, E. Cobos, E. G. Beale, Y. Du and S. C. Williams (2005). "FAM20: an evolutionarily conserved family of secreted proteins expressed in hematopoietic cells." BMC Genomics **6**: 11.
Narayanan, P. K., K. E. LaRue, E. H. Goodwin and B. E. Lehnert (1999). "Alpha particles induce the production of interleukin-8 by human cells." Radiat Res **152**(1): 57-63.

Nayan, R. (2012). "How can countries ensure that the Nuclear Security Summit does not lose momentum and become just another gathering?" Bulletin of the Atomic Scientists **68**(2): 84-86.
NCRP (2008). Management of Persons Contaminated with Radionuclides: Handbook (Report No. 161), Volume 1 - Revision I, National Council on Radiation Protection and Measurements (NCRP).
Nenot, J.-C. (1998). "Radiation accidents: lessons learnt for future radiological protection." International journal of radiation biology **73**(4): 435-442.
Nenot, J. C. (2009). "Radiation accidents over the last 60 years." J Radiol Prot **29**(3): 301-320.
Nikjoo, H., P. O'Neill, M. Terrissol and D. T. Goodhead (1999). "Quantitative modelling of DNA damage using Monte Carlo track structure method." Radiat Environ Biophys **38**(1): 31-38.
Nikjoo, H., P. O'Neill, W. E. Wilson and D. T. Goodhead (2001). "Computational approach for determining the spectrum of DNA damage induced by ionizing radiation." Radiat Res **156**(5 Pt 2): 577-583.
NPG (2010). "Biomarkers on a roll." Nat Biotechnol **28**(5): 431.
Nystrom, T., J. Yang and M. Molin (2012). "Peroxiredoxins, gerontogenes linking aging to genome instability and cancer." Genes Dev **26**(18): 2001-2008.
Oh, J. H., H. P. Wong, X. Wang and J. O. Deasy (2012). "A bioinformatics filtering strategy for identifying radiation response biomarker candidates." PLoS One **7**(6): e38870.
Ozasa, K., E. J. Grant, H. M. Cullings and R. E. Shore (2013). "Invited commentary: missing doses in the life span study of Japanese atomic bomb survivors." Am J Epidemiol **177**(6): 569-573.
Pasquinelli, A. E., B. J. Reinhart, F. Slack, M. Q. Martindale, M. I. Kuroda, B. Maller, D. C. Hayward, E. E. Ball, B. Degnan, P. Muller, J. Spring, A. Srinivasan, M. Fishman, J. Finnerty, J. Corbo, M. Levine, P. Leahy, E. Davidson and G. Ruvkun (2000). "Conservation of the sequence and temporal expression of let-7 heterochronic regulatory RNA." Nature **408**(6808): 86-89.
Paul, S. and S. A. Amundson (2008). "Development of gene expression signatures for practical radiation biodosimetry." International Journal of Radiation Oncology* Biology* Physics **71**(4): 1236-1244. e1276.
Paul, S., C. A. Barker, H. C. Turner, A. McLane, S. L. Wolden and S. A. Amundson (2011). "Prediction of in vivo radiation dose status in radiotherapy patients using ex vivo and in vivo gene expression signatures." Radiation research **175**(3): 257-265.
Paull, T. T., E. P. Rogakou, V. Yamazaki, C. U. Kirchgessner, M. Gellert and W. M. Bonner (2000). "A critical role for histone H2AX in recruitment of repair factors to nuclear foci after DNA damage." Current Biology **10**(15): 886-895.
Pellmar, T. C. and S. Rockwell (2005). "Priority list of research areas for radiological nuclear threat countermeasures." Radiation research **163**(1): 115-123.
Peterson, J., M. MacDonell, L. Haroun, F. Monette, R. D. Hildebrand and A. Taboas (2007). "Radiological and chemical fact sheets to support health risk analyses for contaminated areas." Human Health Fact Sheet, Argonne.
Pinto, M. M., N. F. Santos and A. Amaral (2010). "Current status of biodosimetry based on standard cytogenetic methods." Radiat Environ Biophys **49**(4): 567-581.
Prise, K. M., M. Folkard and B. D. Michael (2006). "Radiation-induced bystander and adaptive responses in cell and tissue models." Dose Response **4**(4): 263-276.
Rana, S., R. Kumar, S. Sultana and R. K. Sharma (2010). "Radiation-induced biomarkers for the detection and assessment of absorbed radiation doses." Journal of Pharmacy And Bioallied Sciences **2**(3): 189.
Raver-Shapira, N., E. Marciano, E. Meiri, Y. Spector, N. Rosenfeld, N. Moskovits, Z. Bentwich and M. Oren (2007). "Transcriptional activation of miR-34a contributes to p53-mediated apoptosis." Mol Cell **26**(5): 731-743.
Riches, L. C., A. M. Lynch and N. J. Gooderham (2008). "Early events in the mammalian response to DNA double-strand breaks." Mutagenesis **23**(5): 331-339.
Riley, T., E. Sontag, P. Chen and A. Levine (2008). "Transcriptional control of human p53-regulated genes." Nat Rev Mol Cell Biol **9**(5): 402-412.

Roch-Lefèvre, S., T. Mandina, P. Voisin, G. Gaëtan, J. E. G. Mesa, M. Valente, P. Bonnesoeur, O. García, P. Voisin and L. Roy (2010). "Quantification of γ-H2AX foci in human lymphocytes: A method for biological dosimetry after ionizing radiation exposure." Radiation research **174**(2): 185-194.
Rogakou, E. P., C. Boon, C. Redon and W. M. Bonner (1999). "Megabase chromatin domains involved in DNA double-strand breaks in vivo." The Journal of cell biology **146**(5): 905-916.
Rogakou, E. P., D. R. Pilch, A. H. Orr, V. S. Ivanova and W. M. Bonner (1998). "DNA double-stranded breaks induce histone H2AX phosphorylation on serine 139." Journal of biological chemistry **273**(10): 5858-5868.
Romm, H., U. Oestreicher and U. Kulka (2009). "Cytogenetic damage analysed by the dicentric assay." Ann Ist Super Sanità **45**(3): 251-259.
Rosemary Siafakas, A. and D. R. Richardson (2009). "Growth arrest and DNA damage-45 alpha (GADD45alpha)." Int J Biochem Cell Biol **41**(5): 986-989.
Rosenthal, J. J., C. E. de Almeida and A. H. Mendonca (1991). "The radiological accident in Goiania: the initial remedial actions." Health Phys **60**(1): 7-15.
Rossnerova, A., M. Spatova, C. Schunck and R. J. Sram (2011). "Automated scoring of lymphocyte micronuclei by the MetaSystems Metafer image cytometry system and its application in studies of human mutagen sensitivity and biodosimetry of genotoxin exposure." Mutagenesis **26**(1): 169-175.
Saenko, V., V. Ivanov, A. Tsyb, T. Bogdanova, M. Tronko, Y. Demidchik and S. Yamashita (2011). "The Chernobyl accident and its consequences." Clin Oncol (R Coll Radiol) **23**(4): 234-243.
Sakata, R., E. J. Grant and K. Ozasa (2012). "Long-term follow-up of atomic bomb survivors." Maturitas **72**(2): 99-103.
Scadden, D. T. (2006). "The stem-cell niche as an entity of action." Nature **441**(7097): 1075-1079.
Schena, M., D. Shalon, R. W. Davis and P. O. Brown (1995). "Quantitative monitoring of gene expression patterns with a complementary DNA microarray." Science **270**(5235): 467-470.
Schmittgen, T. D. and K. J. Livak (2008). "Analyzing real-time PCR data by the comparative C(T) method." Nat Protoc **3**(6): 1101-1108.
Sedelnikova, O. A., E. P. Rogakou, I. G. Panyutin and W. M. Bonner (2002). "Quantitative detection of 125IdU-induced DNA double-strand breaks with γ-H2AX antibody." Radiation research **158**(4): 486-492.
Sharma, A., K. Singh and A. Almasan (2012). "Histone H2AX phosphorylation: a marker for DNA damage." Methods Mol Biol **920**: 613-626.
Shi, Y. and J. Massague (2003). "Mechanisms of TGF-beta signaling from cell membrane to the nucleus." Cell **113**(6): 685-700.
Shigematsu, I. (1998). "Greetings: 50 years of Atomic Bomb Casualty Commission-Radiation Effects Research Foundation studies." Proc Natl Acad Sci U S A **95**(10): 5424-5425.
Shiloh, Y. (2003). "ATM and related protein kinases: safeguarding genome integrity." Nat Rev Cancer **3**(3): 155-168.
Singh, V. K., E. J. Ducey, D. S. Brown and M. H. Whitnall (2012). "A review of radiation countermeasure work ongoing at the Armed Forces Radiobiology Research Institute." Int J Radiat Biol **88**(4): 296-310.
Skrzypski, M. (2008). "Quantitative reverse transcriptase real-time polymerase chain reaction (qRT-PCR) in translational oncology: lung cancer perspective." Lung Cancer **59**(2): 147-154.
Smyth, G. K. (2004). "Linear models and empirical bayes methods for assessing differential expression in microarray experiments." Stat Appl Genet Mol Biol **3**: Article3.
Smyth, G. K. (2005). Limma: linear models for microarray data. Bioinformatics and computational biology solutions using R and Bioconductor, Springer**:** 397-420.
Sontheimer, E. J. (2005). "Assembly and function of RNA silencing complexes." Nat Rev Mol Cell Biol **6**(2): 127-138.
Stewart, F. A., A. V. Akleyev, M. Hauer-Jensen, J. H. Hendry, N. J. Kleiman, T. J. Macvittie, B. M. Aleman, A. B. Edgar, K. Mabuchi, C. R. Muirhead, R. E. Shore and W. H. Wallace (2012). "ICRP publication 118: ICRP statement on tissue reactions and early and late effects of radiation in normal

tissues and organs--threshold doses for tissue reactions in a radiation protection context." Ann ICRP **41**(1-2): 1-322.
Stratz, C., M. Amann, D. D. Berg, D. A. Morrow, F. J. Neumann and W. Hochholzer (2012). "Novel biomarkers in cardiovascular disease: research tools or ready for personalized medicine?" Cardiol Rev **20**(3): 111-117.
Sutton, V. and D. A. Bromley (2005). "Understanding technologies of terror." Technology in Society **27**(3): 263-285.
Szabo-Taylor, K. E., P. Eggleton, C. A. Turner, M. L. Faro, J. M. Tarr, S. Toth, M. Whiteman, R. C. Haigh, J. A. Littlechild and P. G. Winyard (2012). "Lymphocytes from rheumatoid arthritis patients have elevated levels of intracellular peroxiredoxin 2, and a greater frequency of cells with exofacial peroxiredoxin 2, compared with healthy human lymphocytes." Int J Biochem Cell Biol **44**(8): 1223-1231.
Tabocchini, M. A., A. Campa and V. Dini (2012). "DNA and cellular effects of charged particles." Health Physics **103**(5): 547-555.
Tarasov, V., P. Jung, B. Verdoodt, D. Lodygin, A. Epanchintsev, A. Menssen, G. Meister and H. Hermeking (2007). "Differential regulation of microRNAs by p53 revealed by massively parallel sequencing: miR-34a is a p53 target that induces apoptosis and G1-arrest." Cell Cycle **6**(13): 1586-1593.
Thielen, H. (2012). "The Fukushima Daiichi nuclear accident--an overview." Health Phys **103**(2): 169-174.
Turtoi, A., I. Brown, M. Schläger and F. H. Schneeweiss (2010). "Gene Expression Profile of Human Lymphocytes Exposed to 211At α Particles." Radiation research **174**(2): 125-136.
Turtoi, A. and F. H. Schneeweiss (2009). "Effect of 211At α-particle irradiation on expression of selected radiation responsive genes in human lymphocytes." International journal of radiation biology **85**(5): 403-412.
Valentin, J. (2003). "Relative biological effectiveness (RBE), quality factor (Q), and radiation weighting factor (wR): ICRP Publication 92." Annals of the ICRP **33**(4): 1-121.
Valentin, J. (2005). "Protecting people against radiation exposure in the event of a radiological attack. A report of The International Commission on Radiological Protection." Ann ICRP **35**(1): 1-110, iii-iv.
Van Tuyle, G., T. Strub, H. O'Brien, C. Mason and S. Gitomer (2003). Reducing RDD concerns related to large radiological source applications. Los Alamos, NM: Los Alamos National Laboratory, LA-UR-03-6664.
Vousden, K. H. and D. P. Lane (2007). "p53 in health and disease." Nat Rev Mol Cell Biol **8**(4): 275-283.
Vral, A., M. Fenech and H. Thierens (2011). "The micronucleus assay as a biological dosimeter of in vivo ionising radiation exposure." Mutagenesis **26**(1): 11-17.
Wagemaker, G. (1995). "Heterogeneity of radiation sensitivity of hemopoietic stem cell subsets." Stem Cells **13 Suppl 1**: 257-260.
Wang, Y., C. Barbacioru, F. Hyland, W. Xiao, K. L. Hunkapiller, J. Blake, F. Chan, C. Gonzalez, L. Zhang and R. R. Samaha (2006). "Large scale real-time PCR validation on gene expression measurements from two commercial long-oligonucleotide microarrays." BMC Genomics **7**: 59.
Waselenko, J. K., T. J. MacVittie, W. F. Blakely, N. Pesik, A. L. Wiley, W. E. Dickerson, H. Tsu, D. L. Confer, C. N. Coleman, T. Seed, P. Lowry, J. O. Armitage and N. Dainiak (2004). "Medical management of the acute radiation syndrome: recommendations of the Strategic National Stockpile Radiation Working Group." Ann Intern Med **140**(12): 1037-1051.
Whitney, A. R., M. Diehn, S. J. Popper, A. A. Alizadeh, J. C. Boldrick, D. A. Relman and P. O. Brown (2003). "Individuality and variation in gene expression patterns in human blood." Proc Natl Acad Sci U S A **100**(4): 1896-1901.
Wightman, B., I. Ha and G. Ruvkun (1993). "Posttranscriptional regulation of the heterochronic gene lin-14 by lin-4 mediates temporal pattern formation in C. elegans." Cell **75**(5): 855-862.
Winterbourn, C. C. (2008). "Reconciling the chemistry and biology of reactive oxygen species." Nat Chem Biol **4**(5): 278-286.
Wood, R., C. Sharp, P. Gourmelon, B. Le Guen, G. Stradling, D. Taylor and M. Hengé-Napoli (2000). "Decorporation treatment-medical overview." Radiation protection dosimetry **87**(1): 51-56.

Yang, H., Z. Filipovic, D. Brown, S. N. Breit and L. T. Vassilev (2003). "Macrophage inhibitory cytokine-1: a novel biomarker for p53 pathway activation." Mol Cancer Ther **2**(10): 1023-1029.
Zhan, Q. (2005). "Gadd45a, a p53- and BRCA1-regulated stress protein, in cellular response to DNA damage." Mutat Res **569**(1-2): 133-143.
Zhan, Q., I. Bae, M. B. Kastan and A. J. Fornace, Jr. (1994). "The p53-dependent gamma-ray response of GADD45." Cancer Res **54**(10): 2755-2760.
Zhang, B., Y. Wang and Y. Su (2009). "Peroxiredoxins, a novel target in cancer radiotherapy." Cancer Lett **286**(2): 154-160.
Zimmers, T. A., X. Jin, E. C. Hsiao, S. A. McGrath, A. F. Esquela and L. G. Koniaris (2005). "Growth differentiation factor-15/macrophage inhibitory cytokine-1 induction after kidney and lung injury." Shock **23**(6): 543-548.

12 Contribution of Collaborators

Microarray and nCounter analysis was performed as a fee-for-service by the University Health Network – Sick Kids Hospital in Toronto by Dr. Patrick Yau and included RNA hybridization and data acquisition. Statistical analysis was provided by Dr. Pingzhao Hu of Sick Kids Hospital and included mRNA array, miRNA nCounter and WBC qPCR array analysis as well as aid in hierarchical clustering and principal component analysis. H2AX samples were run on the flow-cytometry instrument and data exported by Health Canada technician Barbara Kutzner. Alpha-particle exposure system dosimetry was calculated by Dr. Lindsay Beaton.

13 Appendices

13.1 Appendix I – PBMC RNA Quality Assessment via Bioanalyser

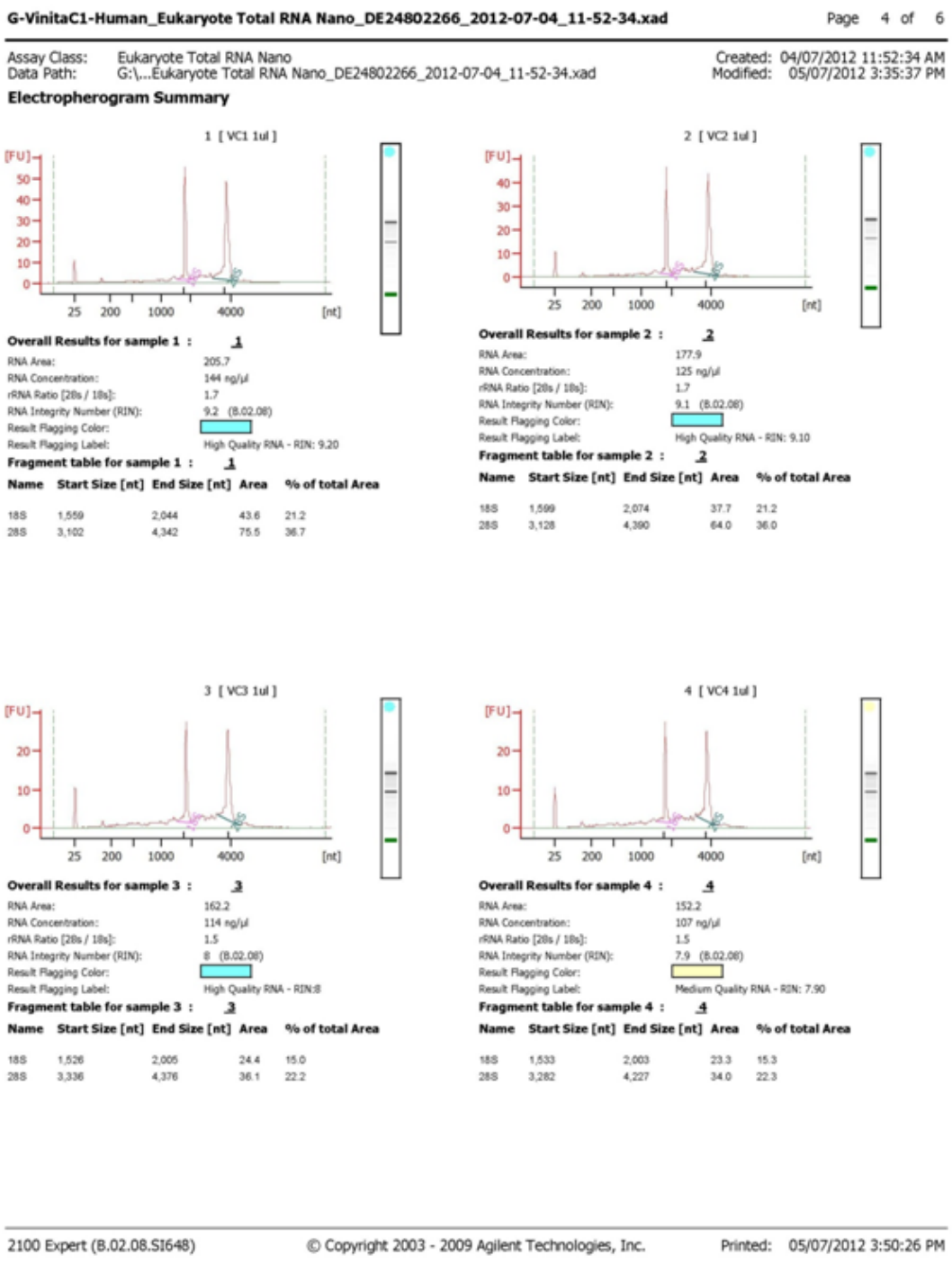

G-VinitaC1-Human_Eukaryote Total RNA Nano_DE24802266_2012-07-04_11-52-34.xad Page 4 of 6

Assay Class: Eukaryote Total RNA Nano
Data Path: G:\...Eukaryote Total RNA Nano_DE24802266_2012-07-04_11-52-34.xad

Created: 04/07/2012 11:52:34 AM
Modified: 05/07/2012 3:35:37 PM

Electropherogram Summary

1 [VC1 1ul]

Overall Results for sample 1 : 1

RNA Area:	205.7
RNA Concentration:	144 ng/µl
rRNA Ratio [28s / 18s]:	1.7
RNA Integrity Number (RIN):	9.2 (B.02.08)
Result Flagging Color:	
Result Flagging Label:	High Quality RNA - RIN: 9.20

Fragment table for sample 1 : 1

Name	Start Size [nt]	End Size [nt]	Area	% of total Area
18S	1,559	2,044	43.6	21.2
28S	3,102	4,342	75.5	36.7

2 [VC2 1ul]

Overall Results for sample 2 : 2

RNA Area:	177.9
RNA Concentration:	125 ng/µl
rRNA Ratio [28s / 18s]:	1.7
RNA Integrity Number (RIN):	9.1 (B.02.08)
Result Flagging Color:	
Result Flagging Label:	High Quality RNA - RIN: 9.10

Fragment table for sample 2 : 2

Name	Start Size [nt]	End Size [nt]	Area	% of total Area
18S	1,599	2,074	37.7	21.2
28S	3,128	4,390	64.0	36.0

3 [VC3 1ul]

Overall Results for sample 3 : 3

RNA Area:	162.2
RNA Concentration:	114 ng/µl
rRNA Ratio [28s / 18s]:	1.5
RNA Integrity Number (RIN):	8 (B.02.08)
Result Flagging Color:	
Result Flagging Label:	High Quality RNA - RIN:8

Fragment table for sample 3 : 3

Name	Start Size [nt]	End Size [nt]	Area	% of total Area
18S	1,526	2,005	24.4	15.0
28S	3,336	4,376	36.1	22.2

4 [VC4 1ul]

Overall Results for sample 4 : 4

RNA Area:	152.2
RNA Concentration:	107 ng/µl
rRNA Ratio [28s / 18s]:	1.5
RNA Integrity Number (RIN):	7.9 (B.02.08)
Result Flagging Color:	
Result Flagging Label:	Medium Quality RNA - RIN: 7.90

Fragment table for sample 4 : 4

Name	Start Size [nt]	End Size [nt]	Area	% of total Area
18S	1,533	2,003	23.3	15.3
28S	3,282	4,227	34.0	22.3

2100 Expert (B.02.08.SI648) © Copyright 2003 - 2009 Agilent Technologies, Inc. Printed: 05/07/2012 3:50:26 PM

Assay Class: Eukaryote Total RNA Nano
Data Path: G:\...Eukaryote Total RNA Nano_DE24802266_2012-07-04_11-52-34.xad

Created: 04/07/2012 11:52:34 AM
Modified: 05/07/2012 3:35:37 PM

Electropherogram Summary Continued ...

5 [VC5 1ul]

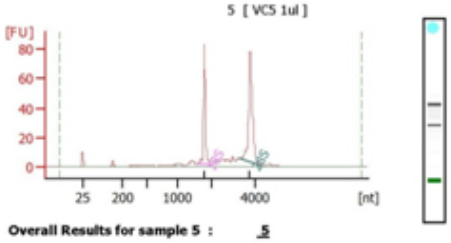

Overall Results for sample 5 : 5

RNA Area:	294.4
RNA Concentration:	206 ng/µl
rRNA Ratio [28s / 18s]:	1.6
RNA Integrity Number (RIN):	9.4 (B.02.08)
Result Flagging Color:	
Result Flagging Label:	High Quality RNA - RIN: 9.40

Fragment table for sample 5 : 5

Name	Start Size [nt]	End Size [nt]	Area	% of total Area
18S	1,538	2,001	67.1	22.8
28S	3,285	4,276	109.7	37.3

6 [VC6 1ul]

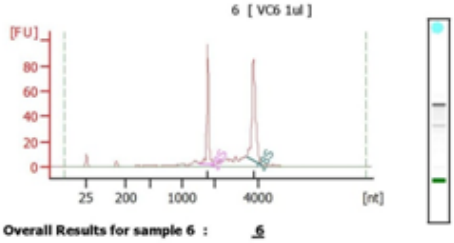

Overall Results for sample 6 : 6

RNA Area:	342.1
RNA Concentration:	240 ng/µl
rRNA Ratio [28s / 18s]:	1.5
RNA Integrity Number (RIN):	9.3 (B.02.08)
Result Flagging Color:	
Result Flagging Label:	High Quality RNA - RIN: 9.30

Fragment table for sample 6 : 6

Name	Start Size [nt]	End Size [nt]	Area	% of total Area
18S	1,535	1,999	79.1	23.1
28S	3,442	4,185	116.4	34.0

7 [VC7 1ul]

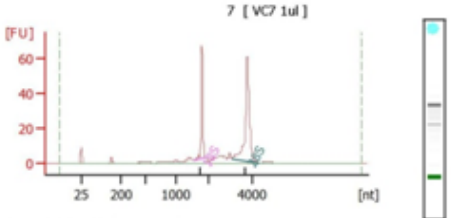

Overall Results for sample 7 : 7

RNA Area:	242.7
RNA Concentration:	170 ng/µl
rRNA Ratio [28s / 18s]:	2.0
RNA Integrity Number (RIN):	9.2 (B.02.08)
Result Flagging Color:	
Result Flagging Label:	High Quality RNA - RIN: 9.20

Fragment table for sample 7 : 7

Name	Start Size [nt]	End Size [nt]	Area	% of total Area
18S	1,550	1,876	47.9	19.7
28S	3,051	4,304	95.2	39.2

8 [VC8 1ul]

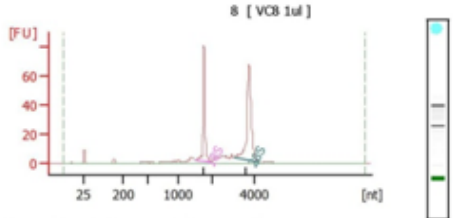

Overall Results for sample 8 : 8

RNA Area:	286.2
RNA Concentration:	201 ng/µl
rRNA Ratio [28s / 18s]:	1.7
RNA Integrity Number (RIN):	9.3 (B.02.08)
Result Flagging Color:	
Result Flagging Label:	High Quality RNA - RIN: 9.30

Fragment table for sample 8 : 8

Name	Start Size [nt]	End Size [nt]	Area	% of total Area
18S	1,527	1,976	64.0	22.4
28S	3,053	4,213	109.8	38.4

Assay Class: Eukaryote Total RNA Nano
Data Path: G:\...Eukaryote Total RNA Nano_DE24802266_2012-07-04_11-52-34.xad

Created: 04/07/2012 11:52:34 AM
Modified: 05/07/2012 3:35:37 PM

Electropherogram Summary Continued ...

9 [VC9 1ul]

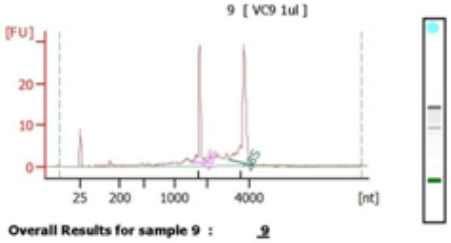

Overall Results for sample 9 : 9

RNA Area:	119.2
RNA Concentration:	84 ng/µl
rRNA Ratio [28s / 18s]:	1.7
RNA Integrity Number (RIN):	9 (B.02.08)
Result Flagging Color:	
Result Flagging Label:	High Quality RNA - RIN:9

Fragment table for sample 9 : 9

Name	Start Size [nt]	End Size [nt]	Area	% of total Area
18S	1,523	1,975	24.2	20.3
28S	3,041	4,177	41.0	34.4

10 [VC10 1ul]

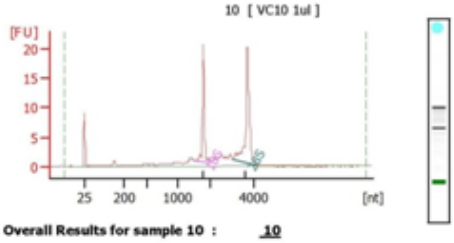

Overall Results for sample 10 : 10

RNA Area:	89.9
RNA Concentration:	63 ng/µl
rRNA Ratio [28s / 18s]:	1.6
RNA Integrity Number (RIN):	9 (B.02.08)
Result Flagging Color:	
Result Flagging Label:	High Quality RNA - RIN:9

Fragment table for sample 10 : 10

Name	Start Size [nt]	End Size [nt]	Area	% of total Area
18S	1,531	1,974	17.3	19.3
28S	3,042	4,166	28.3	31.4

11 [VC11 1ul]

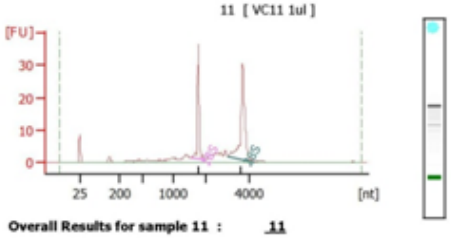

Overall Results for sample 11 : 11

RNA Area:	138.1
RNA Concentration:	97 ng/µl
rRNA Ratio [28s / 18s]:	1.6
RNA Integrity Number (RIN):	8.9 (B.02.08)
Result Flagging Color:	
Result Flagging Label:	High Quality RNA - RIN: 8.90

Fragment table for sample 11 : 11

Name	Start Size [nt]	End Size [nt]	Area	% of total Area
18S	1,521	1,964	28.7	20.7
28S	2,999	4,223	46.3	33.5

12 [VC12 1ul]

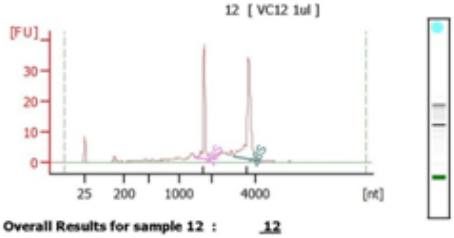

Overall Results for sample 12 : 12

RNA Area:	154.4
RNA Concentration:	108 ng/µl
rRNA Ratio [28s / 18s]:	1.5
RNA Integrity Number (RIN):	8.8 (B.02.08)
Result Flagging Color:	
Result Flagging Label:	High Quality RNA - RIN: 8.80

Fragment table for sample 12 : 12

Name	Start Size [nt]	End Size [nt]	Area	% of total Area
18S	1,516	1,976	32.3	21.0
28S	3,012	4,230	50.1	32.4

Assay Class: Eukaryote Total RNA Nano
Data Path: G:\...Eukaryote Total RNA Nano_DE54700719_2012-07-04_12-01-08.xad

Created: 04/07/2012 12:01:09 PM
Modified: 05/07/2012 3:52:05 PM

Electropherogram Summary

13 [VC13 1ul]

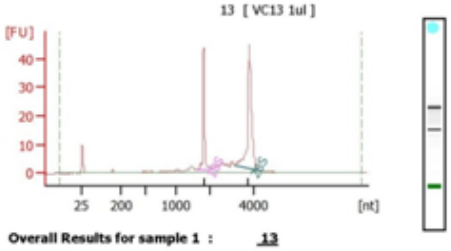

Overall Results for sample 1 : 13

RNA Area:	170.0
RNA Concentration:	141 ng/µl
rRNA Ratio [28s / 18s]:	1.9
RNA Integrity Number (RIN):	9.3 (B.02.08)
Result Flagging Color:	
Result Flagging Label:	High Quality RNA - RIN: 9.30

Fragment table for sample 1 : 13

Name	Start Size [nt]	End Size [nt]	Area	% of total Area
18S	1,609	2,099	34.2	20.1
28S	3,150	4,381	64.9	38.2

14 [VC14 1ul]

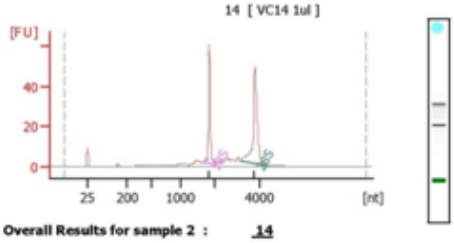

Overall Results for sample 2 : 14

RNA Area:	208.3
RNA Concentration:	172 ng/µl
rRNA Ratio [28s / 18s]:	1.6
RNA Integrity Number (RIN):	9.2 (B.02.08)
Result Flagging Color:	
Result Flagging Label:	High Quality RNA - RIN: 9.20

Fragment table for sample 2 : 14

Name	Start Size [nt]	End Size [nt]	Area	% of total Area
18S	1,594	2,102	47.1	22.6
28S	3,148	4,332	74.0	35.5

15 [VC15 1ul]

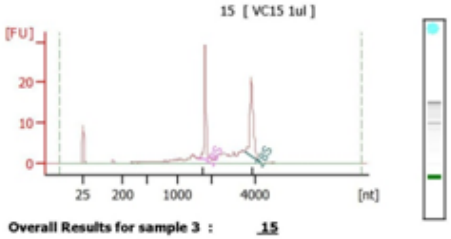

Overall Results for sample 3 : 15

RNA Area:	111.0
RNA Concentration:	92 ng/µl
rRNA Ratio [28s / 18s]:	1.1
RNA Integrity Number (RIN):	8.4 (B.02.08)
Result Flagging Color:	
Result Flagging Label:	High Quality RNA - RIN: 8.40

Fragment table for sample 3 : 15

Name	Start Size [nt]	End Size [nt]	Area	% of total Area
18S	1,605	1,923	21.8	19.7
28S	3,532	4,178	23.8	21.5

16 [VC16 1ul]

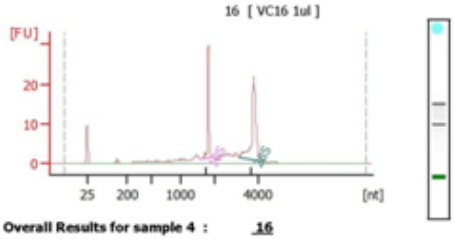

Overall Results for sample 4 : 16

RNA Area:	110.9
RNA Concentration:	92 ng/µl
rRNA Ratio [28s / 18s]:	1.5
RNA Integrity Number (RIN):	8.7 (B.02.08)
Result Flagging Color:	
Result Flagging Label:	High Quality RNA - RIN: 8.70

Fragment table for sample 4 : 16

Name	Start Size [nt]	End Size [nt]	Area	% of total Area
18S	1,583	1,911	21.7	19.6
28S	3,094	4,212	33.1	29.8

Assay Class: Eukaryote Total RNA Nano
Data Path: G:\...Eukaryote Total RNA Nano_DE54700719_2012-07-04_12-01-08.xad

Created: 04/07/2012 12:01:09 PM
Modified: 05/07/2012 3:52:05 PM

Electropherogram Summary Continued ...

17 [VC17 1ul]

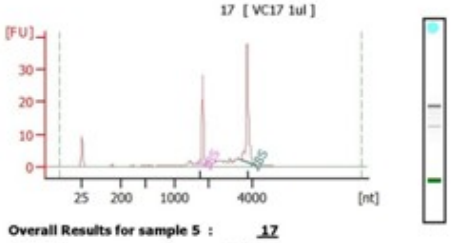

Overall Results for sample 5 : 17

RNA Area:	105.1
RNA Concentration:	87 ng/µl
rRNA Ratio [28s / 18s]:	1.6
RNA Integrity Number (RIN):	9.3 (B.02.08)
Result Flagging Color:	
Result Flagging Label:	High Quality RNA - RIN: 9.30

Fragment table for sample 5 : 17

Name	Start Size [nt]	End Size [nt]	Area	% of total Area
18S	1,588	1,918	20.8	19.8
28S	3,442	4,163	34.2	32.6

18 [VC18 1ul]

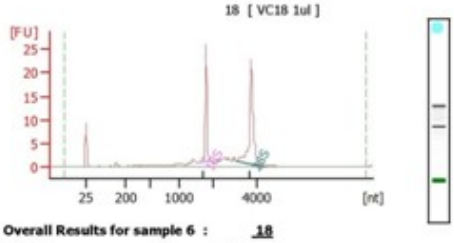

Overall Results for sample 6 : 18

RNA Area:	92.5
RNA Concentration:	77 ng/µl
rRNA Ratio [28s / 18s]:	1.7
RNA Integrity Number (RIN):	9.2 (B.02.08)
Result Flagging Color:	
Result Flagging Label:	High Quality RNA - RIN: 9.20

Fragment table for sample 6 : 18

Name	Start Size [nt]	End Size [nt]	Area	% of total Area
18S	1,587	1,899	18.9	20.5
28S	3,083	4,347	32.7	35.3

19 [VC19 1ul]

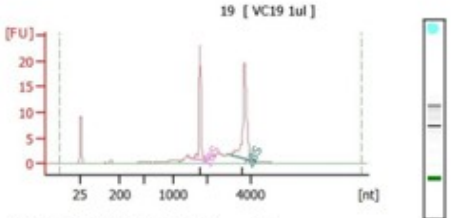

Overall Results for sample 7 : 19

RNA Area:	87.6
RNA Concentration:	72 ng/µl
rRNA Ratio [28s / 18s]:	1.5
RNA Integrity Number (RIN):	9.1 (B.02.08)
Result Flagging Color:	
Result Flagging Label:	High Quality RNA - RIN: 9.10

Fragment table for sample 7 : 19

Name	Start Size [nt]	End Size [nt]	Area	% of total Area
18S	1,581	2,023	19.0	21.7
28S	3,044	4,288	29.3	33.4

20 [VC20 1ul]

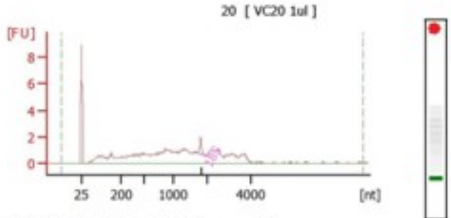

Overall Results for sample 8 : 20

RNA Area:	49.5
RNA Concentration:	41 ng/µl
rRNA Ratio [28s / 18s]:	0.0
RNA Integrity Number (RIN):	4.3 (B.02.08)
Result Flagging Color:	
Result Flagging Label:	Low Quality RNA

Fragment table for sample 8 : 20

Name	Start Size [nt]	End Size [nt]	Area	% of total Area
18S	1,726	1,976	1.1	2.3

Assay Class: Eukaryote Total RNA Nano
Data Path: G:\...Eukaryote Total RNA Nano_DE54700719_2012-07-04_12-01-08.xad

Created: 04/07/2012 12:01:09 PM
Modified: 05/07/2012 3:52:05 PM

Electropherogram Summary Continued ...

21 [VC21 1ul]

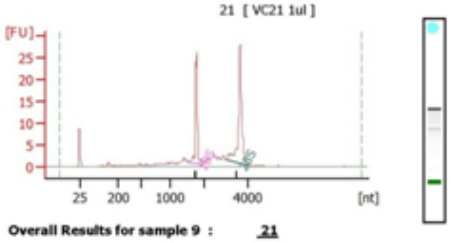

Overall Results for sample 9 : 21

RNA Area:	106.5
RNA Concentration:	88 ng/µl
rRNA Ratio [28s / 18s]:	1.6
RNA Integrity Number (RIN):	8.9 (B.02.08)
Result Flagging Color:	
Result Flagging Label:	High Quality RNA - RIN: 8.90

Fragment table for sample 9 : 21

Name	Start Size [nt]	End Size [nt]	Area	% of total Area
18S	1,527	1,983	21.5	20.2
28S	3,005	4,048	35.4	33.3

22 [VC22 1ul]

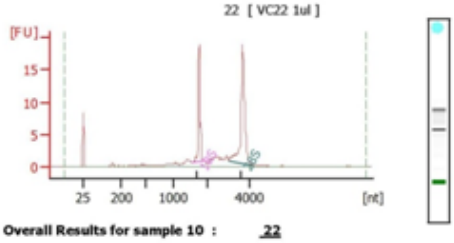

Overall Results for sample 10 : 22

RNA Area:	73.1
RNA Concentration:	60 ng/µl
rRNA Ratio [28s / 18s]:	1.9
RNA Integrity Number (RIN):	9.2 (B.02.08)
Result Flagging Color:	
Result Flagging Label:	High Quality RNA - RIN: 9.20

Fragment table for sample 10 : 22

Name	Start Size [nt]	End Size [nt]	Area	% of total Area
18S	1,558	1,868	13.7	18.8
28S	3,021	4,143	26.6	36.3

23 [VC23 1ul]

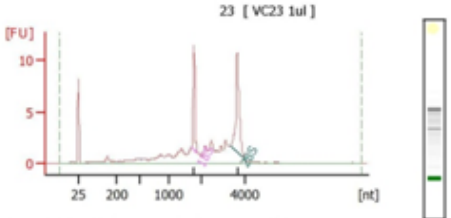

Overall Results for sample 11 : 23

RNA Area:	71.3
RNA Concentration:	59 ng/µl
rRNA Ratio [28s / 18s]:	1.8
RNA Integrity Number (RIN):	7.5 (B.02.08)
Result Flagging Color:	
Result Flagging Label:	Medium Quality RNA - RIN: 7.50

Fragment table for sample 11 : 23

Name	Start Size [nt]	End Size [nt]	Area	% of total Area
18S	1,707	1,867	7.4	10.4
28S	3,335	4,075	13.1	18.4

24 [VC24 1ul]

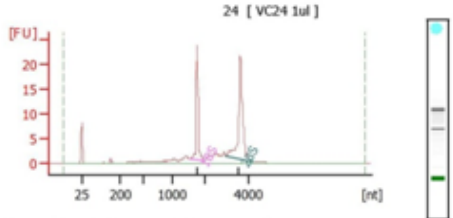

Overall Results for sample 12 : 24

RNA Area:	96.5
RNA Concentration:	80 ng/µl
rRNA Ratio [28s / 18s]:	1.7
RNA Integrity Number (RIN):	9.1 (B.02.08)
Result Flagging Color:	
Result Flagging Label:	High Quality RNA - RIN: 9.10

Fragment table for sample 12 : 24

Name	Start Size [nt]	End Size [nt]	Area	% of total Area
18S	1,538	1,979	19.7	20.4
28S	2,951	4,189	33.2	34.4

Assay Class: Eukaryote Total RNA Nano
Data Path: G:\...Eukaryote Total RNA Nano_DE24802266_2012-07-04_14-15-44.xad

Created: 04/07/2012 2:15:43 PM
Modified: 05/07/2012 3:54:11 PM

Electropherogram Summary

25 [VC25 1ul]

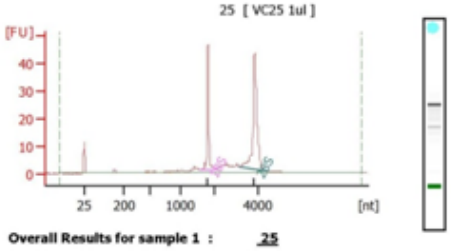

Overall Results for sample 1 : 25

RNA Area:	172.2
RNA Concentration:	110 ng/µl
rRNA Ratio [28s / 18s]:	1.7
RNA Integrity Number (RIN):	9.4 (B.02.08)
Result Flagging Color:	
Result Flagging Label:	High Quality RNA - RIN: 9.40

Fragment table for sample 1 : 25

Name	Start Size [nt]	End Size [nt]	Area	% of total Area
18S	1,585	2,071	37.4	21.7
28S	3,115	4,474	65.0	37.8

26 [VC26 1ul]

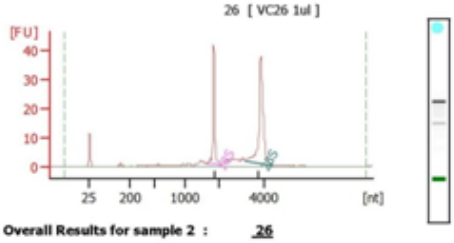

Overall Results for sample 2 : 26

RNA Area:	149.6
RNA Concentration:	95 ng/µl
rRNA Ratio [28s / 18s]:	1.7
RNA Integrity Number (RIN):	9.4 (B.02.08)
Result Flagging Color:	
Result Flagging Label:	High Quality RNA - RIN: 9.40

Fragment table for sample 2 : 26

Name	Start Size [nt]	End Size [nt]	Area	% of total Area
18S	1,625	2,101	32.9	22.0
28S	3,167	4,412	56.8	38.0

27 [VC27 1ul]

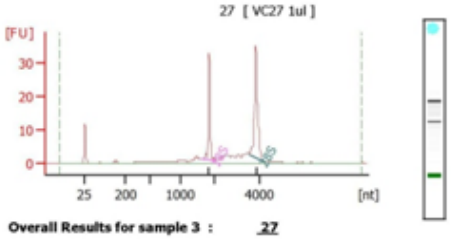

Overall Results for sample 3 : 27

RNA Area:	123.7
RNA Concentration:	79 ng/µl
rRNA Ratio [28s / 18s]:	1.5
RNA Integrity Number (RIN):	9 (B.02.08)
Result Flagging Color:	
Result Flagging Label:	High Quality RNA - RIN:9

Fragment table for sample 3 : 27

Name	Start Size [nt]	End Size [nt]	Area	% of total Area
18S	1,606	2,073	26.0	21.0
28S	3,509	4,193	38.2	30.9

28 [VC28 1ul]

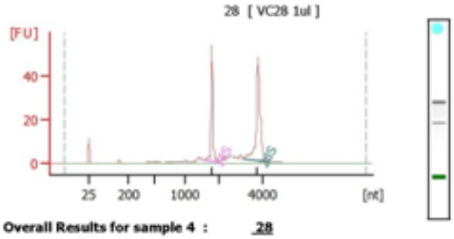

Overall Results for sample 4 : 28

RNA Area:	178.3
RNA Concentration:	113 ng/µl
rRNA Ratio [28s / 18s]:	1.7
RNA Integrity Number (RIN):	9.4 (B.02.08)
Result Flagging Color:	
Result Flagging Label:	High Quality RNA - RIN: 9.40

Fragment table for sample 4 : 28

Name	Start Size [nt]	End Size [nt]	Area	% of total Area
18S	1,576	2,057	41.2	23.1
28S	3,128	4,296	68.9	38.6

Assay Class: Eukaryote Total RNA Nano
Data Path: G:\...Eukaryote Total RNA Nano_DE24802266_2012-07-04_14-15-44.xad

Created: 04/07/2012 2:15:43 PM
Modified: 05/07/2012 3:54:11 PM

Electropherogram Summary Continued ...

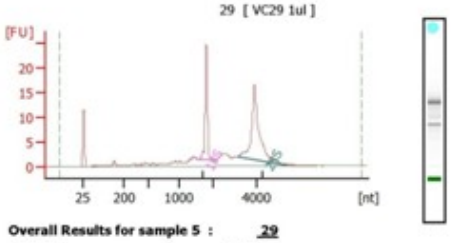

Overall Results for sample 5 : 29

RNA Area:	132.6
RNA Concentration:	84 ng/µl
rRNA Ratio [28s / 18s]:	1.8
RNA Integrity Number (RIN):	9 (B.02.08)
Result Flagging Color:	
Result Flagging Label:	High Quality RNA - RIN:9

Fragment table for sample 5 : 29

Name	Start Size [nt]	End Size [nt]	Area	% of total Area
18S	1,561	1,944	23.1	17.4
28S	3,187	5,426	41.3	31.2

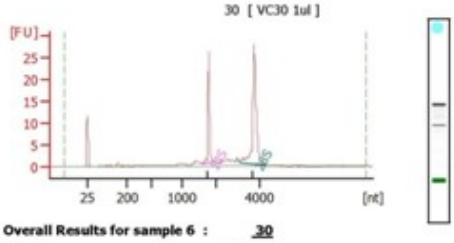

Overall Results for sample 6 : 30

RNA Area:	88.6
RNA Concentration:	56 ng/µl
rRNA Ratio [28s / 18s]:	2.0
RNA Integrity Number (RIN):	9.4 (B.02.08)
Result Flagging Color:	
Result Flagging Label:	High Quality RNA - RIN: 9.40

Fragment table for sample 6 : 30

Name	Start Size [nt]	End Size [nt]	Area	% of total Area
18S	1,603	1,896	18.5	20.9
28S	3,106	4,341	36.3	41.0

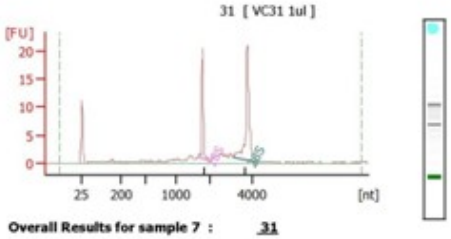

Overall Results for sample 7 : 31

RNA Area:	76.9
RNA Concentration:	49 ng/µl
rRNA Ratio [28s / 18s]:	1.7
RNA Integrity Number (RIN):	9 (B.02.08)
Result Flagging Color:	
Result Flagging Label:	High Quality RNA - RIN:9

Fragment table for sample 7 : 31

Name	Start Size [nt]	End Size [nt]	Area	% of total Area
18S	1,653	2,019	15.5	20.2
28S	3,109	4,143	26.8	34.8

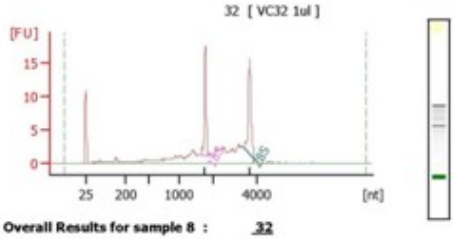

Overall Results for sample 8 : 32

RNA Area:	89.4
RNA Concentration:	57 ng/µl
rRNA Ratio [28s / 18s]:	1.1
RNA Integrity Number (RIN):	7.7 (B.02.08)
Result Flagging Color:	
Result Flagging Label:	Medium Quality RNA - RIN: 7.70

Fragment table for sample 8 : 32

Name	Start Size [nt]	End Size [nt]	Area	% of total Area
18S	1,622	1,872	13.1	14.7
28S	3,434	3,981	15.1	16.9

Assay Class: Eukaryote Total RNA Nano
Data Path: G:\...Eukaryote Total RNA Nano_DE24802266_2012-07-04_14-15-44.xad

Created: 04/07/2012 2:15:43 PM
Modified: 05/07/2012 3:54:11 PM

Electropherogram Summary Continued ...

33 [VC33 1ul]

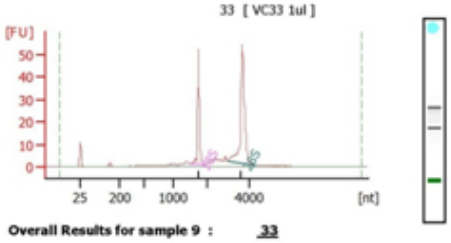

Overall Results for sample 9 : 33

RNA Area:	191.4
RNA Concentration:	122 ng/µl
rRNA Ratio [28s / 18s]:	2.0
RNA Integrity Number (RIN):	9.5 (B.02.08)
Result Flagging Color:	
Result Flagging Label:	High Quality RNA - RIN: 9.50

Fragment table for sample 9 : 33

Name	Start Size [nt]	End Size [nt]	Area	% of total Area
18S	1,552	1,989	41.0	21.4
28S	3,001	4,258	80.5	42.1

34 [VC34 1ul]

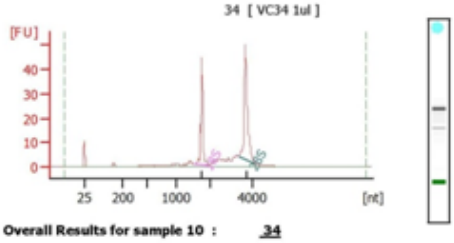

Overall Results for sample 10 : 34

RNA Area:	170.3
RNA Concentration:	108 ng/µl
rRNA Ratio [28s / 18s]:	1.7
RNA Integrity Number (RIN):	9.4 (B.02.08)
Result Flagging Color:	
Result Flagging Label:	High Quality RNA - RIN: 9.40

Fragment table for sample 10 : 34

Name	Start Size [nt]	End Size [nt]	Area	% of total Area
18S	1,539	1,978	36.8	21.6
28S	3,371	4,137	61.2	35.9

35 [VC35 1ul]

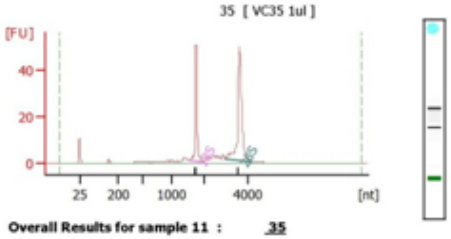

Overall Results for sample 11 : 35

RNA Area:	187.0
RNA Concentration:	119 ng/µl
rRNA Ratio [28s / 18s]:	1.8
RNA Integrity Number (RIN):	9.4 (B.02.08)
Result Flagging Color:	
Result Flagging Label:	High Quality RNA - RIN: 9.40

Fragment table for sample 11 : 35

Name	Start Size [nt]	End Size [nt]	Area	% of total Area
18S	1,527	1,958	40.9	21.9
28S	2,961	4,212	74.4	39.8

36 [VC36 1ul]

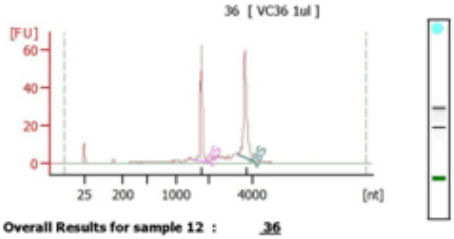

Overall Results for sample 12 : 36

RNA Area:	222.0
RNA Concentration:	141 ng/µl
rRNA Ratio [28s / 18s]:	1.4
RNA Integrity Number (RIN):	9.1 (B.02.08)
Result Flagging Color:	
Result Flagging Label:	High Quality RNA - RIN: 9.10

Fragment table for sample 12 : 36

Name	Start Size [nt]	End Size [nt]	Area	% of total Area
18S	1,537	1,977	51.5	23.2
28S	3,359	4,141	70.5	31.8

Assay Class: Eukaryote Total RNA Nano
Data Path: G:\...Eukaryote Total RNA Nano_DE54700719_2012-07-04_14-23-03.xad

Created: 04/07/2012 2:23:03 PM
Modified: 05/07/2012 3:55:42 PM

Electropherogram Summary

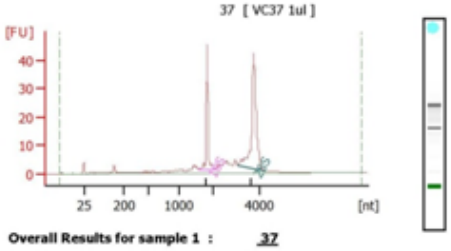

Overall Results for sample 1 : 37

RNA Area:	185.9
RNA Concentration:	178 ng/µl
rRNA Ratio [28s / 18s]:	1.9
RNA Integrity Number (RIN):	9.3 (B.02.08)
Result Flagging Color:	
Result Flagging Label:	High Quality RNA - RIN: 9.30

Fragment table for sample 1 : 37

Name	Start Size [nt]	End Size [nt]	Area	% of total Area
18S	1,572	2,042	37.3	20.1
28S	3,091	4,259	69.7	37.5

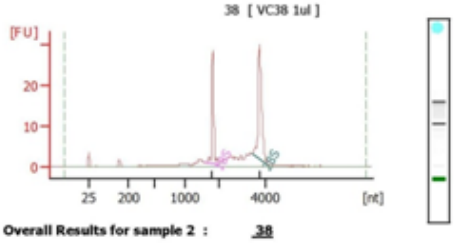

Overall Results for sample 2 : 38

RNA Area:	120.2
RNA Concentration:	115 ng/µl
rRNA Ratio [28s / 18s]:	1.5
RNA Integrity Number (RIN):	9.1 (B.02.08)
Result Flagging Color:	
Result Flagging Label:	High Quality RNA - RIN: 9.10

Fragment table for sample 2 : 38

Name	Start Size [nt]	End Size [nt]	Area	% of total Area
18S	1,557	2,031	24.2	20.1
28S	3,459	4,146	36.8	30.6

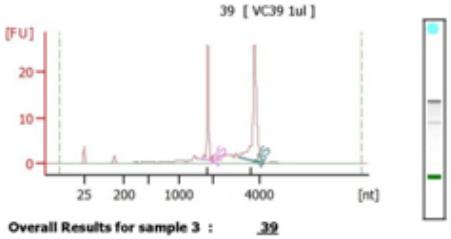

Overall Results for sample 3 : 39

RNA Area:	99.5
RNA Concentration:	95 ng/µl
rRNA Ratio [28s / 18s]:	1.8
RNA Integrity Number (RIN):	9.2 (B.02.08)
Result Flagging Color:	
Result Flagging Label:	High Quality RNA - RIN: 9.20

Fragment table for sample 3 : 39

Name	Start Size [nt]	End Size [nt]	Area	% of total Area
18S	1,574	2,056	20.9	21.0
28S	3,103	4,189	37.1	37.3

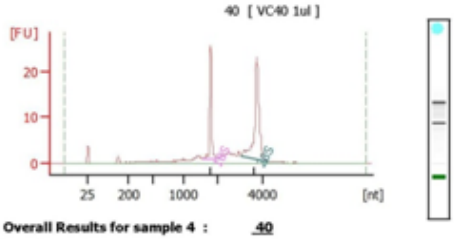

Overall Results for sample 4 : 40

RNA Area:	110.3
RNA Concentration:	106 ng/µl
rRNA Ratio [28s / 18s]:	1.8
RNA Integrity Number (RIN):	8.9 (B.02.08)
Result Flagging Color:	
Result Flagging Label:	High Quality RNA - RIN: 8.90

Fragment table for sample 4 : 40

Name	Start Size [nt]	End Size [nt]	Area	% of total Area
18S	1,561	2,014	20.7	18.7
28S	3,052	4,223	36.9	33.4

Assay Class: Eukaryote Total RNA Nano
Data Path: G:\...Eukaryote Total RNA Nano_DE54700719_2012-07-04_14-23-03.xad

Created: 04/07/2012 2:23:03 PM
Modified: 05/07/2012 3:55:42 PM

Electropherogram Summary Continued ...

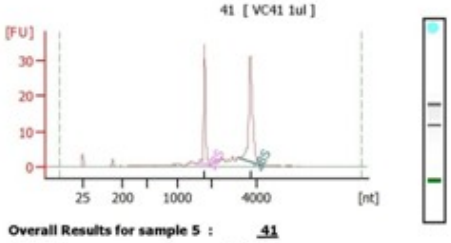

Overall Results for sample 5 : 41

RNA Area:	120.6
RNA Concentration:	115 ng/µl
rRNA Ratio [28s / 18s]:	1.6
RNA Integrity Number (RIN):	9.3 (B.02.08)
Result Flagging Color:	
Result Flagging Label:	High Quality RNA - RIN: 9.30

Fragment table for sample 5 : 41

Name	Start Size [nt]	End Size [nt]	Area	% of total Area
18S	1,548	2,012	27.7	23.0
28S	3,241	4,230	44.6	37.0

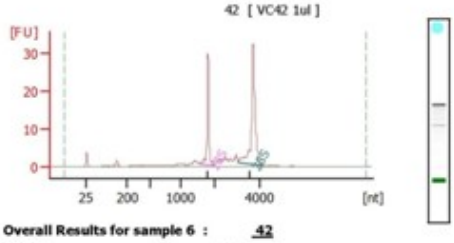

Overall Results for sample 6 : 42

RNA Area:	117.6
RNA Concentration:	113 ng/µl
rRNA Ratio [28s / 18s]:	1.8
RNA Integrity Number (RIN):	9.3 (B.02.08)
Result Flagging Color:	
Result Flagging Label:	High Quality RNA - RIN: 9.30

Fragment table for sample 6 : 42

Name	Start Size [nt]	End Size [nt]	Area	% of total Area
18S	1,544	1,997	24.1	20.5
28S	3,015	4,089	43.7	37.2

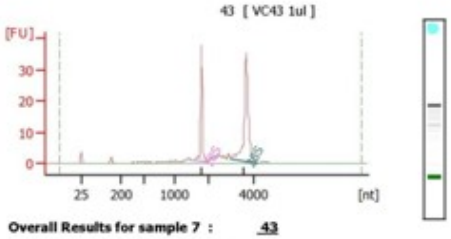

Overall Results for sample 7 : 43

RNA Area:	133.9
RNA Concentration:	128 ng/µl
rRNA Ratio [28s / 18s]:	1.8
RNA Integrity Number (RIN):	9.3 (B.02.08)
Result Flagging Color:	
Result Flagging Label:	High Quality RNA - RIN: 9.30

Fragment table for sample 7 : 43

Name	Start Size [nt]	End Size [nt]	Area	% of total Area
18S	1,548	1,985	30.1	22.5
28S	3,005	4,180	53.6	40.0

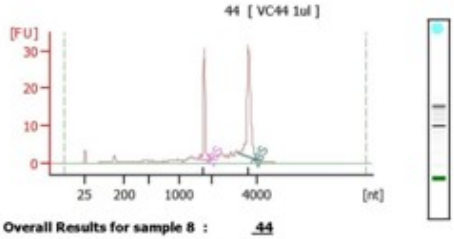

Overall Results for sample 8 : 44

RNA Area:	141.5
RNA Concentration:	136 ng/µl
rRNA Ratio [28s / 18s]:	1.6
RNA Integrity Number (RIN):	8.7 (B.02.08)
Result Flagging Color:	
Result Flagging Label:	High Quality RNA - RIN: 8.70

Fragment table for sample 8 : 44

Name	Start Size [nt]	End Size [nt]	Area	% of total Area
18S	1,525	1,964	26.1	18.4
28S	3,169	4,064	41.3	29.2

Assay Class: Eukaryote Total RNA Nano
Data Path: G:\...Eukaryote Total RNA Nano_DE54700719_2012-07-04_14-23-03.xad

Created: 04/07/2012 2:23:03 PM
Modified: 05/07/2012 3:55:42 PM

Electropherogram Summary Continued ...

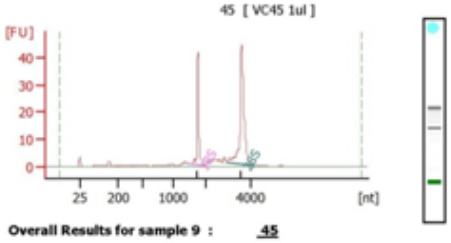

Overall Results for sample 9 : 45

RNA Area:	158.0
RNA Concentration:	151 ng/µl
rRNA Ratio [28s / 18s]:	2.0
RNA Integrity Number (RIN):	9.6 (B.02.08)
Result Flagging Color:	
Result Flagging Label:	High Quality RNA - RIN: 9.60

Fragment table for sample 9 : 45

Name	Start Size [nt]	End Size [nt]	Area	% of total Area
18S	1,548	1,971	34.0	21.5
28S	2,954	4,129	67.8	42.9

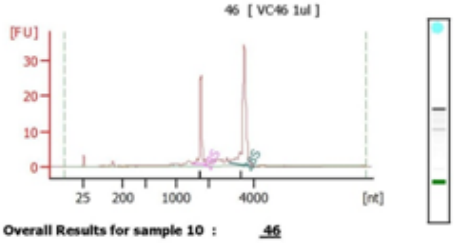

Overall Results for sample 10 : 46

RNA Area:	105.7
RNA Concentration:	101 ng/µl
rRNA Ratio [28s / 18s]:	2.1
RNA Integrity Number (RIN):	9.5 (B.02.08)
Result Flagging Color:	
Result Flagging Label:	High Quality RNA - RIN: 9.50

Fragment table for sample 10 : 46

Name	Start Size [nt]	End Size [nt]	Area	% of total Area
18S	1,506	1,940	20.9	19.8
28S	2,928	4,025	44.6	42.2

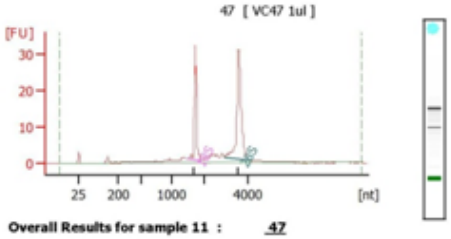

Overall Results for sample 11 : 47

RNA Area:	134.0
RNA Concentration:	128 ng/µl
rRNA Ratio [28s / 18s]:	1.9
RNA Integrity Number (RIN):	9.3 (B.02.08)
Result Flagging Color:	
Result Flagging Label:	High Quality RNA - RIN: 9.30

Fragment table for sample 11 : 47

Name	Start Size [nt]	End Size [nt]	Area	% of total Area
18S	1,495	1,930	27.4	20.5
28S	2,929	4,139	52.0	38.8

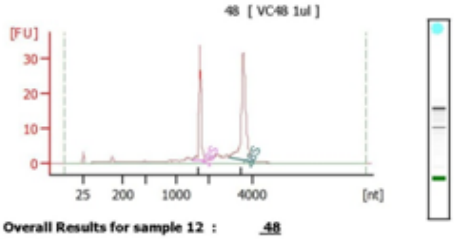

Overall Results for sample 12 : 48

RNA Area:	145.4
RNA Concentration:	139 ng/µl
rRNA Ratio [28s / 18s]:	1.9
RNA Integrity Number (RIN):	9 (B.02.08)
Result Flagging Color:	
Result Flagging Label:	High Quality RNA - RIN:9

Fragment table for sample 12 : 48

Name	Start Size [nt]	End Size [nt]	Area	% of total Area
18S	1,514	1,939	28.4	19.5
28S	2,915	4,070	52.7	36.3

13.2 Appendix II – WBC RNA Quality Assessment via Bioanalyser

Assay Class: Eukaryote Total RNA Nano
Data Path: C:\...Eukaryote Total RNA Nano_DE72904889_2011-10-24_13-38-26.xad

Created: 10/24/2011 1:38:25 PM
Modified: 10/24/2011 2:02:17 PM

Electropherogram Summary

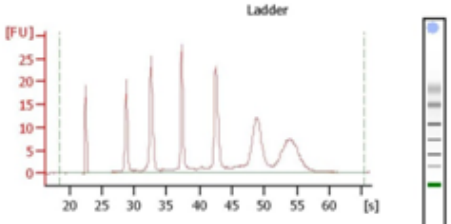

Overall Results for Ladder

RNA Area:	271.3
RNA Concentration:	150 ng/µl
Result Flagging Color:	
Result Flagging Label:	All Other Samples

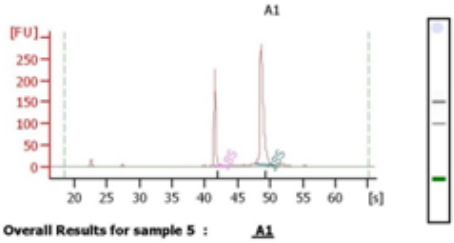

Overall Results for sample 5 : A1

RNA Area:	630.3
RNA Concentration:	348 ng/µl
rRNA Ratio [28s / 18s]:	2.1
RNA Integrity Number (RIN):	10 (B.02.08)
Result Flagging Color:	
Result Flagging Label:	RIN:10

Fragment table for sample 5 : A1

Name	Start Time [s]	End Time [s]	Area	% of total Area
18S	41.17	42.78	169.3	26.9
28S	47.65	50.96	353.7	56.1

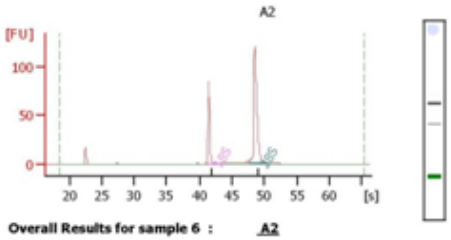

Overall Results for sample 6 : A2

RNA Area:	243.7
RNA Concentration:	135 ng/µl
rRNA Ratio [28s / 18s]:	2.1
RNA Integrity Number (RIN):	10 (B.02.08)
Result Flagging Color:	
Result Flagging Label:	RIN:10

Fragment table for sample 6 : A2

Name	Start Time [s]	End Time [s]	Area	% of total Area
18S	41.16	42.67	63.1	25.9
28S	47.61	50.65	134.7	55.3

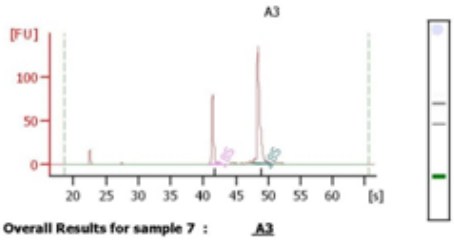

Overall Results for sample 7 : A3

RNA Area:	237.5
RNA Concentration:	131 ng/µl
rRNA Ratio [28s / 18s]:	2.4
RNA Integrity Number (RIN):	10 (B.02.08)
Result Flagging Color:	
Result Flagging Label:	RIN:10

Fragment table for sample 7 : A3

Name	Start Time [s]	End Time [s]	Area	% of total Area
18S	41.10	42.72	58.9	24.8
28S	47.52	50.61	139.5	58.7

Assay Class: Eukaryote Total RNA Nano
Data Path: C:\...Eukaryote Total RNA Nano_DE72904889_2011-10-24_13-38-26.xad

Created: 10/24/2011 1:38:25 PM
Modified: 10/24/2011 2:02:17 PM

Electropherogram Summary Continued ...

A4

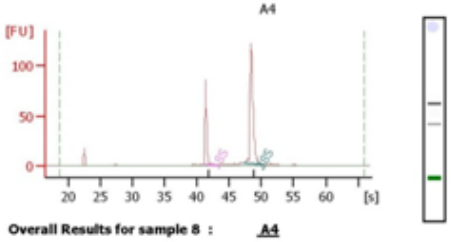

Overall Results for sample 8 : A4

RNA Area:	244.3
RNA Concentration:	135 ng/µl
rRNA Ratio [28s / 18s]:	2.1
RNA Integrity Number (RIN):	10 (B.02.08)
Result Flagging Color:	
Result Flagging Label:	RIN:10

Fragment table for sample 8 : A4

Name	Start Time [s]	End Time [s]	Area	% of total Area
18S	41.03	42.65	62.8	25.7
28S	47.30	50.36	133.3	54.6

A5

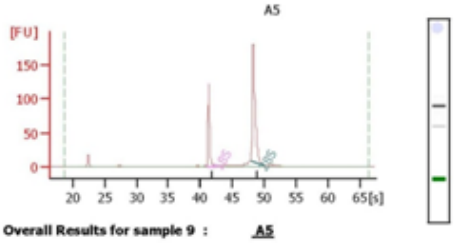

Overall Results for sample 9 : A5

RNA Area:	353.4
RNA Concentration:	195 ng/µl
rRNA Ratio [28s / 18s]:	2.0
RNA Integrity Number (RIN):	10 (B.02.08)
Result Flagging Color:	
Result Flagging Label:	RIN:10

Fragment table for sample 9 : A5

Name	Start Time [s]	End Time [s]	Area	% of total Area
18S	40.96	42.50	93.7	26.5
28S	47.88	50.00	183.1	51.8

A6

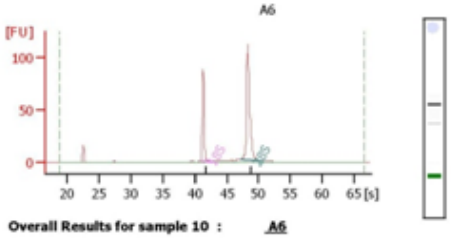

Overall Results for sample 10 : A6

RNA Area:	254.0
RNA Concentration:	140 ng/µl
rRNA Ratio [28s / 18s]:	2.1
RNA Integrity Number (RIN):	10 (B.02.08)
Result Flagging Color:	
Result Flagging Label:	RIN:10

Fragment table for sample 10 : A6

Name	Start Time [s]	End Time [s]	Area	% of total Area
18S	40.99	42.49	64.5	25.4
28S	47.17	50.55	134.3	52.9

A7

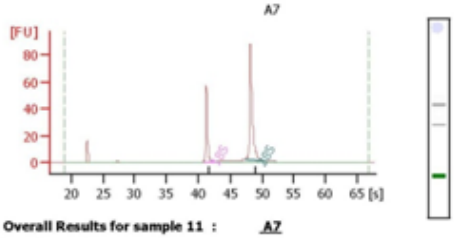

Overall Results for sample 11 : A7

RNA Area:	175.5
RNA Concentration:	97 ng/µl
rRNA Ratio [28s / 18s]:	2.1
RNA Integrity Number (RIN):	10 (B.02.08)
Result Flagging Color:	
Result Flagging Label:	RIN:10

Fragment table for sample 11 : A7

Name	Start Time [s]	End Time [s]	Area	% of total Area
18S	40.98	42.58	43.6	24.9
28S	47.28	50.48	92.8	52.9

Assay Class: Eukaryote Total RNA Nano
Data Path: C:\...Eukaryote Total RNA Nano_DE72904889_2011-10-24_13-38-26.xad

Created: 10/24/2011 1:38:25 PM
Modified: 10/24/2011 2:02:17 PM

Electropherogram Summary Continued ...

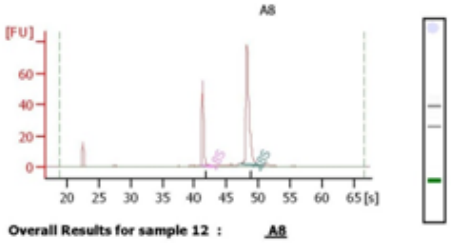

Overall Results for sample 12 : A8

RNA Area:	162.5
RNA Concentration:	90 ng/µl
rRNA Ratio [28s / 18s]:	2.2
RNA Integrity Number (RIN):	10 (B.02.08)
Result Flagging Color:	
Result Flagging Label:	RIN:10

Fragment table for sample 12 : A8

Name	Start Time [s]	End Time [s]	Area	% of total Area
18S	40.98	42.58	40.0	24.6
28S	47.27	50.66	89.7	55.2

Assay Class: EukaryoteTotal RNA Nano
Data Path: C:\..._EukaryoteTotal RNA Nano_DE02000304_2011-10-24_14-02-12.xad

Created: 10/24/2011 2:02:12 PM
Modified: 10/24/2011 2:25:21 PM

Electropherogram Summary

Ladder

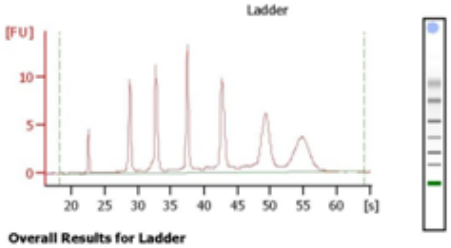

Overall Results for Ladder

RNA Area:	123.1
RNA Concentration:	150 ng/µl
Result Flagging Color:	
Result Flagging Label:	All Other Samples

A9

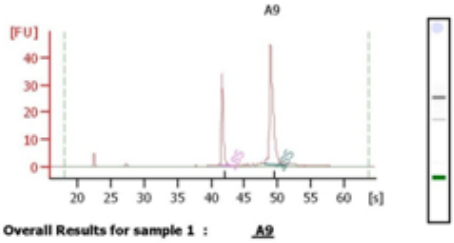

Overall Results for sample 1 : A9

RNA Area:	111.6
RNA Concentration:	136 ng/µl
rRNA Ratio [28s / 18s]:	2.0
RNA Integrity Number (RIN):	10 (A.01.01)
Result Flagging Color:	
Result Flagging Label:	RIN:10

Fragment table for sample 1 : A9

Name	Start Time [s]	End Time [s]	Area	% of total Area
18S	41.35	42.92	27.6	24.8
28S	47.96	51.28	56.3	50.5

A10

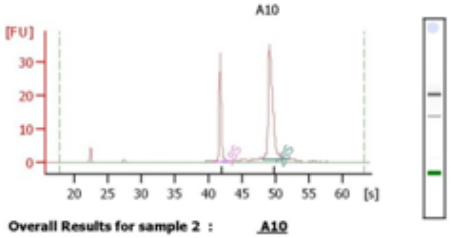

Overall Results for sample 2 : A10

RNA Area:	104.9
RNA Concentration:	128 ng/µl
rRNA Ratio [28s / 18s]:	1.9
RNA Integrity Number (RIN):	10 (A.01.01)
Result Flagging Color:	
Result Flagging Label:	RIN:10

Fragment table for sample 2 : A10

Name	Start Time [s]	End Time [s]	Area	% of total Area
18S	40.74	43.08	27.5	26.2
28S	48.07	51.64	52.7	50.3

A11

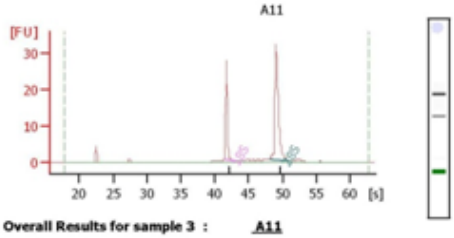

Overall Results for sample 3 : A11

RNA Area:	83.1
RNA Concentration:	101 ng/µl
rRNA Ratio [28s / 18s]:	1.8
RNA Integrity Number (RIN):	10 (A.01.01)
Result Flagging Color:	
Result Flagging Label:	RIN:10

Fragment table for sample 3 : A11

Name	Start Time [s]	End Time [s]	Area	% of total Area
18S	41.36	42.95	21.0	25.3
28S	48.05	51.19	38.1	45.8

Assay Class: EukaryoteTotal RNA Nano
Data Path: C:\..._EukaryoteTotal RNA Nano_DE02000304_2011-10-24_14-02-12.xad

Created: 10/24/2011 2:02:12 PM
Modified: 10/24/2011 2:25:21 PM

Electropherogram Summary Continued ...

A12

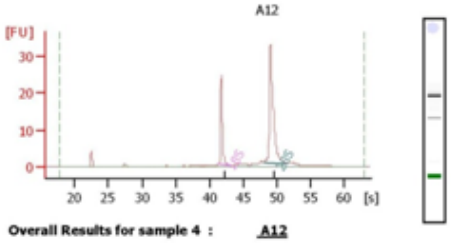

Overall Results for sample 4 : A12

RNA Area:	89.7
RNA Concentration:	109 ng/µl
rRNA Ratio [28s / 18s]:	2.1
RNA Integrity Number (RIN):	10 (A.01.01)
Result Flagging Color:	
Result Flagging Label:	RIN:10

Fragment table for sample 4 : A12

Name	Start Time [s]	End Time [s]	Area	% of total Area
18S	41.35	43.08	19.9	22.2
28S	48.06	51.34	42.5	47.4

A13

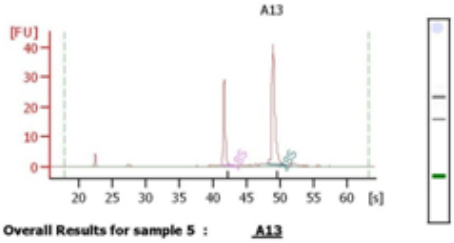

Overall Results for sample 5 : A13

RNA Area:	84.8
RNA Concentration:	103 ng/µl
rRNA Ratio [28s / 18s]:	1.9
RNA Integrity Number (RIN):	10 (A.01.01)
Result Flagging Color:	
Result Flagging Label:	RIN:10

Fragment table for sample 5 : A13

Name	Start Time [s]	End Time [s]	Area	% of total Area
18S	41.29	42.96	22.2	26.2
28S	47.93	50.96	41.3	48.7

A14

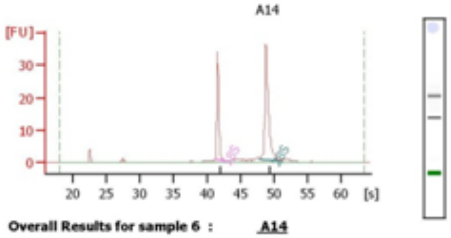

Overall Results for sample 6 : A14

RNA Area:	100.3
RNA Concentration:	122 ng/µl
rRNA Ratio [28s / 18s]:	1.7
RNA Integrity Number (RIN):	9.9 (A.01.01)
Result Flagging Color:	
Result Flagging Label:	RIN: 9.90

Fragment table for sample 6 : A14

Name	Start Time [s]	End Time [s]	Area	% of total Area
18S	41.27	42.79	26.5	26.4
28S	47.90	51.18	45.1	44.9

A15

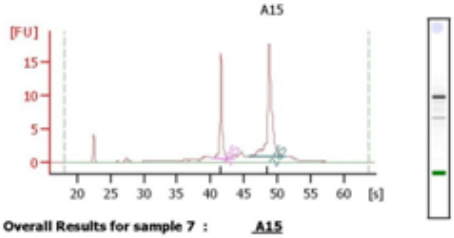

Overall Results for sample 7 : A15

RNA Area:	79.3
RNA Concentration:	97 ng/µl
rRNA Ratio [28s / 18s]:	1.9
RNA Integrity Number (RIN):	9.2 (A.01.01)
Result Flagging Color:	
Result Flagging Label:	RIN: 9.20

Fragment table for sample 7 : A15

Name	Start Time [s]	End Time [s]	Area	% of total Area
18S	40.32	42.78	14.4	18.1
28S	45.74	51.30	27.8	35.1

Assay Class: EukaryoteTotal RNA Nano
Data Path: C:\..._EukaryoteTotal RNA Nano_DE02000304_2011-10-24_14-02-12.xad

Created: 10/24/2011 2:02:12 PM
Modified: 10/24/2011 2:25:21 PM

Electropherogram Summary Continued ...

A16

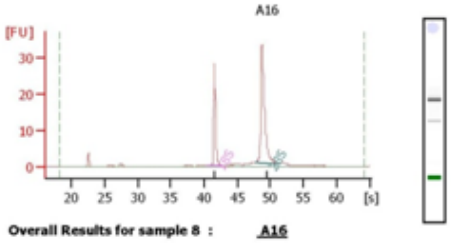

Overall Results for sample 8 : A16

RNA Area:	92.6
RNA Concentration:	113 ng/µl
rRNA Ratio [28s / 18s]:	1.8
RNA Integrity Number (RIN):	10 (A.01.01)
Result Flagging Color:	
Result Flagging Label:	RIN:10

Fragment table for sample 8 : A16

Name	Start Time [s]	End Time [s]	Area	% of total Area
18S	40.34	42.95	23.6	25.5
28S	47.75	51.15	43.4	46.9

A17

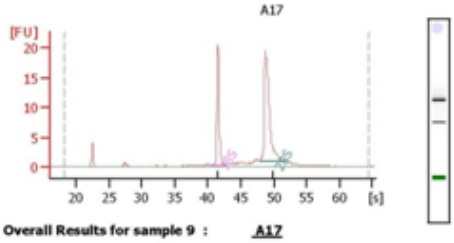

Overall Results for sample 9 : A17

RNA Area:	75.5
RNA Concentration:	92 ng/µl
rRNA Ratio [28s / 18s]:	1.9
RNA Integrity Number (RIN):	9.9 (A.01.01)
Result Flagging Color:	
Result Flagging Label:	RIN: 9.90

Fragment table for sample 9 : A17

Name	Start Time [s]	End Time [s]	Area	% of total Area
18S	40.37	42.85	17.4	23.1
28S	47.85	51.83	33.4	44.2

A18

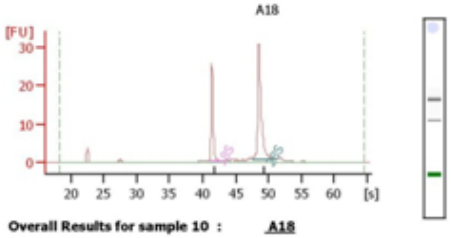

Overall Results for sample 10 : A18

RNA Area:	81.1
RNA Concentration:	99 ng/µl
rRNA Ratio [28s / 18s]:	1.9
RNA Integrity Number (RIN):	10 (A.01.01)
Result Flagging Color:	
Result Flagging Label:	RIN:10

Fragment table for sample 10 : A18

Name	Start Time [s]	End Time [s]	Area	% of total Area
18S	41.11	42.70	20.1	24.8
28S	47.63	51.00	37.9	46.8

A19

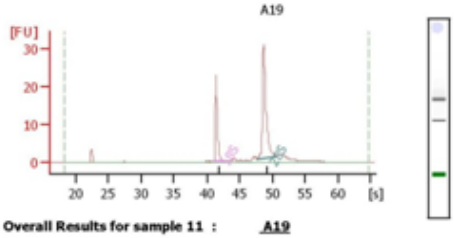

Overall Results for sample 11 : A19

RNA Area:	86.5
RNA Concentration:	105 ng/µl
rRNA Ratio [28s / 18s]:	2.0
RNA Integrity Number (RIN):	10 (A.01.01)
Result Flagging Color:	
Result Flagging Label:	RIN:10

Fragment table for sample 11 : A19

Name	Start Time [s]	End Time [s]	Area	% of total Area
18S	41.05	42.65	20.4	23.5
28S	47.72	50.68	40.5	46.8

Assay Class: EukaryoteTotal RNA Nano
Data Path: C:\..._EukaryoteTotal RNA Nano_DE02000304_2011-10-24_14-02-12.xad

Created: 10/24/2011 2:02:12 PM
Modified: 10/24/2011 2:25:21 PM

Electropherogram Summary Continued ...

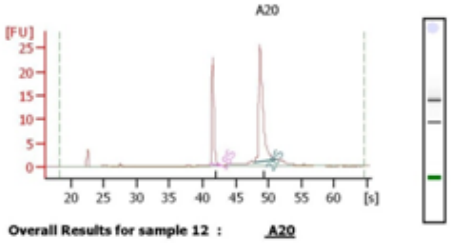

Overall Results for sample 12 : A20

RNA Area:	80.3
RNA Concentration:	98 ng/µl
rRNA Ratio [28s / 18s]:	2.1
RNA Integrity Number (RIN):	10 (A.01.01)
Result Flagging Color:	
Result Flagging Label:	RIN:10

Fragment table for sample 12 : A20

Name	Start Time [s]	End Time [s]	Area	% of total Area
18S	41.20	42.84	18.3	22.7
28S	47.81	51.09	37.6	46.8

13.3 Appendix III – Whole Blood Exposure and DNA Damage Response

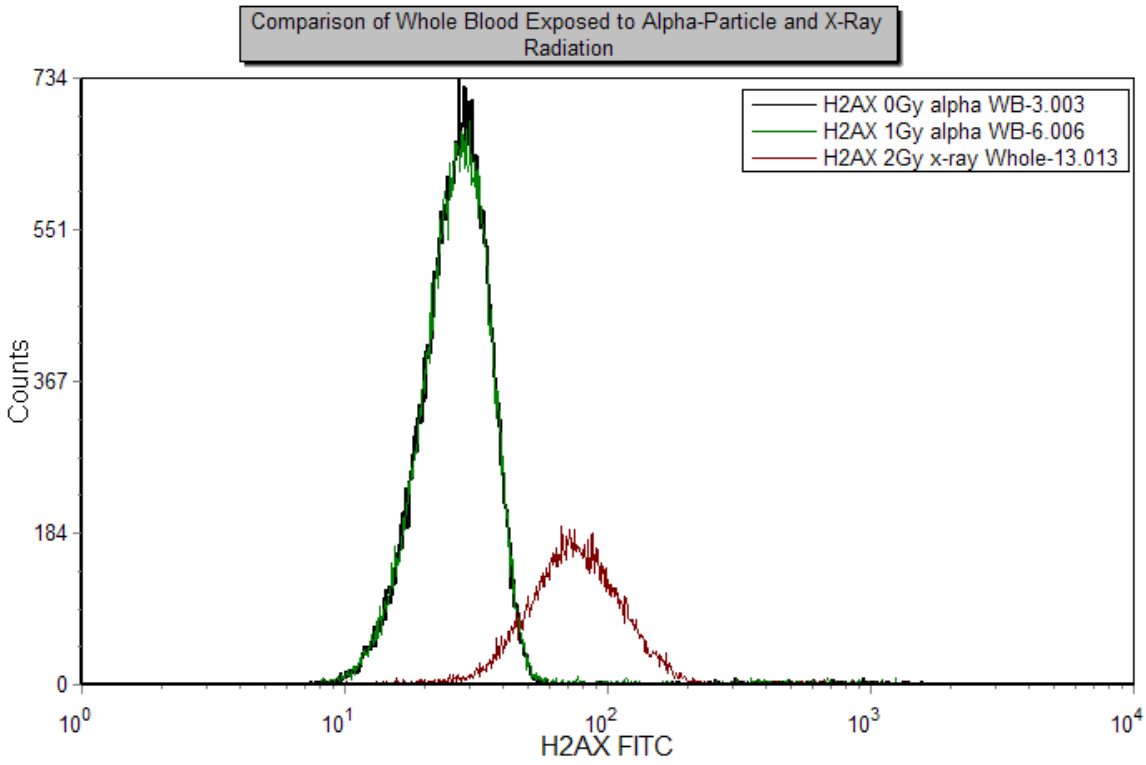

13.4 Appendix IV – Genes Identified as Significant After Alpha-Particle Exposure via Microarray

13.4.1 Low Dose

Dose	0.5 Gy Alpha		1.0 Gy Alpha		1.5 Gy Alpha	
Symbol	FC	PV	FC	PV	FC	PV
DDB2	3.56	0.00	4.41	0.00	5.49	0.00
ISG20L1	3.63	0.00	4.45	0.00	5.23	0.00
PHLDA3	3.18	0.00	3.96	0.00	4.89	0.00
TNFSF4	2.93	0.00	3.69	0.00	4.67	0.00
APOBEC3H	2.52	0.04	3.20	0.00	3.91	0.00
ACTA2	2.54	0.01	3.07	0.00	3.60	0.00
CMBL	2.52	0.01	2.90	0.00	3.57	0.00
GADD45A	2.27	0.01	2.77	0.00	3.38	0.00
DCDC2B	-1.62	0.01	-1.18	1.00	-1.26	0.64
MAMDC4	2.06	0.04	2.82	0.00	3.23	0.00
BAX	2.31	0.00	2.88	0.00	3.23	0.00
ASTN2	2.07	0.01	2.67	0.00	3.15	0.00
AEN	2.16	0.01	2.80	0.00	3.14	0.00
MIR1204	2.32	0.01	2.71	0.00	3.06	0.00
PHPT1	2.23	0.00	2.57	0.00	3.03	0.00
PCNA	2.02	0.00	2.44	0.00	2.88	0.00
LOC650612	-1.40	0.04	1.01	1.00	-1.01	1.00
TNFRSF10B	2.02	0.01	2.32	0.00	2.72	0.00
GLS2	1.87	0.01	2.37	0.00	2.62	0.00
TRIAP1	1.81	0.00	2.14	0.00	2.57	0.00
TMEM30A	1.72	0.01	2.13	0.00	2.45	0.00
SESN1	1.90	0.00	2.14	0.00	2.44	0.00
IER5	1.82	0.01	2.10	0.00	2.41	0.00
TNFRSF10D	1.81	0.01	2.08	0.00	2.39	0.00
ASCC3	1.84	0.00	2.22	0.00	2.37	0.00
XPC	1.81	0.01	2.12	0.00	2.31	0.00
FAS	1.79	0.00	2.06	0.00	2.23	0.00
CCNG1	1.80	0.00	1.97	0.00	2.14	0.00
PPM1D	1.63	0.01	1.81	0.00	2.11	0.00
RPS27L	1.67	0.01	1.90	0.00	2.04	0.00
TP53INP1	1.53	0.04	1.81	0.00	2.02	0.00
MAP4K4	1.40	0.05	1.54	0.00	1.69	0.00
FBXO22	1.39	0.03	1.56	0.00	1.65	0.00

13.4.2 Medium Dose

Dose	0.5 Gy Alpha		1.0 Gy Alpha		1.5 Gy Alpha	
Symbol	FC	PV	FC	PV	FC	PV
DDB2	3.56	0.00	4.41	0.00	5.49	0.00
ISG20L1	3.63	0.00	4.45	0.00	5.23	0.00
ANKRA2	1.39	0.27	1.48	0.02	1.60	0.00
PHLDA3	3.18	0.00	3.96	0.00	4.89	0.00
ARHGEF3	1.32	0.59	1.51	0.00	1.55	0.00
TNFSF4	2.93	0.00	3.69	0.00	4.67	0.00
APOBEC3H	2.52	0.04	3.20	0.00	3.91	0.00
ACTA2	2.54	0.01	3.07	0.00	3.60	0.00
BBC3	1.40	0.66	1.65	0.01	1.83	0.00
BTG3	1.30	0.21	1.41	0.00	1.54	0.00
CCDC90B	1.20	0.64	1.29	0.02	1.35	0.00
CMBL	2.52	0.01	2.90	0.00	3.57	0.00
CD70	2.04	0.75	2.50	0.04	3.01	0.00
CDKN1A	2.30	0.11	2.94	0.00	3.58	0.00
GADD45A	2.27	0.01	2.77	0.00	3.38	0.00
DCP1B	1.17	1.00	1.45	0.01	1.51	0.00
MAMDC4	2.06	0.04	2.82	0.00	3.23	0.00
DRAM1	1.32	1.00	1.55	0.03	1.66	0.00
E2F7	1.33	1.00	1.49	0.05	1.72	0.00
EDA2R	1.31	1.00	1.57	0.02	1.67	0.00
FAM127B	1.21	0.54	1.31	0.00	1.38	0.00
FAM20B	1.08	1.00	1.25	0.03	1.35	0.00
BAX	2.31	0.00	2.88	0.00	3.23	0.00
ASTN2	2.07	0.01	2.67	0.00	3.15	0.00
FDXR	1.47	0.85	1.76	0.01	1.88	0.00
FHL2	1.50	0.44	1.82	0.00	2.20	0.00
AEN	2.16	0.01	2.80	0.00	3.14	0.00
GDF15	1.49	1.00	1.98	0.03	2.26	0.00
MIR1204	2.32	0.01	2.71	0.00	3.06	0.00
GSS	1.15	1.00	1.29	0.03	1.34	0.00
HIST1H4B	1.83	0.75	2.21	0.03	2.59	0.00
PHPT1	2.23	0.00	2.57	0.00	3.03	0.00
IGFBP4	1.19	1.00	1.45	0.01	1.52	0.00
ISCU	1.18	0.98	1.24	0.05	1.26	0.01
ISG20	-1.44	1.00	-1.92	0.00	-2.30	0.00
PCNA	2.02	0.00	2.44	0.00	2.88	0.00
LAMC3	1.54	1.00	1.93	0.02	2.13	0.00
LOC100133328	1.27	1.00	1.53	0.01	1.57	0.00
LOC387882	-1.18	1.00	-1.41	0.04	-1.45	0.01

LOC729204	-1.07	1.00	-1.37	0.03	-1.26	0.21
LOC90120	1.10	1.00	1.43	0.00	1.31	0.00
TNFRSF10B	2.02	0.01	2.32	0.00	2.72	0.00
GLS2	1.87	0.01	2.37	0.00	2.62	0.00
MDM2	1.24	0.31	1.30	0.02	1.45	0.00
TRIAP1	1.81	0.00	2.14	0.00	2.57	0.00
MYO1A	1.18	1.00	1.43	0.04	1.37	0.07
NUDT15	1.21	0.24	1.31	0.00	1.38	0.00
TMEM30A	1.72	0.01	2.13	0.00	2.45	0.00
PCNXL2	1.19	1.00	1.33	0.01	1.40	0.00
SESN1	1.90	0.00	2.14	0.00	2.44	0.00
IER5	1.82	0.01	2.10	0.00	2.41	0.00
POLH	1.39	0.24	1.60	0.00	1.92	0.00
TNFRSF10D	1.81	0.01	2.08	0.00	2.39	0.00
PRKAB1	1.29	0.59	1.49	0.00	1.60	0.00
PVT1	1.42	1.00	1.68	0.02	1.85	0.00
RETSAT	1.21	1.00	1.38	0.03	1.45	0.00
ASCC3	1.84	0.00	2.22	0.00	2.37	0.00
SAC3D1	1.26	0.24	1.29	0.04	1.33	0.01
SCARNA10	1.29	1.00	1.57	0.03	1.81	0.00
XPC	1.81	0.01	2.12	0.00	2.31	0.00
SLC7A6	1.62	0.15	1.89	0.00	2.15	0.00
FAS	1.79	0.00	2.06	0.00	2.23	0.00
TMPRSS7	1.24	1.00	1.53	0.00	1.52	0.00
CCNG1	1.80	0.00	1.97	0.00	2.14	0.00
PPM1D	1.63	0.01	1.81	0.00	2.11	0.00
RPS27L	1.67	0.01	1.90	0.00	2.04	0.00
TNFSF8	1.92	0.08	2.33	0.00	2.61	0.00
TOB1	1.23	0.69	1.38	0.00	1.47	0.00
TP53AP1	1.20	1.00	1.39	0.03	1.45	0.01
TP53INP1	1.53	0.04	1.81	0.00	2.02	0.00
TP53TG1	1.23	1.00	1.40	0.03	1.43	0.01
MAP4K4	1.40	0.05	1.54	0.00	1.69	0.00
TRIM22	1.69	0.25	2.06	0.00	2.16	0.00
TRIM32	1.25	0.45	1.34	0.02	1.37	0.00
FBXO22	1.39	0.03	1.56	0.00	1.65	0.00
ZNF337	1.34	0.25	1.44	0.01	1.52	0.00
ZNF79	1.39	0.47	1.74	0.00	1.95	0.00

13.4.3 High Dose

Dose	0.5 Gy Alpha		1.0 Gy Alpha		1.5 Gy Alpha	
Symbol	FC	PV	FC	PV	FC	PV
DDB2	3.56	0.00	4.41	0.00	5.49	0.00
ISG20L1	3.63	0.00	4.45	0.00	5.23	0.00
AGRN	1.14	1.00	1.22	0.15	1.26	0.02
ALB	1.33	1.00	1.49	0.58	1.75	0.03
ANKRA2	1.39	0.27	1.48	0.02	1.60	0.00
ANKRD16	-1.10	1.00	-1.13	0.80	-1.22	0.03
APBB3	1.22	1.00	1.32	0.22	1.39	0.02
APOBEC3C	1.14	1.00	1.31	0.15	1.35	0.04
PHLDA3	3.18	0.00	3.96	0.00	4.89	0.00
ARHGEF3	1.32	0.59	1.51	0.00	1.55	0.00
TNFSF4	2.93	0.00	3.69	0.00	4.67	0.00
APOBEC3H	2.52	0.04	3.20	0.00	3.91	0.00
ACTA2	2.54	0.01	3.07	0.00	3.60	0.00
BBC3	1.40	0.66	1.65	0.01	1.83	0.00
BTG3	1.30	0.21	1.41	0.00	1.54	0.00
CCDC28B	-1.06	1.00	-1.13	0.84	-1.21	0.04
CCDC34	1.21	1.00	1.32	0.14	1.42	0.01
CCDC90B	1.20	0.64	1.29	0.02	1.35	0.00
CMBL	2.52	0.01	2.90	0.00	3.57	0.00
CD70	2.04	0.75	2.50	0.04	3.01	0.00
CDCA7	-1.18	1.00	-1.24	0.38	-1.38	0.01
CDKN1A	2.30	0.11	2.94	0.00	3.58	0.00
GADD45A	2.27	0.01	2.77	0.00	3.38	0.00
DCP1B	1.17	1.00	1.45	0.01	1.51	0.00
MAMDC4	2.06	0.04	2.82	0.00	3.23	0.00
DRAM1	1.32	1.00	1.55	0.03	1.66	0.00
E2F7	1.33	1.00	1.49	0.05	1.72	0.00
EDA2R	1.31	1.00	1.57	0.02	1.67	0.00
EI24	1.24	0.82	1.30	0.06	1.37	0.01
ETHE1	-1.24	1.00	-1.27	0.38	-1.37	0.03
F5	1.32	1.00	1.45	0.33	1.60	0.03
FAM127B	1.21	0.54	1.31	0.00	1.38	0.00
FAM20B	1.08	1.00	1.25	0.03	1.35	0.00
BAX	2.31	0.00	2.88	0.00	3.23	0.00
ASTN2	2.07	0.01	2.67	0.00	3.15	0.00
FDXR	1.47	0.85	1.76	0.01	1.88	0.00
FHL2	1.50	0.44	1.82	0.00	2.20	0.00
AEN	2.16	0.01	2.80	0.00	3.14	0.00
GAMT	1.19	1.00	1.35	0.19	1.42	0.02

GDF15	1.49	1.00	1.98	0.03	2.26	0.00
MIR1204	2.32	0.01	2.71	0.00	3.06	0.00
GPR172B	1.21	1.00	1.25	0.36	1.39	0.01
GSS	1.15	1.00	1.29	0.03	1.34	0.00
HIST1H2AB	1.07	1.00	1.14	1.00	1.49	0.03
HIST1H2AG	1.20	1.00	1.28	0.38	1.43	0.01
HIST1H2AH	1.37	1.00	1.38	0.75	1.65	0.03
HIST1H2AM	1.29	1.00	1.41	0.74	1.82	0.01
HIST1H2BG	1.40	1.00	1.58	0.10	1.87	0.00
HIST1H3A	1.26	1.00	1.42	0.55	1.71	0.01
HIST1H4A	1.41	1.00	1.66	0.38	1.94	0.03
HIST1H4B	1.83	0.75	2.21	0.03	2.59	0.00
HIST1H4E	1.28	1.00	1.54	0.14	1.63	0.03
HIST1H4F	1.26	1.00	1.27	0.85	1.52	0.02
HIST1H4L	1.30	1.00	1.38	0.33	1.53	0.02
HIST2H3A	1.53	1.00	1.66	0.19	1.92	0.01
HIST2H3D	1.11	1.00	1.25	0.55	1.38	0.02
PHPT1	2.23	0.00	2.57	0.00	3.03	0.00
IFITM1	-1.26	1.00	-1.43	0.14	-1.61	0.00
IGFBP4	1.19	1.00	1.45	0.01	1.52	0.00
IKBIP	1.14	1.00	1.23	0.15	1.29	0.01
ISCU	1.18	0.98	1.24	0.05	1.26	0.01
ISG20	-1.44	1.00	-1.92	0.00	-2.30	0.00
PCNA	2.02	0.00	2.44	0.00	2.88	0.00
KCNK17	-1.28	1.00	-1.26	0.91	-1.54	0.02
LAMC3	1.54	1.00	1.93	0.02	2.13	0.00
LIG1	1.47	1.00	1.78	0.08	2.03	0.00
LOC100129866	1.12	1.00	1.18	0.58	1.31	0.01
LOC100132139	1.20	1.00	1.26	0.42	1.39	0.02
LOC100132564	2.73	0.56	3.32	0.05	4.92	0.00
LOC100133328	1.27	1.00	1.53	0.01	1.57	0.00
LOC387882	-1.18	1.00	-1.41	0.04	-1.45	0.01
LOC641978	1.26	1.00	1.37	0.23	1.56	0.00
LOC653604	1.07	1.00	1.20	0.86	1.37	0.03
LOC728671	-1.36	1.00	-1.21	1.00	-1.62	0.03
LOC728953	1.21	1.00	1.25	0.29	1.36	0.01
LOC90120	1.10	1.00	1.43	0.00	1.31	0.00
LRP5	1.31	1.00	1.56	0.22	1.69	0.03
MAD1L1	1.14	1.00	1.28	0.17	1.32	0.03
TNFRSF10B	2.02	0.01	2.32	0.00	2.72	0.00
GLS2	1.87	0.01	2.37	0.00	2.62	0.00
MDM2	1.24	0.31	1.30	0.02	1.45	0.00
MGAT3	1.20	1.00	1.31	0.11	1.40	0.01

MGC27348	1.10	1.00	1.27	0.15	1.32	0.02
TRIAP1	1.81	0.00	2.14	0.00	2.57	0.00
MIR888	1.19	1.00	1.21	1.00	1.46	0.04
MRPL49	1.12	1.00	1.24	0.12	1.32	0.00
MTHFD1L	1.20	1.00	1.35	0.72	1.67	0.01
MYC	-1.34	1.00	-1.69	0.12	-1.94	0.01
NAALADL1	-1.20	1.00	-1.26	0.52	-1.36	0.05
NACC2	1.19	1.00	1.28	0.25	1.43	0.00
NIN	1.13	1.00	1.20	0.32	1.25	0.03
NUDT15	1.21	0.24	1.31	0.00	1.38	0.00
OSBPL3	1.17	1.00	1.29	0.15	1.35	0.02
PACSIN1	-1.15	1.00	-1.37	0.15	-1.56	0.00
PACSIN3	1.29	1.00	1.41	0.33	1.55	0.03
PAICS	-1.14	1.00	-1.30	0.05	-1.35	0.01
TMEM30A	1.72	0.01	2.13	0.00	2.45	0.00
PCNP	1.15	1.00	1.21	0.08	1.22	0.03
PCNXL2	1.19	1.00	1.33	0.01	1.40	0.00
PEX5	-1.09	1.00	-1.15	0.20	-1.18	0.03
SESN1	1.90	0.00	2.14	0.00	2.44	0.00
IER5	1.82	0.01	2.10	0.00	2.41	0.00
PLLP	1.29	1.00	1.49	0.18	1.58	0.03
PMAIP1	1.14	1.00	1.37	0.10	1.44	0.01
POLH	1.39	0.24	1.60	0.00	1.92	0.00
TNFRSF10D	1.81	0.01	2.08	0.00	2.39	0.00
PRKAB1	1.29	0.59	1.49	0.00	1.60	0.00
PRKD2	1.19	1.00	1.28	0.16	1.32	0.03
PRMT7	1.13	1.00	1.15	1.00	1.33	0.03
PTP4A1	1.22	1.00	1.39	0.06	1.45	0.01
PVT1	1.42	1.00	1.68	0.02	1.85	0.00
RETSAT	1.21	1.00	1.38	0.03	1.45	0.00
REV3L	1.21	1.00	1.41	0.08	1.52	0.00
RN7SK	1.59	1.00	1.79	0.29	2.24	0.01
RNU6-1	1.43	1.00	1.56	0.62	1.87	0.04
RPPH1	1.36	1.00	1.64	0.20	1.92	0.01
ASCC3	1.84	0.00	2.22	0.00	2.37	0.00
SAC3D1	1.26	0.24	1.29	0.04	1.33	0.01
SCARNA10	1.29	1.00	1.57	0.03	1.81	0.00
XPC	1.81	0.01	2.12	0.00	2.31	0.00
SGIP1	1.08	1.00	1.30	0.20	1.37	0.02
SIPA1	-1.09	1.00	-1.16	0.19	-1.24	0.00
SLC7A6	1.62	0.15	1.89	0.00	2.15	0.00
SNORD68	1.22	1.00	1.31	0.71	1.49	0.04
SNORD96B	1.30	1.00	1.39	0.30	1.57	0.01

SOX4	1.31	1.00	1.48	0.34	1.69	0.02
SPATA18	1.34	1.00	1.58	0.55	2.07	0.01
SPDEF	-1.17	1.00	-1.10	1.00	-1.40	0.04
SRA1	1.12	1.00	1.26	0.14	1.31	0.02
STAT3	1.14	1.00	1.19	0.34	1.24	0.05
FAS	1.79	0.00	2.06	0.00	2.23	0.00
TMEM43	-1.16	1.00	-1.24	0.25	-1.28	0.04
TMPRSS7	1.24	1.00	1.53	0.00	1.52	0.00
CCNG1	1.80	0.00	1.97	0.00	2.14	0.00
PPM1D	1.63	0.01	1.81	0.00	2.11	0.00
RPS27L	1.67	0.01	1.90	0.00	2.04	0.00
TNFSF8	1.92	0.08	2.33	0.00	2.61	0.00
TNFSF9	1.16	1.00	1.39	0.19	1.49	0.02
TOB1	1.23	0.69	1.38	0.00	1.47	0.00
TP53AP1	1.20	1.00	1.39	0.03	1.45	0.01
TP53INP1	1.53	0.04	1.81	0.00	2.02	0.00
TP53TG1	1.23	1.00	1.40	0.03	1.43	0.01
MAP4K4	1.40	0.05	1.54	0.00	1.69	0.00
TRIM22	1.69	0.25	2.06	0.00	2.16	0.00
TRIM32	1.25	0.45	1.34	0.02	1.37	0.00
UROD	1.10	1.00	1.18	0.09	1.20	0.03
VWCE	1.63	1.00	1.94	0.08	2.28	0.00
FBXO22	1.39	0.03	1.56	0.00	1.65	0.00
ZNF195	1.18	1.00	1.16	0.86	1.32	0.01
ZNF296	-1.09	1.00	-1.15	0.88	-1.29	0.01
ZNF319	-1.06	1.00	-1.09	0.98	-1.18	0.03
ZNF337	1.34	0.25	1.44	0.01	1.52	0.00
ZNF541	1.33	1.00	1.72	0.06	1.94	0.00
ZNF79	1.39	0.47	1.74	0.00	1.95	0.00

13.5 Appendix V – miRNA Transcripts Identified as Significant after Alpha-Particle Exposure via nCounter Analysis

13.5.1 Low Dose

Dose	0.5 Gy Alpha		1.0 Gy Alpha		1.5 Gy Alpha	
miRNA Symbol	**FC**	**PV**	**FC**	**PV**	**FC**	**PV**
hsa-miR-34a	2.42	0.00	3.13	0.00	3.34	0.00

13.5.2 Medium Dose

Dose	0.5 Gy Alpha		1.0 Gy Alpha		1.5 Gy Alpha	
miRNA Symbol	**FC**	**PV**	**FC**	**PV**	**FC**	**PV**
hsa-miR-34a	2.42	0.00	3.13	0.00	3.34	0.00
hsa-miR-492	-2.25	0.19	2.00	0.01	1.81	0.00

13.5.3 High Dose

Dose	0.5 Gy Alpha		1.0 Gy Alpha		1.5 Gy Alpha	
miRNA Symbol	**FC**	**PV**	**FC**	**PV**	**FC**	**PV**
hsa-miR-34a	2.42	0.00	3.13	0.00	3.34	0.00
hsa-miR-492	-2.25	0.19	2.00	0.01	1.81	0.00
hsa-miR-494	1.47	0.36	1.55	0.07	2.05	0.00

13.6 Appendix VI – Individual Clinical Chemistry Results

Analyte	Units	0 Gy	0.5 Gy	1.0 Gy	1.5 Gy
GLU	mg/dL	96	97	99	100
BUN	mg/dL	16	16	16	16
CA	mg/dL	9.0	9	9	9.2
CRE	mg/dL	0.5	0.6	0.8	0.5
NA+	mmol/L	137	136	143	136
K+	mmol/L	4.4	4.3	4.4	4.4
CL-	mmol/L	103	105	106	101
tCO2	mmol/L	26	26	26	26
GLU	mg/dL	102	103	104	103
BUN	mg/dL	16	17	17	17
CRE	mg/dL	0.6*	0.8	0.8	0.6
UA	mg/dL	3.6	3.6	3.6	3.5
CA	mg/dL	9.3	9.3	9.5	9.4
ALB	g/dL	3.6	3.7	3.7	3.6
TP	g/dL	6.7	6.6	6.9	6.6
ALT	U/L	20	19	19	17
AST	U/L	19	18	19	19
ALP	U/L	51	55	49	53
GGT	U/L	18	20	22	19
AMY	U/L	39	41	40	39
CRP	mg/L	<5.0	<5.0	<5.0	<5.0
CHOL	mg/dL	182	180	174	179
HDL	mg/dL	60	61	58	60
TRIG	mg/dL	72	72	69	71
ALT	U/L	11	15	13	15
AST	U/L	18	17	17	19
GLU	mg/dL	99	99	96	99
TC/H		3	3	3	3
LDL	mg/dL	107	105	102	105
VLDL	mg/dL	14	14	14	14
ALB	g/dL	3.8	3.7	3.5	3.9
ALP	U/L	50	45	39	44
ALT	U/L	13	14	17	14
AST	U/L	17	17	15	14
DBIL	mg/dL	0.3	0.3	0.2	0.2
TBIL	mg/dL	1	1	1	1.1
TP	g/dL	6.6	6.5	6.1	6.9

Analyte	Units	0 Gy	0.5 Gy	1.0 Gy	1.5 Gy
GLU	mg/dL	98	98	98	99
BUN	mg/dL	20	21	20	21
CA	mg/dL	9.1	9	9.3	9.4
CRE	mg/dL	1	0.9	1	1
NA+	mmol/L	133	132	136	134
K+	mmol/L	4.3	4.1	4.4	4.3
CL-	mmol/L	100	101	103	104
tCO2	mmol/L	26	26	27	27
GLU	mg/dL	103	103	104	104
BUN	mg/dL	21	21	21	21
CRE	mg/dL	1.1	1.2	1.1	1.2
UA	mg/dL	6.1	6.3	6.5	6.4
CA	mg/dL	9.4	9.2	9.4	9.3
ALB	g/dL	4.1	4.1	4.1	3.9
TP	g/dL	6.9	6.9	7	7
ALT	U/L	23	33	25	26
AST	U/L	27	26	27	27
ALP	U/L	43	40	47	43
GGT	U/L	35	34	36	35
AMY	U/L	29	29	29	28
CRP	mg/L	<5.0	<5.0	<5.0	<5.0
CHOL	mg/dL	219	224	226	223
HDL	mg/dL	65	65	65	64
TRIG	mg/dL	170	171	173	170
ALT	U/L	20	24	23	21
AST	U/L	25	27	23	25
GLU	mg/dL	97	96	99	99
TC/H		3.4	3.5	3.5	3.5
LDL	mg/dL	120	125	126	126
VLDL	mg/dL	34	34	35	34
ALB	g/dL	4.1	4.1	4.1	4.2
ALP	U/L	33	36	39	38
ALT	U/L	28	27	25	21
AST	U/L	24	24	26	25
DBIL	mg/dL	0.3	0.2	0.2	0.2
TBIL	mg/dL	0.9	0.9	1	0.9
TP	g/dL	6.8	6.9	6.9	7

Analyte	Units	0 Gy	0.5 Gy	1.0 Gy	1.5 Gy
GLU	mg/dL	108	110	106	106
BUN	mg/dL	18	19	18	18
CA	mg/dL	9.6	9.8	9.6	9.6
CRE	mg/dL	1	1.1	1.2	1.1
NA+	mmol/L	134	138	133	134
K+	mmol/L	4.5	4.6	4.5	4.4
CL-	mmol/L	101	103	100	100
tCO2	mmol/L	29	29	31	30
GLU	mg/dL	114	110	111	112
BUN	mg/dL	19	18	19	19
CRE	mg/dL	1.1	1.1	1.1	1.2
UA	mg/dL	4	4.1	4.1	4.1
CA	mg/dL	9.8	9.6	9.8	10.1
ALB	g/dL	4	4	3.9	4
TP	g/dL	7.3	7	7.1	7.2
ALT	U/L	30	27	30	27
AST	U/L	44	41	39	42
ALP	U/L	39	32	33	37
GGT	U/L	28	26	26	28
AMY	U/L	46	43	43	45
CRP	mg/L	< 5.0	< 5.0	< 5.0	< 5.0
CHOL	mg/dL	280	272	276	270
HDL	mg/dL	68	68	66	64
TRIG	mg/dL	203	198	203	194
ALT	U/L	22	25	26	27
AST	U/L	41	39	42	43
GLU	mg/dL	110	108	109	107
TC/H		4.1	4	4.2	4.2
LDL	mg/dL	172	164	170	167
VLDL	mg/dL	41	40	41	39
ALB	g/dL	4	4.1	4	4
ALP	U/L	33	31	32	29
ALT	U/L	31	23	27	26
AST	U/L	41	41	41	41
DBIL	mg/dL	0.3	0.2	0.2	0.2
TBIL	mg/dL	0.8	0.8	0.7	0.7
TP	g/dL	7.3	7.2	7	7.1

Analyte	Units	0 Gy	0.5 Gy	1.0 Gy	1.5 Gy
GLU	mg/dL	109	110	106	111
BUN	mg/dL	21	21	20	20
CA	mg/dL	8.9	8.9	8.7	8.8
CRE	mg/dL	1.1	1.1	1	1
NA+	mmol/L	134	130	133	135
K+	mmol/L	4.4	4.5	4.2	4.5
CL-	mmol/L	99	99	102	100
tCO2	mmol/L	27	26	27	25
GLU	mg/dL	113	116	112	114
BUN	mg/dL	23	22	22	22
CRE	mg/dL	1.1	1.1	1.1	1
UA	mg/dL	5.7	5.9	5.7	5.9
CA	mg/dL	9.1	9.1	9	8.9
ALB	g/dL	3.9	3.8	3.7	3.7
TP	g/dL	7.3	7.3	7.2	7.2
ALT	U/L	24	21	20	24
AST	U/L	25	25	23	16
ALP	U/L	59	52	50	52
GGT	U/L	37	36	35	37
AMY	U/L	50	50	48	50
CRP	mg/L	< 5.0	< 5.0	< 5.0	< 5.0
CHOL	mg/dL	213	208	209	210
HDL	mg/dL	40	40	36	41
TRIG	mg/dL	262	262	259	259
ALT	U/L	17	18	19	19
AST	U/L	23	26	20	22
GLU	mg/dL	110	114	109	112
TC/H		5.3	5.2	5.8	5.1
LDL	mg/dL	120	116	121	116
VLDL	mg/dL	52	52	52	52
ALB	g/dL	3.9	3.9	3.9	4
ALP	U/L	50	54	49	52
ALT	U/L	20	22	19	21
AST	U/L	25	22	25	25
DBIL	mg/dL	0.2	0.3	0.3	0.3
TBIL	mg/dL	0.6	0.6	0.6	0.6
TP	g/dL	7.3	7.2	7.3	7.3

Analyte	Units	0 Gy	0.5 Gy	1.0 Gy	1.5 Gy
GLU	mg/dL	91	89	87	89
BUN	mg/dL	9	9	9	9
CA	mg/dL	9	8.9	8.8	8.6
CRE	mg/dL	0.7	0.6	0.6	0.6
NA+	mmol/L	134	134	133	130
K+	mmol/L	4.7	4.5	4.6	4.6
CL-	mmol/L	101	104	104	106
tCO2	mmol/L	21	21	21	20
GLU	mg/dL	95	91	92	92
BUN	mg/dL	9	10	9	10
CRE	mg/dL	0.8	0.8	0.9	0.8
UA	mg/dL	4	4	4.1	4
CA	mg/dL	9	8.8	8.9	10.4
ALB	g/dL	3.5	3.5	3.6	3.4
TP	g/dL	6.5	6.4	6.6	6.4
ALT	U/L	17	24	22	21
AST	U/L	22	22	20	20
ALP	U/L	38	37	33	37
GGT	U/L	17	16	16	18
AMY	U/L	28	24	29	29
CRP	mg/L	< 5.0	< 5.0	< 5.0	< 5.0
CHOL	mg/dL	176	173	171	172
HDL	mg/dL	70	67	67	70
TRIG	mg/dL	124	125	124	131
ALT	U/L	9	19	22	19
AST	U/L	23	20	18	19
GLU	mg/dL	90	88	87	90
TC/H		2.5	2.6	2.6	2.5
LDL	mg/dL	82	81	79	76
VLDL	mg/dL	25	25	25	26
ALB	g/dL	3.7	3.5	3.6	3.7
ALP	U/L	35	36	34	33
ALT	U/L	14	22	21	20
AST	U/L	22	21	22	22
DBIL	mg/dL	0.2	0.2	0.3	0.3
TBIL	mg/dL	0.7	0.6	0.6	0.6
TP	g/dL	6.5	6.3	6.4	6.4

Analyte	Units	0 Gy	0.5 Gy	1.0 Gy	1.5 Gy
GLU	mg/dL	76	74	74	72
BUN	mg/dL	12	12	13	12
CA	mg/dL	8.9	8.8	9	8.7
CRE	mg/dL	0.6	0.6	0.6	0.8
NA+	mmol/L	134	132	132	128
K+	mmol/L	4	4.2	4.6	4.1
CL-	mmol/L	101	104	100	100
tCO2	mmol/L	26	26	23	26
GLU	mg/dL	81	80	77	78
BUN	mg/dL	13	13	12	13
CRE	mg/dL	0.8	0.6	0.8	0.7
UA	mg/dL	4.8	4.8	4.5	4.7
CA	mg/dL	9	9.2	8.8	8.8
ALB	g/dL	3.8	3.6	3.6	3.5
TP	g/dL	6.7	6.6	6.5	6.5
ALT	U/L	19	17	14	19
AST	U/L	18	17	21	17
ALP	U/L	19	25	19	23
GGT	U/L	7	8	6	6
AMY	U/L	43	43	42	41
CRP	mg/L	< 5.0	< 5.0	< 5.0	< 5.0
CHOL	mg/dL	164	158	167	149
HDL	mg/dL	60	58	60	56
TRIG	mg/dL	61	58	61	58
ALT	U/L	13	11	10	15
AST	U/L	18	16	18	15
GLU	mg/dL	78	74	77	73
TC/H		2.7	2.7	2.8	2.6
LDL	mg/dL	91	89	95	81
VLDL	mg/dL	12	12	12	12
ALB	g/dL	3.8	3.7	3.6	3.6
ALP	U/L	21	26	15	22
ALT	U/L	15	15	14	10
AST	U/L	17	18	19	16
DBIL	mg/dL	0.3	0.3	0.1	0.2
TBIL	mg/dL	0.8	0.7	0.7	0.7
TP	g/dL	6.5	6.4	6.5	6.2

Analyte	Units	0 Gy	0.5 Gy	1.0 Gy	1.5 Gy
GLU	mg/dL	77	77	79	79
BUN	mg/dL	17	16	17	17
CA	mg/dL	8.8	8.8	8.7	8.8
CRE	mg/dL	1.1	1	1	1.1
NA+	mmol/L	138	138	136	136
K+	mmol/L	4.4	4.4	4.4	4.4
CL-	mmol/L	102	103	101	102
tCO2	mmol/L	28	29	26	28
GLU	mg/dL	82	82	84	83
BUN	mg/dL	18	19	18	18
CRE	mg/dL	1.1	1.1	1	1.2
UA	mg/dL	5.8	5.9	5.7	5.7
CA	mg/dL	9.2	9.2	9	8.9
ALB	g/dL	4.1	4.1	3.9	3.9
TP	g/dL	7.2	7.2	7.1	7
ALT	U/L	20	15	13	18
AST	U/L	28	28	25	27
ALP	U/L	42	46	45	45
GGT	U/L	20	20	18	18
AMY	U/L	45	46	45	50
CRP	mg/L	< 5.0	< 5.0	< 5.0	< 5.0
CHOL	mg/dL	206	208	203	201
HDL	mg/dL	80	80	80	81
TRIG	mg/dL	83	85	82	85
ALT	U/L	15	12	18	10
AST	U/L	25	25	25	28
GLU	mg/dL	78	78	79	81
TC/H		2.6	2.6	2.5	2.5
LDL	mg/dL	109	111	107	103
VLDL	mg/dL	17	17	16	17
ALB	g/dL	4	4.1	4.1	4.1
ALP	U/L	46	48	41	42
ALT	U/L	18	15	11	14
AST	U/L	26	25	24	26
DBIL	mg/dL	0.2	0.2	0.2	0.3
TBIL	mg/dL	0.6	0.6	0.7	0.6
TP	g/dL	7.1	7.1	7	7.1

Analyte	Units	0 Gy	0.5 Gy	1.0 Gy	1.5 Gy
GLU	mg/dL	155	158	159	156
BUN	mg/dL	13	13	13	14
CA	mg/dL	9.6	9.7	9.9	10
CRE	mg/dL	0.5	0.5	0.6	0.7
NA+	mmol/L	126	127	133	133
K+	mmol/L	4	3.9	4.1	4
CL-	mmol/L	99	98	105	103
tCO2	mmol/L	23	24	23	23
GLU	mg/dL	166	166	166	163
BUN	mg/dL	13	13	14	13
CRE	mg/dL	0.7	0.7	0.7	0.7
UA	mg/dL	5.8	5.7	5.7	5.6
CA	mg/dL	10.4	10.2	10.3	10.1
ALB	g/dL	4	3.9	3.9	3.8
TP	g/dL	7.1	7	7.2	7
ALT	U/L	29	29	23	26
AST	U/L	18	18	19	22
ALP	U/L	90	80	87	82
GGT	U/L	47	45	45	45
AMY	U/L	17	19	19	19
CRP	mg/L	< 5.0	< 5.0	< 5.0	< 5.0
CHOL	mg/dL	175	179	180	189
HDL	mg/dL	35	36	38	38
TRIG	mg/dL	166	168	170	175
ALT	U/L	19	20	18	21
AST	U/L	23	16	19	21
GLU	mg/dL	156	158	157	161
TC/H		4.9	5	4.7	5
LDL	mg/dL	106	110	108	116
VLDL	mg/dL	33	34	34	35
ALB	g/dL	3.9	4.3	3.8	4
ALP	U/L	76	90	75	73
ALT	U/L	26	24	24	24
AST	U/L	17	19	20	21
DBIL	mg/dL	0.3	0.3	0.3	0.3
TBIL	mg/dL	1	1.1	1	1.1
TP	g/dL	6.9	7.5	6.8	7.1

Analyte	Units	0 Gy	0.5 Gy	1.0 Gy	1.5 Gy
GLU	mg/dL	91	93	90	92
BUN	mg/dL	11	10	10	10
CA	mg/dL	9.1	9.1	8.9	8.8
CRE	mg/dL	0.7	0.7	0.6	0.7
NA+	mmol/L	136	134	132	134
K+	mmol/L	4.7	4.4	4.6	4.5
CL-	mmol/L	105	105	102	104
tCO2	mmol/L	26	26	25	25
GLU	mg/dL	97	98	96	96
BUN	mg/dL	11	12	11	12
CRE	mg/dL	0.7	0.8	0.8	0.9
UA	mg/dL	2.9	3	3	3
CA	mg/dL	9.1	9	9	9
ALB	g/dL	3.9	4	3.9	3.9
TP	g/dL	6.8	6.7	6.9	6.8
ALT	U/L	12	20	10	13
AST	U/L	22	20	20	18
ALP	U/L	44	44	40	41
GGT	U/L	<5	5	5	<5
AMY	U/L	35	35	37	35
CRP	mg/L	< 5.0	< 5.0	< 5.0	< 5.0
CHOL	mg/dL	190		192	186
HDL	mg/dL	51		50	50
TRIG	mg/dL	118		116	118
ALT	U/L	11		7	8
AST	U/L	23		19	18
GLU	mg/dL	94		92	93
TC/H		3.7		3.8	3.7
LDL	mg/dL	115		118	112
VLDL	mg/dL	24		23	24
ALB	g/dL	4.1	4.1	4.1	4.1
ALP	U/L	40	42	40	37
ALT	U/L	6	11	10	11
AST	U/L	20	17	19	16
DBIL	mg/dL	0.2	0.3	0.2	0.2
TBIL	mg/dL	0.7	0.7	0.8	0.7
TP	g/dL	6.8	6.8	6.8	c

Analyte	Units	0 Gy	0.5 Gy	1.0 Gy	1.5 Gy
GLU	mg/dL	98	103	99	103
BUN	mg/dL	13	14	13	14
CA	mg/dL	8.4	8.7	8.4	8.7
CRE	mg/dL	0.5	0.6	0.5	0.7
NA+	mmol/L	131	134	127	135
K+	mmol/L	4.4	4.5	4.2	4.5
CL-	mmol/L	98	100	98	102
tCO2	mmol/L	24	25	24	25
GLU	mg/dL	109	101	108	108
BUN	mg/dL	15	14	15	15
CRE	mg/dL	0.8	0.8	0.9	0.7
UA	mg/dL	4.7	4.5	4.8	4.7
CA	mg/dL	9.1	8.5	9.2	9.3
ALB	g/dL	3.9	3.7	4.1	4
TP	g/dL	6.8	6.3	6.9	6.8
ALT	U/L	27	21	24	25
AST	U/L	25	23	26	25
ALP	U/L	62	54	60	61
GGT	U/L	37	31	36	35
AMY	U/L	23	21	23	22
CRP	mg/L	< 5.0	< 5.0	< 5.0	< 5.0
CHOL	mg/dL	179	195	175	180
HDL	mg/dL	100	>100	97	99
TRIG	mg/dL	67	71	68	68
ALT	U/L	19	22	25	23
AST	U/L	25	28	24	27
GLU	mg/dL	105	112	104	108
TC/H		1.8	-	1.8	1.8
LDL	mg/dL	66	-	64	67
VLDL	mg/dL	13	14	14	14
ALB	g/dL	4.2	4.2	3.7	4.1
ALP	U/L	55	52	45	55
ALT	U/L	18	21	16	22
AST	U/L	24	22	21	23
DBIL	mg/dL	0.2	0.3	0.3	0.3
TBIL	mg/dL	0.7	0.7	0.6	0.7
TP	g/dL	6.8	6.7	5.9	6.8

Analyte	Units	0 Gy	0.5 Gy	1.0 Gy	1.5 Gy
GLU	mg/dL	250	252	250	253
BUN	mg/dL	10	9	10	9
CA	mg/dL	8.8	8.7	8.5	8.9
CRE	mg/dL	0.7	0.6	0.7	0.7
NA+	mmol/L	134	131	133	135
K+	mmol/L	4.6	4.4	4.6	4.5
CL-	mmol/L	102	104	103	102
tCO2	mmol/L	25	24	25	24
GLU	mg/dL	258	260	260	260
BUN	mg/dL	10	10	11	11
CRE	mg/dL	0.9	0.9	0.8	0.8
UA	mg/dL	6.5	6.6	6.4	6.5
CA	mg/dL	9.1	9	8.9	8.9
ALB	g/dL	3.4	3.6	3.6	3.6
TP	g/dL	7.1	7.2	7.1	7.2
ALT	U/L	40	36	20	35
AST	U/L	31	28	28	27
ALP	U/L	64	70	66	64
GGT	U/L	49	49	49	50
AMY	U/L	28	27	27	28
CRP	mg/L	22.5	23.2	23.1	23.5
CHOL	mg/dL	223	219	223	220
HDL	mg/dL	39	34	36	33
TRIG	mg/dL	316	309	311	313
ALT	U/L	35	40	18	35
AST	U/L	28	27	28	28
GLU	mg/dL	258	256	258	257
TC/H		6.2	6.4	6.3	6.7
LDL	mg/dL	124	123	126	124
VLDL	mg/dL	63	62	62	63
ALB	g/dL	3.7	3.7	3.7	3.6
ALP	U/L	62	64	58	64
ALT	U/L	35	37	16	36
AST	U/L	28	27	29	25
DBIL	mg/dL	0.3	0.3	0.3	0.3
TBIL	mg/dL	0.8	0.8	0.8	0.8
TP	g/dL	7.2	7.4	7.1	7.2

Analyte	Units	0 Gy	0.5 Gy	1.0 Gy	1.5 Gy
GLU	mg/dL	138	135	128	134
BUN	mg/dL	15	14	14	14
CA	mg/dL	9.2	9.1	8.7	8.9
CRE	mg/dL	0.7	0.8	0.7	0.7
NA+	mmol/L	140	139	132	139
K+	mmol/L	4.7	4.6	4.4	4.6
CL-	mmol/L	110	110	103	108
tCO2	mmol/L	26	26	24	26
GLU	mg/dL	129	137	131	136
BUN	mg/dL	14	15	14	15
CRE	mg/dL	0.6	0.8	0.7	0.8
UA	mg/dL	4.8	5.1	4.9	5.2
CA	mg/dL	8.4	8.9	8.8	8.9
ALB	g/dL	3.5	3.7	3.4	3.7
TP	g/dL	6.1	6.6	6.5	6.7
ALT	U/L	19	26	20	22
AST	U/L	22	23	25	24
ALP	U/L	50	54	51	56
GGT	U/L	12	15	15	14
AMY	U/L	75	78	84	79
CRP	mg/L	< 5.0	< 5.0	< 5.0	< 5.0
CHOL	mg/dL	172	177	192	173
HDL	mg/dL	52	54	59	54
TRIG	mg/dL	77	75	80	75
ALT	U/L	20	19	20	19
AST	U/L	24	24	25	26
GLU	mg/dL	134	138	145	136
TC/H		3.3	3.3	3.3	3.2
LDL	mg/dL	104	109	117	103
VLDL	mg/dL	15	15	16	15
ALB	g/dL	3.7	3.9	3.8	4
ALP	U/L	51	51	54	54
ALT	U/L	25	23	20	20
AST	U/L	23	24	22	24
DBIL	mg/dL	0.3	0.3	0.3	0.3
TBIL	mg/dL	0.8	0.8	0.8	0.8
TP	g/dL	6.3	6.7	6.6	6.9

14 Curriculum Vitae

WORK EXPERIENCE

January 2009 to Present Health Canada **Ottawa, ON**

Molecular Biologist / Student

- Member of a team tasked with examining the biological ramifications of alpha particle radiation. This research project has implications for bio-nuclear forensics and is relevant as the general public is exposed to alpha particle radiation through ubiquitous radon exposure

. Responsibilities include:

- All aspect of the experimental process including experimental design and performance as well as data acquisition and analysis
- Collaborating with other members within Health Canada to fulfill experimental mandate
- Presenting data and conclusions in various forms such as published articles, manuscripts, posters, and at national and international conferences
- Negotiating with suppliers to acquire optimal lab equipment solutions

January 2012 to Present University of Ottawa **Ottawa, ON**

Laboratory Teaching Assistant

- Instructor and laboratory demonstrator for a third year biochemistry laboratory course

Responsibilities include:

- Demonstrating experimental techniques and assisting students with the various lab tasks
- Grading and evaluating laboratory reports and project proposals submitted by course participants
- Providing constructive feedback to students and on-going communications with teaching staff

EDUCATION

2011-2013 University of Ottawa **Ottawa, ON**

Master of Science in Biochemistry

- Published seven (7) peer-reviewed articles in scientific journals
- Presented findings at international scientific conferences

2006-2011 University of Ottawa **Ottawa, ON**

Bachelor of Science (Co-op) Honours in Biochemistry.

- Graduated Cum Laude

PUBLICATION LIST

Chauhan, V., & **Howland, M.** (2012). Genomic Profiling of a Human Leukemic Monocytic Cell-Line (THP-1) Exposed to Alpha Particle Radiation. *The Scientific World Journal, 2012*.

Chauhan, V., **Howland, M.**, Greene, H. B., & Wilkins, R. C. (2012). Transcriptional and Secretomic Profiling of Epidermal Cells Exposed to Alpha Particle Radiation. *The Open Biochemistry Journal, 6*, 103.

Chauhan, V., **Howland, M**., Kutzner, B., McNamee, J. P., Bellier, P. V., & Wilkins, R. C. (2012). Biological effects of alpha particle radiation exposure on human monocytic cells. *International Journal of Hygiene and Environmental Health,* 215(3), 339-344.

Chauhan, V., **Howland, M.**, Mendenhall, A., O'Hara, S., Stocki, T. J., McNamee, J. P., & Wilkins, R. C. (2012). Effects of alpha particle radiation on gene expression in human pulmonary epithelial cells. *International Journal of Hygiene and Environmental Health.* 2012 215(5):522-35

Chauhan, V., **Howland, M**., & Wilkins, R. (2012). A Comparitive Assessement of Cytokine Expression in Human-Derived Cell Lines Exposed to Alpha Particles and X-Rays. *The Scientific World Journal,* 2012.

Chauhan, V., **Howland, M**., & Wilkins, R. (2012). Effects of α-Particle Radiation on MicroRNA Responses in Human Cell-Lines. *The Open Biochemistry Journal, 6*, 16.

Chauhan, V., **Howland, M**., Chen, J., Kutzner, B., & Wilkins, R. C. (2011). Differential effects of alpha-particle radiation and X-irradiation on genes associated with apoptosis. *Radiology Research and Practice,* 2011.

AWARDS RECIEVED

- North American Radiation Research Scholar-in-Training travel bursary recipient (2012)
- CTPNL Conference Travel Award (2012)
- International Congress on Radiation Research travel bursary (2011)
- Health Canada National Science Forum Student Award recipient (2010)
- Tony MacKay Student Paper Award (Presented annually by the Canadian Radiation Protection Association for the best article written by a student) (2009)

0